The Pennsylvania State University

The Graduate School

The Eberly College of Science

A NOVEL SMALL MOLECULE DNA INTERCALATOR PZ1225 IN CANCER CELL APOPTOSIS AND A HISTONE MODIFIER PAD4 IN MACROPHAGE EXTRACELLULAR TRAP FORMATION

A Dissertation in

Molecular Cellular and Integrative Biosciences

by

Jinquan Sun

Submitted in Partial Fulfillment
of the Requirements
for the Degree of

Doctor of Philosophy

December 2016

The dissertation of Jinquan Sun was reviewed and approved* by the following committee members:

Yanming Wang
Associate Professor of Biochemistry and Molecular Biology
Dissertation Advisor

Zhi-Chun Lai
Professor of Biology
Professor of Biochemistry and Molecular Biology
Chair of Committee

Douglas R. Cavener
Professor and Verne M. Williaman Dean,
Eberly College of Science

Robert F. Paulson
Professor of Veterinary and Biomedical Sciences

Lu Bai
Assistant Professor of Biochemistry and Molecular Biology
Assistant Professor of Physics

Melissa Rolls
Associate Professor of Biochemistry and Molecular Biology
Chair of the Molecular, Cellular and Integrative Biosciences Graduate Program

*Signatures are on file in the Graduate School

ABSTRACT

In the beginning of the 21th century, Douglas Hanahan and Robert Weinberg published couple papers that discussed our understanding of cancer based on studies in the past decades. The authors discussed8 hallmarks of cancerthat define the tumor tissue. These hallmarks include, "*1) self-sufficiency in growth signals, 2) insensitivity to antigrowth signals, 3) evading apoptosis(lack of cell attrition mechanisms), 4) limitless replicative potential, 5) sustained angiogenesis, 6) tissue invasion and metastasis"*[1], *7) the reprogramming of energy metabolism, and 8) the evading immune destruction"*[2]. They also specified that the genome instability of cancer cells is the underlying mechanism that enables the hallmarks.The traits mentioned above provided a constitutive framework to understand the process of neoplasm. In this Ph.D. dissertation, I will report my exploration on cancer treatment regarding to two of the hallmarks—genomic instability and the invading immune destruction.

In one aspect of my Ph.D. study, I have explored the cellular mechanisms of a novel small molecule PZ1225, which intercalate into and distort DNA with a two-indole-ring structure. PZ1225 induced DNA damage results in apoptotic cell death in cancer. In addition, the molecule activates ER stress and UPR response, inhibits autophagy efflux, and activates MAPK signaling. Most importantly, I explored the function of the cell signaling pathways in mediating PZ1225 induced cell death. Using a combination of high through put analyses and cellular biology means, I developed a

combination treatment of PZ1225 and a MEK inhibitor U0126. The combination treatment induces apoptosis in cancer cells by more than 2 fold compared to PZ1225 alone and 5 fold compared to U0126 alone.

In another aspect, various immune cells grow in the cancer tissue and create a microenvironment benefiting the progression and metastasis of cancer. The extracellular traps formed by neutrophils have been reported to assist cancer metastasis. In my Ph.D. study, I also explored the function of macrophages in forming extracellular traps (ETs). Using the peritoneal macrophages extracted from PAD4 transgenic mice, I observed formation of extracellular traps by macrophages and histone hypercitrullination on the structure. In addition, I elucidated the requirement of the protein arginine deiminase 4 (PAD4) but not PAD2 in hypercitrullination of histones and ET formation.

Based on the findings that neutrophil extracellular traps play a role in multiple disease models, I also explored the effects of PAD4 on a mouse stroke model. In the Appendix chapter, I presented the preliminary data that suggest absence of PAD4 protects brain tissue, especially the neuron cells, from ischemia/reperfusion injuries.

TABLE OF CONTENTS

LIST OF FIGURES

LIST OF TABLES

LIST OF ABBREVIATIONS

CML	Chronic myelogenous leukemia
DDR	DNA damage response
HNPCC	Hereditary non-polyposis colon cancer
MMR	Mismatch repair
5-FU	5-Fluorouracil
ABC	ATP-binding cassette
MAPK	Mitogen-activated protein kinase
mTOR	mammalian target of rapamycin
PS	Phosphatidylserine
DC	Dendritic cells
UPR	Unfolded protein response
ER	Endoplasmic reticulum
ERAD	Endoplasmic reticulum-associated degradation
SEM	Scanning electron microscopy
TEM	Transmission electron microscopy
TUNEL	Terminal deoxynuleotidyl transferase (TdT) dUTP nick-end labeling
NETs	Neutrophil extracellular traps
METs	Macrophage extracellular traps
ETs	Extracellular traps
ETL	Extracellular traps-like
PAD	Protein arginine deiminase
PCM	Peritoneal cavity macrophage
LPS	Lipopolysaccharide

ACKNOWLEDGEMENTS

This thesis summarizes my work at Penn State University for my Ph. D study. There are so many people to thank for helping me during the last 5 years and a half.

First and foremost, I would like to express my sincere gratitude to my advisor, professor Yanming Wang, for the continuous support of my Ph. D study and for his patience, dedication and immense knowledge in the research. His guidance helped me in all time of research and in writing of this thesis. He has set an example for everyone in the lab on hard working, critical thinking, and keeping curiosity of the world. I feel especially grateful to his support for me to explore the research topics I have a great passion with, even at times when our ideas don't agree with each other. He has shown to me the spirit of science. I will try my best to carry on the same spirit and pass on the generosity in my journeys to come.

Besides my advisor, I would like to thank the rest of my thesis committee: Dr. Zhichun Lai, Dr. Douglas Cavener, Dr. Robert Paulson and Dr. Lu Bai. They have helped me in my research with great encouragement and insightful comments. Thank you to Dr. Zhi-chun Lai, who takes the responsibility to be my committee chair. I am honored to work with Dr. Douglas Cavener while rotating in his lab. I am grateful for Dr. Paulson's help whenever I stepped into his office with a question and Dr. Bai, who has a sharp mind in science and a big smile on the face.

My sincere thanks go to Dr. Na Xiong and Dr. Gong Chen, who provided insightful suggestions in the collaboration projects. Luming Zhao in Xiong lab generously shared reagents and invested time into the flow cytometry experiments. Yuting Bai in Chen lab has generously shared the murine models of Alzheimer's diseases.

My sincere thanks also go to professors Dr. Frank Pugh, Dr. Song Tan, Dr. Joseph Reese, Dr. David Gilmour, Dr. Shaun Mahony, and all the members

in the gene regulation center, for offering me research materials and thoughtful ideas on my research.

I want to thank all the members in Wang lab—the graduate students Dr. Jing Hu, Dr. Shu Wang, Dr. Xiangyun Chen, Lai Shi and the undergraduate students Luxin Pei, Sarah Moore, Jiayan Zhou, Lu Yang, Nicholas Schultheis and Alexander Radaoui. They have inspired me in research and helped me much more in life.

I would also like to thank Dr. Gregory Broussard and Dr. Ola Sodeinde for their instructions in teaching, and Melissa Long for her generous help and honest advice in career development.

Xiaoyu Zhu, Fan Wang, Chao Yan and my other pleasant friends at PSU are much appreciated. They have helped me greatly in my research and also shared with me the happy moments in my life and keep me accompanied during hard time.

Last but not least, I would like to thank my family, especially my mother Mrs. Yiping Sun and my husband Mr. Yuchen Chen. They have been my best friends as always, shown to me unconditional love and encouraged me to keep a positive attitude at all times. My love goes to them in the same way.

Chapter 1

Literature Review

1.1 Abstract

The use of chemotherapy in cancer treatment has a history of nearly half century. After many years of research into tumor development, chemotherapy is still one of the most effective and widely used methods to treat tumors. At the same time, our understanding of tumor progression and metastasis has been developed deeply. Until now, we have known that cancer is a genetic disease and systematic disease that incorporates multiple machineries for disease progression, such as the immune system, the circulation system, and the DNA damage repair system. Great complexity of the disease requires an integrative regimen in the treatment. Combinatorial treatment is one of the solutions to the complicated question. In addition, with more and more understanding in the microenvironment of the tumor tissues, especially the molecular mechanisms of immuno-oncology, future therapies are expected to target the great ecology of tumor tissue, instead of focusing on the tumor cells *per se*.

1.2 DNA-damage inducers as chemotherapy agents

1.2.1 Cancer is a genetic disease

Human endeavors to fight cancer have a history of more than 100 years[3]. But until now, cancer still ranks second as the leading cause of death right after heart disease. In the United States, American Cancer Society (ACS) reported an estimate of more than 1.6 million people to be newly diagnosed with cancer in the year of 2016[4]. Researchers have been spending a lot of effort trying to figure out the cause of cancer since the late nineteenth century. In the early time, cancer is considered caused by "changing in the environment", which is vague and provided little clue for cancer treatment. In 1890, David von Hansemann first described that cancer cells undergo aberrant mitosis[5]. The aberrant mitosis leads to change of chromatin content thus results in tumor. The idea was largely ignored until the beginning of the twentieth century when Theodor Boveri did a series of experiments, which led to the discovery of centrosome and the unequal distribution of chromosomes during mitosis[6]. Although most of the cells with incorrect separation of chromosome cannot survive, he proposed, cells that bypass the defect would potentially develop into tumor. This discovery laid the foundation for the current prevailing view that multitude of genetic and epigenetic changes in cells lead to tumor development. Later in the mid and late twentieth century, a series of discoveries made this view solid.

In 1960, the first case of chromosome translocation resulted tumor is reported by researchers at the University of Pennsylvania. Peter Nowell and David Hungerford found the *Philadelphia chromosome* in the autosome in chronic myelogenous leukemia (CML)[7]. Later, it was discovered that this abnormal chromosome contains a fusion gene that expresses a constantly active tyrosine kinase signaling protein. The similar chromosome translocation was observed in leukemia with abnormal expression of MYC gene in 1980s[8,9]. In accordance with the discovery of Philadelphia chromosome encoded protein, from 1970s to 1980s, Robert Weinberg, Michael Wigler and Mariano Barbacid discovered the first oncogene independently[10-13].The gene was later found to be *Ras* gene that is the cellular homolog of the *ras* genes from the sarcoma viruses. In addition, Weinberg and colleagues reported in the 1980s that oncogenes such as *MYC* and *Ras* or *MCL* and *MYC* collaboratively induce tumors. This discovery is in accordance with the work of Alfred Knudson in the 1970s, when he developed the Knudson model to demonstrate the proposition that multiple mutations are required for retinoblastoma development[14].

1.2.2 DNA damage responses are defective in fast-proliferating cancer cells

DNA damage is introduced to genome via physiological process such as DNA mismatch or DNA strand breaks during replication; or chemicals such as reactive oxygen species, which are produced as by-product in stress

response or respiration (Table 1-1). Environment also contains DNA damaging agents such as UV light and ionizing radiation. Although DNA damages are induced by different stimuli, normal cells have a set of DNA repair mechanisms, namely DNA damage response (DDR), to guarantee genome stability. The repair system consists of but not limited to mismatch repair, nucleotide excision repair, single stranded break repair and double-stranded break repair[3,15-18](Table 1-1).

In cancer cells, constant activation of oncogenes such as *MYC* and *Ras* promoted cell growth. However, fast proliferation of cancer cells created the pressure in DNA replication and DNA damage repair. Almost all of the cancer cells lack an intact DDR system[16]. The defects in DDR initially allow cancer cells to bypass the cell cycle checkpoints, promote the fast replication and lead to tumor development. For example, the genome of hereditary non-polyposis colon cancer (HNPCC) patient contains multiple mutations in the *MSH2* and *MLH1* genes, whose functions are required for mismatch repair (MMR)[19,20]. Defects in MMR in colon cells result in unrepaired mismatch and a phenotype known as microsatellite instability, which lead to cancer development together with multiple mutations that increase the genome instability[21,22].But as a double-sided sword, the defects in DDR also increase the frequency of DNA damage and result in the cancer cell relying heavily on the remaining DDR mechanisms. When DNA damage accumulates, it will trigger programed cell death such as apoptosis and autophagy and kill cancer

cell eventually. The defects in DDR make the cancer cells more susceptible to DNA damage agents thus create a therapeutic window for anti-cancer therapy.

Table 1-1. DNA damage inducers and repair mechanisms in mammalian cells.

DNA damage inducer	DNA damage	DNA Damage Repair Mechanism	Factors involved in the DDR
Radiation (X-ray), oxygen radicals, alkylating agents	Abnormal bases (Uracil), single strand break, abasic site	Base-excision repair (BER)	DNA glycosylase, AP endonuclease
UV irradiation, chemical mutagens (polycyclic aromatic, hydrocarbons)	Bulky adducts (6,4-photoproducts , Thymidine dimers)	Nucleotide-excision repair (NER)	Global Genomic NER (DNA damage binding and XPC-Rad23B complex, DDB1, DDB2, XPA); Transcription Coupled NER (RNA polymerase stall, CSA, CSB)
Radiation (X-ray), oxygen radicals, anti-tumor agents	Double-strand break, inter-strand break	Homologous recombination repair, non-homologous end joining	ATM, BRCA1, BRCA2, P53, RAD51, KU70, KU80, DNA-PKCs.
Replication errors	A-G/T-C mismatch, insertion and deletion	Mismatch repair	MLH1, MLH3, MSH2, MSH3, MSH4, MSH5, MSH6, PMS1, PMS2

1.2.3 DNA damage inducers are effective chemotherapy agents

DNA damaging reagents have a long history in anti-cancer chemotherapy. The first DNA damage inducer used for treating cancer dated back to the 1940s when Alfred Gilman and Louis Goodman were studying the victims of chemical weapon sulfur mustard gas. They found depleted bone marrow and reduced lymph nodes in the soldiers exposed to the gas[23]. Led by this discovery, they treated the late stage non-Hodgkins lymphoma patients with a more stable nitrogen mustard reagent tris β-chloroethyl amine and observed recession of tumors[24]. Later in 1949, Sidney Farber

reported stimulated proliferation of acute lymphoblastic leukemia cells by folic acid[25]. He and colleagues later designed folate analogs that block folic acid function and were able to briefly alleviate the tumor development[26]. In 1958, Li and colleagues designed another folate analog, methotrexate, which becomes the first reagent to cure a solid tumor[27]. Since then, DNA damage reagents have become widely used and effective candidates in cancer chemotherapy.

Many successful DNA damage inducers have been developed, including the DNA crosslinking reagent cisplatin, the DNA base analog reagent 5-fluorouracil (5-FU), the topoisomerase-DNA complex inhibit or etoposide and the multi-functional anthracycline drugs such as doxorubicin. Among them, cisplatin and doxorubicin (Fig. 1-1) are the most successful anti-cancer compounds and are still widely used today.

Cisplatin was discovered accidentally in 1965 by Barnett Rosenberg[28]. When Rosenberg was studying the division of E.coli, he chose platinum as the electrodes to create the magnetic field because they had “no biological activity”. In the experiment, they were excited to find E.coli cells stopped dividing when the magnetic field was on and restored dividing when it was off. In the following two years, Rosenberg and colleagues tried to untangle the mechanism behind it and finally realized that it was not the current but the platinum compound released from the electrodes changed the dividing

behavior of E.coli. Cisplatin, a small molecule that contains a platinum ion, was then discovered and approved by FDA for treatment of testicular and bladder cancers in 1978. Until now, cisplatin has been applied in the treatment of testicular cancer, cervical cancer, non-small cell lung cancer and the list is still expanding.

Daunorubicin is a multi-functional anthracycline antibiotic that targets DNA by multiple ways. It acts as a topoisomerase II inhibitor, a DNA intercalator and a free radical generator. It can also alkylate and crosslink DNA.It is discovered in an effort to isolate anti-tumor compounds from soil-based microbes. Daunorubicin was purified from a train of Streptomyces peucetius and shown a promising efficacy in clinical trials to treat acute leukemia and lymphoma. In the 1960s, doxorubicin is discovered as a substitute to daunorubicin in an effort to overcome the detrimental cardiac toxicity of the later[29,30]. Later on, more and more analogs to doxorubicin and daunorubicin were developed and belonged to the same anthracyclines family. Since then, more than 500 anthracycline molecules had been evaluated by National Cancer Institute (NCI) but no candidate shows a better efficacy in tumor inhibition than the original two. Doxorubicin has an efficacy towards a wide range of tumor types (more than 20 by far), including acute lymphoblastic/myeloblastic leukemia, breast cancer, bone sarcoma, gastric cancer, Hodgkin lymphoma, liver cancer, Wilm's tumor and so on.

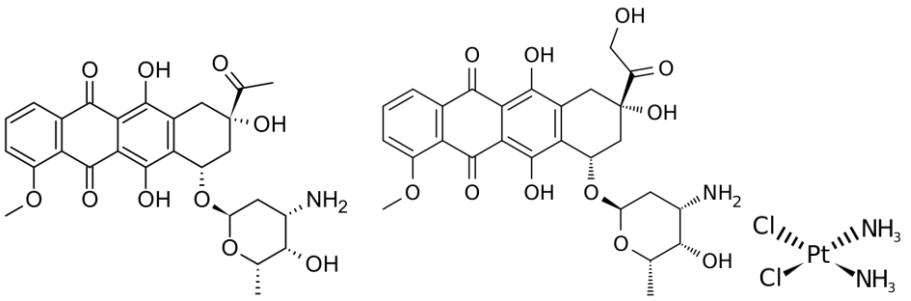

Figure 1-1. Structures of widely used chemotherapy agents. Daunorubicin (left), doxorubicin (middle) and cisplatin (right).

1.2.4 Limitation of DNA damage inducers as chemotherapy agents and possible solutions

Although the DNA damage inducers like cisplatin and doxorubicin shown significant efficacy in killing of cancer cells, the major limitations are drug resistance of tumor tissues and toxicity to healthy tissues.

Multiple mechanisms in the cancer cells lead to drug resistance. One of the chemo-resistance mechanisms exerts through multidrug resistance protein pumps in the cell membrane. The ATP-Binding Cassette (ABC) protein is the major family of proteins located in the cancer cell membrane that is responsible for multidrug resistance. This family of proteins is conserved in both eukaryotes and prokaryotes. In human genome, 48 functional ABC proteins are identified[31]. Among them, 3 proteins are well known and are reported to export chemotherapy reagents out of the cancer cell *in vivo*, namely P-glycoprotein, multidrug resistance-associated protein

1(MRP1) and mitoxantrone resistance protein 1 (MXR1)[32,33]. Although these proteins exhibit similar functions in chemotherapy drug efflux, they are quite different in their protein structures and targeted molecules.

Mutations in the cancer genome are another way for cancer cells to acquire drug resistance. The mutations happen in different levels include mutations that result in deficiency in cell death signaling pathways, mutations that lead to increased DNA repair, and mutations in the replication process that allows by-pass of DNA crosslinking sites. Moreover, mutations in the cancer genome are inheritable, which finally lead to development of a drug resistance tumor tissue. Mutations on p53 gene and MAPK signaling pathways are well known to be responsible for tumorigenesis[34,35]. In addition, both signaling pathways play a role in chemo-resistance[35-38]. p53 gene signals many cell fate deciding processes including apoptotic cell death, cell cycle arrest and cell senescence[39,40]. Disruption of p53 gene function may result in deficit in these processes and protect cancer cells from programmed cell death[39]. Ras in the MAPK signaling also plays a role in p53 activation[41]. At the same time, both p53 and MAPK signaling pathways are reported to inhibit the expression of ABC transporter protein[42,43]. Once mutated, these signaling pathways can no longer inhibit the expression of efflux proteins thus alleviate the effect of chemo-reagents. Most importantly, in cancer cells, mutations in these drug resistant pathways often happen concurrently.

Besides the mechanisms mentioned above, many other chemo-resistant mechanisms exist, such as inactivation of chemotherapy reagent and epithelial-mesenchymal transition. In addition, cancer cell heterogeneity contributes significantly to chemo-resistance. In the cancer cell population, a small fraction of cell is resistant to chemo-reagents and may also acquire stem cell properties. Thus the chemotherapy might be selecting the drug-resistant cells from the population and only able to kill the chemo-sensitive cancer cells[44,45].

Besides chemo-resistance, toxic side effects are another limitation of chemo-reagents. The toxicity mainly comes from the poor specificity of DNA damage reagents and is mostly dose-dependent. Normally, the toxicity affects fast proliferating cells the most. But in the case of cisplatin, proximal tubule cells in the kidney are significantly affected although they are quiescent cells[46,47], while doxorubicin mainly causes cardiotoxicity[48,49].

Research have put lots of effort to overcome the limitations of chemo-reagents while preserve their cell-killing efficacy. Although strategies to overcome drug resistance depend heavily on the specific type of tumors, some strategies are reported to be effective among many tumors, such as combination therapy[50,51]. The inhibitors in combination target different pathways the cancer cells rely on for proliferation. With combination therapy, we are able to achieve 1) higher efficacy of cancer cell killing 2) overcoming

the chemo-resistance; and 3) lowered toxicity to healthy tissues. For example, in melanoma, constant activation of kinases in the MAPK signaling pathway is always observed, and inhibitors are designed to target each kinase specifically (Fig. 1-2). However, a single inhibitor only recesses tumor growth for a short period of time and over time, melanoma cells acquire additional activation of candidate(s) in the MAPK kinase cascade to antagonize the inhibition effect[52,53]. Since melanoma cell proliferation depends heavily on the MAPK signaling, a combination therapy of MEK and BRAF inhibitors are designed to achieve a long-lasting inhibition effect[54,55]. In 2014, FDA approved the combination therapy of vemurafenib, a BRAF inhibitor, and cobimetinib, a MEK inhibitor, to treat advanced melanoma.

With the development in the biotechnology, nanotechnology is applied to the delivery of chemotherapy reagents in recent years. Delivery through nanoparticle achieved better specificity to tumor tissue compared with traditional chemotherapy[56]. As a result, chemotherapy agents packaged in nanoparticle could 1) kill chemo-resistant cancer cells or cancer stem cells and 2) decrease the toxicity to healthy tissues.

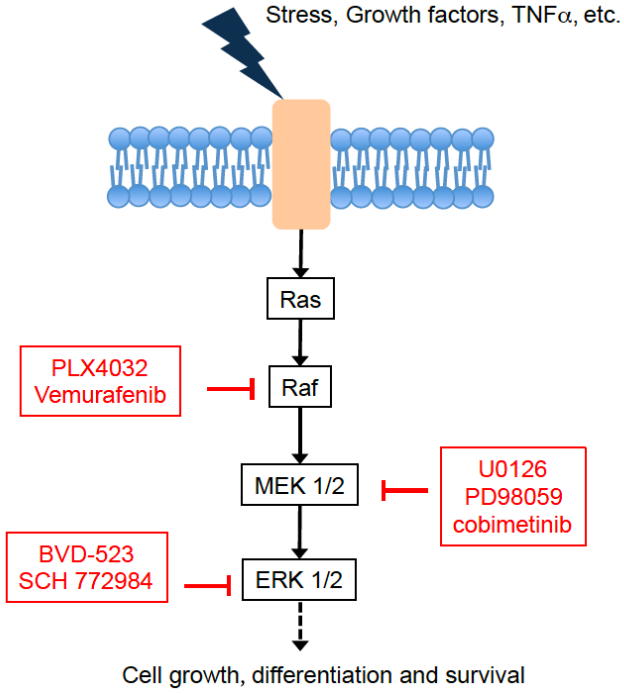

Figure 1-2. MAPK kinase cascade consists of Ras, Raf, MEK and ERK kinases. Mutations in MAPK kinases result in constant activation of the pathway. Inhibitors are designed to target the kinases specifically, including some of the mutated forms.

1.3 Cell Death or Survival Signaling Pathways in Cancer cells

DNA damage agents in chemotherapy induce a variety of DNA lesions in the cancer genome. The lesions lead to genomic mutations and when accumulate to a certain point, activate programmed cell death pathways in cancer cells including apoptosis, autophagy, necrosis, mitotic catastrophe, senescence and cell cycle arrest. Mutations in the programmed cell death pathways promoted tumor development, metastasis as well as cancer cellresistance to chemotherapy[14,15,20,36,57,58]. Thus, understanding the

molecular mechanisms of different cell death pathways is important for chemotherapy design and drug resistance study.

1.3.1 Apoptosis is an important pathway that programs tumor cell death in chemotherapy

Apoptosis is the most common pathway that is mutated in cancer cells and plays an important role in tumorigenesis as well as chemotherapy resistance[39,59,60]. Most of the chemotherapy agents induce DNA damage and program cancer cells towards apoptotic cell death. However, most of the tumor cells also have deficits in the apoptosis pathway and the mainreason of malignancy is the dysregulation of apoptosis, which results in imbalance between proliferation and cell death.

Apoptosis is firstly named by Kerr *et al* in the 1970s. At that time, people have observed the characteristic structure change during apoptosis and named it apoptosis aiming to separate the cell death process from necrosis[61,62]. In the early stage of apoptosis, nucleus undergoes condensation and fragmentation. During late apoptosis, cell membrane undergoes blebbing and finally loses its integrity. The signature morphological changes of apoptosis are important for distinguishing apoptosis from other cell death pathways[63].

Apoptosis is regulated through three major signaling pathways: the intrinsic pathways mediated through 1) mitochondria or 2) endoplasmic reticulum, and the extrinsic pathway mediated by 3) various death signals and the caspase protease cascade[64] (Figure 1-3).

The extrinsic pathway is activated by death signals such as tumor necrosis factor (TNF)[65,66] and executed by activation of pre-caspase 8 and the downstream cleavage of other caspases. The intrinsic mitochondrial pathway is triggered by stress signals such as excess level of calcium ion in the cytoplasm and oxidative stress. In mitochondria, the balance between two classes of genes, most of which belongs to the Bcl-2 protein family, is responsible for cell fate determination. One group of proteins is pro-apoptotic, including Bak, Bax, Bad, Bik and Bim. The other group is anti-apoptotic, including Bcl-2, Bcl-X_L and Mcl-1[67,68]. In addition, mitochondria release cytochrome c that activates caspase 3[69,70]. The intrinsic and extrinsic pathways converge at caspase 3 activation. Caspase 3 then mediates apoptosis by cleavage of key proteins such as poly (ADP-ribose) polymerase 1 (PARP-1), which is considered a hallmark of apoptosis[71]. Under physiological conditions, PARP-1 protein detects and aids in the repair of DNA damage. Under stressed conditions, however, cleavage of PARP-1 by caspase 3, or by caspase 7, promotes apoptosis. The cleavage produces two fragments of 89 kDa and 24 kDa respectively. The larger 89kDa fragment consists of a catalytic domain and is relocated from nucleus to cytosol. The

24 kDa domain, instead, irreversibly binds to the damaged DNA with its zinc-finger motif. The binding inhibits DNA damage repair and project cells to apoptosis[59,72,73].

Another hallmark of apoptosis is the H2A.X phosphorylated on serine 139 (γ-H2A.X)[74]. It is detected in apoptotic cells at the DNA damage site, especially at DNA double strand breaks[74]. Researchers have reported thatγ-H2A.X locates in the periphery nucleus area, which forms a "ring" structure under the microscope, inside the nuclear envelope and co-localized with TUNEL assay- labeled DNA damage sites[75].

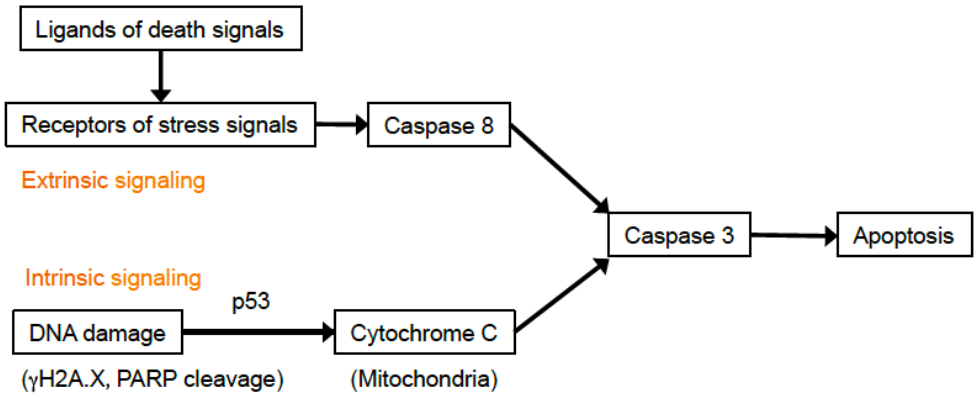

Figure 1-3. Intrinsic and extrinsic signaling pathways that induce apoptotic cell death in cancer cells. The intrinsic pathway is mediated through DNA damage and regulated by tumor repressor gene p53 and signaling pathways in mitochondria. The extrinsic pathway is triggered by death signals from extracellular space, mediated through stress signal receptors and caspase 8. Both pathways induced cleavage of caspase 3 and leads to apoptosis.

1.3.2 Regulation of autophagy in cancer cells

Autophagy pathway is vital for cells to maintain homeostasis under stressed conditions. It degrades wrongly folded proteins and cell organelles and recycles cell building blocks and energy. In cancer cells, fast proliferation creates stresses in protein folding, processing and transportation. Thus, the autophagy pathway is essential for cancer cell living and also promotes cancer cell survival in chemotherapy[76-78]. For example, mice without the ubiquitin-binding protein p62/SQSTM are protected from Ras-induced transformation and tumorigenesis of lung adenocarcinomas[79]. At the same time, disruption in autophagy pathway was found in nearly half of human breast, prostate and ovarian cancers[80]. The complicated role of autophagy in cancer cells needs a detailed evaluation in the design of chemotherapy.

Autophagy happens mainly in three steps. Firstly, double membrane structure enclosed wrongly folded protein or broken cellular organelles. The vesicle formed is called the autophagosome. LC3-II protein in the cell membrane is one of the hallmarks of autophagosomes[81,82]. Then autophagosomes merge with lysosomes, which provides a low pH environment for various enzyme reactions. Finally, debris is degraded in the fused structure called autophagolysosome and cellular building blocks such as amino acid recycle[83,84].

The initiation of autophagy is regulated by different stress response pathways such as ER stress and mammalian target of rapamycin (mTOR)[85-89]. It is reported that ER stress activation triggers autophagosome formation. The three proteins involved in ER stress response, namely PERK, IRE1 and ATF6 regulate autophagy in their unique ways[83,90,91]. The unfolded protein response induced by ER stress can also regulate autophagy by inhibiting mTOR signaling pathway[92-94]. TOR in yeast is firstly reported to be the target of the immunosuppressant rapamycin in 1991 and was thus named based on this connection[95]. In response to various signals *in vivo and in vitro*, such as serum starvation and cellular oxidative stress, mTOR pathway coordinates cellular metabolism and balances cell death and survival, including the autophagy pathway[90].Inhibition of mTOR by rapamycin dephosphorylates ULK1 at Serine 757 and Atg13 and results in the stimulation of autophagy.

In addition, genetic studies have identified a series of Atg genes required for healthy flow of autophagy, for example, Atg5, 12 and 16 form a complex that recruits LC3-II onto the autophagosome membrane and Atg7 and Atg3 are required for processing LC3 to produce LC3-II[96,97].Besides degradation happened in autophagolysosome, LC3-II binds to p62 and facilitate degradation of ubiquitinated protein aggregations[98,99].

1.3.3 Necrotic cell death is a well regulated cell death pathway in cancer

When cells undergo severe environmental changes that disrupt cell membrane integrity and die after that, we normally think the death is not well regulated but instead a passive and catastrophic process. So not surprisingly, necrosis is considered an accidental and unregulated form of cell death decades ago. Not until recently, scientists discovered the key regulators of necrosis such as kinase receptor-interacting serine/threonine-protein kinase 1 (RIP1) and TNF, FAS or TRAIL receptors[62,100-102]. These molecules regulate necrotic cell death in cancer cells, especially when apoptosis is defective and autophagy is suppressed at the same time[103].

Necrosis happens when cells are faced with harsh environmental changes such as extreme temperature and significant change in pH. Under the circumstances, cells firstly lose its membrane integrity. Unlike apoptosis where externalization of phosphatidylserine (PS) happens before cell break and cell content loss, necrotic cells cannot be recognized by phagocytes at the first place. As a result, necrosis triggers a series of immune response after the cell contents are released to the extracellular space. Hsp 70 is one of the molecules that are passively released when cell membrane breaks in necrotic cell death. Besides its role as a hallmark of necrosis, Hsp 70 signals immunogenicity by 1) interacting with other immune cells such as macrophage or dendritic cells (DC) and 2) stimulating antigen presentation to T lymphocytes and finally 3) activating immune responses[104]. The necrotic cancer cell promotes maturation of dendritic cell and their capability of

presenting antigens. Mature dendritic cells further stimulate $CD4^+$ and $CD8^+$ T cells that recognize cancer cells[105,106].

1.4 Immune system plays an important role in cancer development and cancer cells' response to chemotherapy

The cancer tissue consists of a various types of cells including the heterogeneous cancer cell population and a mixture of immune cells including T cells, neutrophil, macrophage, and dendritic cells. Cancer cells present antigens that can be recognized by host T cells and dendritic cells, which laid the foundation for immunologic targeting of cancer cells. The dynamic microenvironment of cancer cells affects cancer proliferation and development as well as their reaction to chemotherapy and radiotherapy[105].

1.4.1 The dynamic microenvironment in the tumor tissue affects chemotherapy efficiency

Many chemotherapy agents induce apoptotic cell death in cancer. Although apoptotic cells send out the "eat me" signal to macrophage by exposing PS, many apoptosis-inducing chemotherapy agents, such as mitomycin C and etoposide, show an immunosuppressive effect and do not induce immunogenic cell death. However, DNA damaging agents such as

anthracyclines and 5-FU stimulate anti-cancer immune responses in the tumor tissue.

As one of the most effective anthracycline agent, doxorubicin elicited immune responses have been well characterized in the last decades[107,108].In an experiment using a combination therapy of DNA damage agents—such as doxorubicin and cisplatin—and IL-12, mice survival is significantly prolonged in the combination treatment but not in the chemotherapy or IL-12 alone groups[72,109]. It is reported that anthracyclines elicit T-cell mediated immune response with chaperone protein calreticulin[72]. Calreticulin proteins are exposed to the cell surface to form the ecto-calreticulin during the early apoptotic stage. It is important for mediating dendritic cells to engulf the dying tumor cells. However, apoptosis induced by other chemotherapy agents do not normally present ecto-calreticulin in the cell membranes. Thus the calreticulin exposure is a hallmark for immunogenic cell death.

In another example, mice model have confirmed that 5-FU, a fluorepyrimidine DNA damage inducer, stimulates the uptake of tumor cells by DC and the antigen presentation to T cells as well as the expression of heat-shock proteins in immune cells[110,111].

In addition, DNA damage also induces expression of natural-killer group 2 member D (NKG2D) ligands in an ATM-/ATR-dependent manner on

the cell surface of tumor. NKG2D is a lectin-type activating receptor that is required by NK-cells mediated cell lysis[112].

1.4.2 PAD4 mediates tumor progression and metastasis via neutrophil extracellular traps formation

Extracellular traps formation is firstly reported in neutrophil (NETs) by Brinkmann and colleagues in 2004[113].It is reported as a suicide mechanism exempted by neutrophil to inhibit spread of bacteria in the circulating system (**Figure 1-4**). NETs structure contains different types of hydrolyses that kills invading bacteria or inhibit proliferation of bacteria. When NETs are produced, other immune cells will also be attracted to the infection site to aid the killing of microbes and clearance of remaining extracellular chromatin. Later on, other cells in the innate immune system such as macrophage, eosinophil and mast cell are also found to produce the similar extracellular traps-like structure[114,115].

NETs are made of decondensed chromatin and other components from the cell organelles like myeloperoxidase, neutrophil elastase *et al*[116]. Besides its function in the bacteria killing and trapping, NETs are found to be involved in multiple disease pathologies such as atherosclerosis, thrombosis and ischemic injuries[117-122]. Protein arginine deiminase 4 (PAD4) is the enzyme that cintrullinates histones at multiple site such as H1, H2A, H2B, H3

and H4[188-191]. Human genome contains 5 PADs, which are PAD1, 2, PAD4 knockout mice or PAD4 inhibitor were reported to alleviate disease pathologies of the above mentioned disease models[119]. The alleviation is largely due to the requirement of PAD4 in the process of NETs formation. Without PAD4, NETs are abolished and the clearance of NETs at the site of inflammation rescues disease phenotype[122,123]. The stimulation of NETs by microorganisms and inflammatory diseases were mediated by molecules such as bacterial products lipopolysaccharide (LPS) and phorbol myristate acetate (PMA)[113]. Calcium ion could also induce NETs formation by activating PAD4 activity[124,125]. In the disease pathology, cytokines and chemokines potentially primes neutrophil cells to produce extracellular traps[126].

Recently, NETs was found to exert facilitative functions in tumor development and metastasis. However, the molecular mechanism of the effect is poorly understood. Zychlinsky and colleagues (2013) reported existence of tumor-associated neutrophils (TANs) and NETs in the tumor tissue and hypothesized a positive role of Ewing sarcoma cells in promoting NETs formation and vice versa[127]. In another infection model in mice, Janothan Cools et al (2013) reported the trapping of circulating lung carcinoma cells by extracellular DNA snares. They also observed increased formation of hepatic metastatic burden at 2 weeks following injection of tumor cells[128]. Most recently, Samer Tohme from Allan Tsung group reported NETs in promoting metastasis after surgery in human patients[121]. In the

patients with metastatic colorectal cancer and perform of liver resection, higher level of NETs was found in the blood serum of the patients. They also observed a negative correlation between NETs formation and reduction in disease-free survival. The result is further confirmed in a murine model where accelerated metastasis of tumor is correlated with NETs formation. Administration of DNase I digestion of NETs or PAD4 inhibitor abrogated the promoting effect[121].

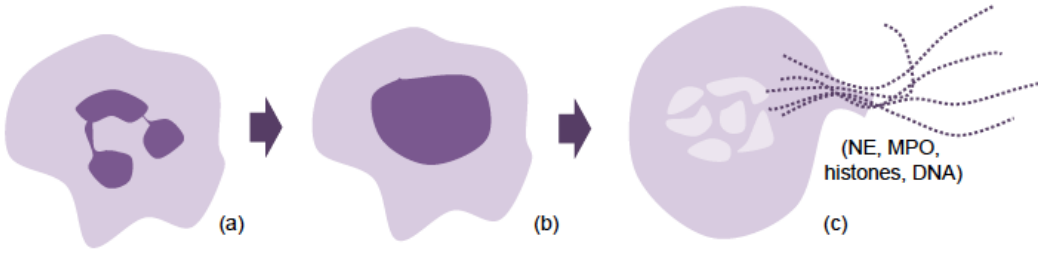

Figure 1-4. Netotic cell death in neutrophil results in release of decondensed chromatin into the extracellular space. (a) Neutrophil nucleus shows a signature lobular structure. (b) PAD4 activation, ROS, and hypercitrullinationon histones decondenses chromatin. (c) Decondensed chromatin released into extracellular space.

Chapter 2

Method and Materials

2.1 Mammalian Cell culture

2.1.1 Medium and culture conditions

Mammalian cells were cultured in DMEM medium (life technologies, 11965-084) supplemented with 10% FBS (Sigma, 12306C) and 1% penicillin-streptomycin (life technologies, 15140-122) in a 5% CO2 incubator at 37 °C.

2.1.2 Cell lines

Mammalian cancer cell lines used in the thesis work were obtained from ATCC. Cell lines includingU2OS, WM115, HacaT, 293T, HepG2, HL60, and MES-SA/Dx5, RAW 264.7 and J774A.1 were obtained from ATCC within the last five years and used at early passages stored within 6 month after the receipt of the original stock. NHF cells were a generous gift from Dr. Jiyue Zhu at Penn State University College of Medicine at Hershey. HCT116 $p53^{+/+}$ and $p53^{-/-}$ were a generous gift from Dr. Bert Vogelstein at Johns Hopkins University and obtained in 2008 and stored at early passages.

2.1.3 Cell splitting, Freezing and Recovery

DMEM medium was warmed under room temperature before use. Adherent cells in 10cm dish were rinsed briefly with DPBS (Invitrogen, 14190) and digested with 2ml 0.05% trypsin solution (Invitrogen, 11875) at 37°C for less than 5 min. Before harvest of cell, at least equal volume of DMEM medium was added to suspend cells. Cells were then harvested into 15ml Falcon centrifuge tubes (VWR 21008-918) and centrifuged at 1,000 rpm for 5 min under 4°C. At 1:4 to 1:10 ratio, cells were seeded into new plates with fresh DMEM medium. Floating cells were centrifuged and diluted to new plates without treatment of trypsin.

When confluent, cells were stored in 1.2 ml cryogenic vials (VWR 89094-810) after cell number counting that performed with a hemocytometer (Hausser Scientific, 1492). Medium used to store cells contained 50 % culture medium, 10 % DMSO and 40 % FBS.

For recovery, cells were quickly thawed under room temperature or using water bath. Melted cell solution was added into at least 9ml of fresh medium and centrifuged at 1,000 rpm under 4°C. After centrifuge, top medium was aspirated and cell pellet was re-suspended using fresh medium into a new culture dish. The next day, cell morphology was checked under

microscope and fresh medium was changed after 2-3 days of culture and cells were ready to use.

2.2 Primary Cell Extraction and Cell Culture

2.2.1 Mouse Embryonic Fibroblast

To obtain mouse embryonic fibroblast, mouse embryos in the age of 12.5 to 13.5 days were dissected from abdomen of pregnant female C57BL/6 mice. Embryos from one mouse were processed together. Mouse head and embryonic internal organ tissues were removed. The remaining embryonic tissues were rinsed with DPBS and transferred to a clean culture dish. Embryos were then minced with a sterile blade in 3-5 ml trypsin solution and incubated at 37°C. After 10 minutes, equal volume of MEF medium was added to inactivate the trypsin and the mixture was placed under room temperature allowing precipitation of undigested large pieces of tissue. The upper solution without large tissue pieces was centrifuged at 1000 x g at room temperature for 5 minutes. Cell pellet was then re-suspended in pre-warmed fresh MEF medium and cultured for 2-3 days until confluence.MEF cells were then used for experiment or stored in liquid nitrogen for future use.

2.2.2 Murine Macrophage

Mouse macrophages were extracted from wild-type or PAD4 transgenic mice in C57BL/6J background at the age of 6-10 weeks. After euthanasia, 5 ml 3% FBS (Gibco 10438026) in DPBS (Gibco 14190144) was injected into the mouse peritoneal cavity. Mouse belly was massaged for 2-3 minutes before retraction of the solution from the abdomen. Extracted cells were centrifuged at 1000 rpm for 5 minutes under 4°C, re-suspended in DMEM medium and cultured under 37°C. After 3-3.5 hours culture, floating cells were washed away with DPBS. Macrophage cells remained attached to the culture dish. The macrophage medium was DMEM medium containing 10% FBS and 1% Penicillin-Streptomycin (10,000U/ml, Gibco 15140122). Murine peritoneal macrophage cells were extracted and used freshly.

2.3 Analyses of RNA

2.3.1 RNA Extraction

Cells prepared for RNA extraction were pelleted and used for extraction immediately upon collection. RNA was extracted using the PureLink® RNA purification kit (Life Technologies 12183018A) following manufacture's instruction. Concentration of each RNA sample was measured with Nanodrop ND-100.

2.3.2 Reverse Transcription

1 μg of RNA was used for reverse transcription. Each reaction also contained 4 μg of 5 X qScript cDNA SuperMix (Quanta Biosciences, 95048) and complemented with RNase free water to 20 μl. The program for reverse transcription was 1) 5 min at 25°C, 2) 30 min at 42°C, 3) 5 min at 85°C, and 4) hold at 4°C. Then obtained cDNA solution is diluted by 50 fold and used for quantitative PCR measurement.

2.3.3 SYBR Green-based Real-Time quantitative PCR

6μl of the SYBR Green SuperMix (Quanta, 95055) for realtime PCR was used in the reaction mixture. The mixture also contained 4 μl of diluted cDNA template and 2 μl of Forward and Reverse primers. The reactions were run in the StepOne Plus Real-time PCR system from Applied Biosystems. The program ran at 95°C for 10 min followed by 40 cycles of program at 1) 95 °C for 15 sec and 2) 70°C for 15 sec. Data were collected automatically by the machine. Melting curve, amplification plot and other parameters were used to check primer quality and reliability of the data. The data were then exported from the StepOne Software and plotted in Excel.

2.3.4 Analysis of Microarray Data

U2OS cells were treated with 30 μM PZ1225 for 6 hr before harvesting. Control cells were mock treated with DMSO. Total RNA was purified with

Purelink®RNA mini kit (life technologies, 12183018A). The Affymetrix GeneChip Human Gene 1.0 ST arrays were used. Data from all Affymetrix GeneChips were normalized and analyzed as previously described[86]. Then genes shown more than 2 fold change were processed using MATLAB to produce heatmap and analyzed using IPA (Ingenuity System, www.ingenuity.com) core analysis to identify canonical pathways, upstream regulators, and establish networks. Realtime PCR was performed to confirm microarray results. Primer sets including:

SESN2 Forward 5”-AGAAGGTCCACGTGAACTTGCT-3”,

Reverse 5”-TCAGGTCATGTAGCGGGT GAT-3”;

DDIT3 Froward 5”-CGCCTGACCAGGGAAGTAGA-3”,

Reverse 5”- TCA TGC TTG GTG CAG ATT CAC -3”;

ATF4 Forward 5”-CAGTCCCTCCAACAACAGCAA-3”,

Reverse 5”- CCATTTTCTCCAACATCCAATCT-3”;

DDIT3 Forward 5”- CGCCTGACCAGGGAAGTAGA-3”,

Reverse 5”- TCATGCTTGGTGCAGATTCAC-3”

DDIT4 Forward 5”-CAC TCT GAG TTC ATC AGC AAA CG-3”,

Reverse 5”-ACGAGAAGCGGTCCCAAAG-3”;

PTEN Forward 5”-AAGGGACGAACTGGTGTAATG-3”,

Reverse 5”-GCCTCTGACTGGGAATAGTTAC-3”;

IL8 Forward 5”-ATACTCCAAACCTTTCCACCC-3”,

Reverse 5”-TCTGCACCCAGTTTTCCTTG-3”;

MCL1 Forward 5”-AAGGACAAAACGGGACTGG-3”,

Reverse 5”-ATATGCCAAACCAGCTCCTAC-3”;

ETV5 Forward 5”-CAGTTTGTCCCAGATTTTCAGTC-3”,

Reverse 5”-ATAGTTAGCACCAAGAGCCTG-3”;

EGR1 Forward 5”-TGTCACCAACTCCTTCAGC-3”,

Reverse 5”-TCCTGTCCTTTAAGTCTCTTGTG-3”;

FOSL1 Forward 5”-GGGCATGTTCCGAGACTTC-3”,

Reverse 5”-CTCATGGTGTTGATGCTTGG-3”;

MYC Forward 5”-TTCGGGTAGTGGAAAACCAG-3”,

Reverse 5”-AGTAGAAATACGGCTGCACC-3”.

Top canonical pathways were identified using IPA pathway analysis. Upstream regulators such as ATF4 and EIF2AK3 were confirmed with realtime PCR and western blot. Result shows target molecules of ATF4 in dataset and their expression changes were graphed. Network analyses visualized the gene networks based on the correlation of genes signaling UPR, MAPK and DNA damage responses. Moreover, medicines regulating similar group of genes were analyzed together with PZ1225. Inhibitors in the MAPK pathway antagonize PZ1225 over the same group of genes.

2.4 Analyses of Protein

2.4.1 Extract Protein from Whole Cell Lysate

Cells were collect from the culture dish by trypsinization and centrifuge (adherent cells), by direct centrifuge (floating cells) or by scraping in the cell lysis buffer in the culture dish (macrophage cells). Cells were lysed in RIPA buffer (10 mM Tris-Cl pH 8.0, 1 mM EDTA, 0.5 mM EGTA, 1% Triton X-100, 0.1% sodium deoxycholate, 0.1% SDS, 140 mM NaCl, before use, add proteinase inhibitor cocktail).

Protein solutions were further sheared by sonication using Bioruptor (Diagenode Inc.) in ice-cold dd$H_2O$for three times 10 minutes each. To get rid of cell debris, protein solution was centrifuged at maximum speed (~14,000 rpm) at 4°C for 10 min. Supernatant after spin was collect as protein sample for further analyses.

2.4.2 Running SDS-PAGE and Transferring onto Nitrocellulose Membrane

Proteins are denatured and loaded in SDS-PAGE and transferred onto nitrocellulose membrane using the Semi-dry transfer system (Amersham Biosciences TE 77 ECL Semi-Dry Transfer Unit) at constant current for 1 hour.

Recipe for SDS-PAGE (11 ml for three gels):

	8%	10%	12%	15%
Resolving Gel (ml)				
ddH_2O	3.8	3.1	2.35	1.25
30% Acrylamide/Bis-acrylamide solution	2.95	3.65	4.4	5.5
1 M Tris, pH 8.8	4.1			
10% SDS	0.1			
10% ammonium persulfate	0.06			
TEMED	6 μl			
Stacking Gel (ml)				
ddH_2O	0.665			
30% Acrylamide/Bis-acrylamide solution	3.62			
1 M Tris, pH 6.8	0.63			
10% SDS	0.05			
10% ammonium persulfate	0.05			
TEMED	5 μl			

2.4.3 Coomassie Blue Staining

After running SDS-PAGE, the protein gel was firstly fixed with fixation buffer (40% methanol, 10% acetic acid, diluted in ddH_2O) at RT for 15 min on a shaker. Then the gel was stained with Coomassie Blue R250 solution at RT for 15-30 min. Gel was then emerged in destaining buffer (10% methanol, 5% acetic acid, diluted in ddH_2O) at RT for O/N or heated in a microwave machine quickly to reveal protein bands on the gel. According to total

staining in each lane, the amount of protein sample was adjusted to reach an equal loading.

2.4.4 Western Blotting

After transferring of protein sample, the nitrocellulose membrane is quickly stained with Ponceau S solution (0.1% Ponceau S (w/v) in 5% acetic acid (w/v)) to reveal the equal loading of protein. Before continuing to western blot, membrane was rinsed with dd$H_2O$to wash away any Ponceau S staining.

The membranes were cut at appropriate size and position and blocked with 5% non-fat milk in TBST buffer (1 x TBS is diluted from 10 x TBS stocking solution (in 1L solution, dissolve 30g Tris.HCl, 80g NaCl, 2g KCl, adjust pH to 7.4 using HCl) supplied with 0.1% Tween 20) at RT for 10-30 min. Primary antibody was administrated in 5% non-fat milk in a sealed bag (tubular rollstock, item #TRS-95250-2) at 4°C for O/N on a rocker. On the second day, wash the membrane in TBST 10 min each for three times. Secondary antibody was then administered at 1:2000 dilutions as primary antibody. After 2-4 hours incubation, membranes were administered with final wash of 10 min each for three times, incubated with HRP western blot substrate (VisiGlo Select HRP Chemiluminescent Substrate Kit, 1B1583-KIT-100ml or Roche Lum-Light ^{PLUS} Western Blotting Substrate, 12015196001) and proceeded to expose in a dark room. Antibodies used in Western blot

were anti-PERK (cell signaling, 3192S), anti-ATF4 (Santa cruz, sc-200), anti-SESN2 (Abcam,ab57810), anti-DDIT3 (Santa cruz, sc7351), antip70S6K (Cell Signaling, 9202), anti-p70S6K-pT389 (Cell Signaling, 9205), anti-p70S6K-pT421(Cell Signaling, 9204S), anti-LC3B (Cell Signaling, 2275S), anti-p62/SQSTM1 (Bethyl Laboratories, A302-855A), anti-cleaved-PARP (Asp214) (Cell signaling, 9546), anti-eIF2α (Cell signaling, 2103), anti-eIF2α-pS51 (Cell signaling, 3398), anti-ERK pT202/204 (Cell Signaling, 4370S),anti-ERK (Cell Signaling, 9107S) anti-H2A.X pS139(Abcam, 39117), anti-H3cit 2,8,17 ()and anti-β-actin (Sigma, A1978) at appropriate dilutions.

2.5 Cell Death and Viability Assays

2.5.1 ATP-titer Assay

For viability assays, cells are seeded in 96-well plate at a concentration of 2000 cells/well, cultured for 24 hours before treatment. Cells are then treated with gradient anti-cancer drugs for 48 hours. Cell viability is evaluated with Promega CellTiter-Glo® Luminescent Cell Viability Assay (G7572) following manufacture's instruction.

2.5.2 TUNEL assay

TUNEL assay is used to analyze DNA double stranded break in the genome of cells treated with the target reagent(s). Cells were cultured on a

coverslip in the 6-well plate. After appropriate treatment was administered, coverslips are immersed in fixative solution (4 % paraformaldehyde in PBS) at 4°C for 25 minutes. 2 washes of PBS of 5 min each were administered and cells on the coverslip were then permeabilized with 0.2 % Triton X-100 in PBS for 5 minutes. After another two washes with PBS, cells were treated with equilibration buffer at room temperature for 5-10 min. Then 50 μl of TdT reaction mix was evenly distributed on the coverslips covering a small area such that the cells are not dried. Coverslips were then incubated at 37°C for 60 min in a humid chamber. Exposure to light should be avoided from this step forward. After wash with 2 X SSC and PBS, coverslips were stained quickly with Hoechst (1mg/ml, 1:1000) in PBS and mounted on the slide. Cells were then observed under the Axioskop 40 fluorescence microscope (Carl Zeiss, Inc.). DNA double stranded breaks will be seen under both GPF and RFP channels.

2.5.3 Measurement of Apoptosis

To measure apoptosis, mammalian cells are cultured and induced with certain reagents for apoptosis. Then cells trypsinized into single cell and collected and fixed with 70% ethanol and analyzed following the instruction of FITC Annexin V Apoptosis Detection Kit I (BD Pharmingen, 556547). In each sample, 1-5 X 10^5 cells are resuspended in 500 μl of 1 X Annexin V Binding Buffer. Then 5 μl Annexin V-Cy5 and 5 μl propidium iodide (PI) were

added in to the solution and incubated at room temperature for 5 min in the dark. Cells are then analyzed using flow cytometer (Beckman Coulter FC500) in the Penn State Flow Cytometry Center. Data are processed using the Flowjo software.

2.6 Cell Imaging

2.6.1 Live Cell Imaging of mCherry-GFP-LC3 Transfected Cells

U2OS cells were transfected with the mCherry-GFP-LC3B reporter plasmid. The transfection was performed using Lipofectamine 2000 (Invitrogen) in a 35 mm glass bottom dish according to the manufacturer's instructions. Cells were cultured for 12 hr after transfection, before the addition of PZ1225. After incubation with PZ1225 for 12 or 24 hr, the live cell imaging was done essentially as previously described[86]. The processing and analysis of images were done using Metamorph (Molecular Devices) and the NIH Image J software.

2.6.2 Immunohistochemistry and Fluorescent Microscopy

Mammalian cells are seeded on the coverslip in a 6-well plate, cultured until more than 80% confluence in the culture medium supplemented with FBS and antibiotics. Cells are stimulated as designed and fixed with 3.7% paraformaldehyde in PBS buffer containing 0.1% Triton X-

100 and 0.2% NP-40, pH 7.4. Coverslips with the fixed cells are rinsed with PBS twice blocked in 2% BSA in PBST for at least half hour at RT. Primary antibodies were diluted in 2% BSA and 5% normal goat serum in PBST and was performed in a humid chamber for overnight at 4°C. The second day, coverslips are washed with PBST 10 minutes each for three times. Cells were then stained with the appropriate secondary antibodies conjugated with Cy3, Alexa488 or Cy5 at 1:200 to 1:500 dilutions in a humid chamber for 1-2 hour at room temperature. Another round of PBST wash was administrated. Nuclear DNA was visualized by quick Hoechst staining at 1μg/ml (Sigma, 94403) in PBST for 15s-1min followed by a final wash with H_2O. Imaging was obtained using an Axioskop 40 fluorescence microscope (Carl Zeiss, Inc.) equipped with an AxioCam MRM camera and the AxioVision AC software. Images were later processed using the Adobe Photoshop program, Adobe Illustrator or the Image J program as appropriate.

To visualize the LC3B subcellular localization, U2OS cells stably expressing LC3 protein fused with GFP fluorescence were transfected with ER dsRED or RFP lamp1 plasmid. 12 hrs after transfection, cells were treated with 30 μM PZ1225 for 12 or 24 hr, and processed for immunostaining.

To investigate extracellular trap formation in peritoneal cavity macrophages, primary murine macrophage and macrophage cell lines RAW 264.7 and J774A.1 were treated with calcium ionophore (5μM), LPS (3-5

μg/ml), YW3-56 (5μM) or serum starvation (15-24h) for 3.5 hours or overnight and immunostaining was performed. Antibodies used in immunostaining includeα-HA (Sigma, H9658, mouse mAb, 1:200 dilution), α-H3Cit (Abcam, Ab5103, rabbit pAb,1:200 dilution), α –PAD4 (rabbit pAb, 1:200 dilution), F4/80 conjugated with Alexa 488 (Biolegend 123119, 1:200 dilution),α-H3cit26(rabbit pAb, 1:200 dilution), and secondary antibodies Cy™3 AffiniPure goat anti-rabbit IgG (H+L) (Jackson ImmunoResearch, 111-165-144) or Alexa Fluor® 488 goat anti-mouse IgG (H+L) (abcam, ab150113). DNA was stained with 1μg/ml Hoechst (Sigma, 94403).

2.6.3 Transmission Electron Microscopy

TEM samples were processed and imaged in the Penn State Electron Microscopy Facility. For transmission electronic microscopy (TEM) analyses, cells were treated as designed and 1) fixed in 2% glutaraldehyde in 0.1 M phosphate buffer (PB), pH 7.4 for 2-3 hours, 2) washed in 0.2 M phosphate buffer, 3) immersed in 1% osmium tetroxide in 0.1 M PB, 4) washed with distilled water for at least 5 times to remove any excess phosphate ion, 5) En bloc stained with 2% aqueous uranyl acetate (UA) for 2 hours at 4°C in dark, and 6) dehydrated with gradients of ethanol (25%, 50%, 70%, 85%, 95%, 100%) on ice. After dehydration, cell pellet was washed with propylene oxide twice and infiltrated with increased concentration of resin until samples are embedded in 100% resin. Samples were then sliced and imaged with FEI

Tecnai G2 Spirit BioTwin transmission electron microscope. Images were processed in Adobe Illustrator when necessary.

2.6.4 Scanning Electron Microscopy

SEM sample preparation and microscopy were performed at the Pennsylvania State University Microscope Facility. To visualize the METs structure, peritoneal cavity macrophages were extracted, cultured on the 18x18mm glass coverslip, and treated with calcium ionophore, LPS or serum starvation before SEM analysis. Cells were then fixed in 1% Glutaraldehyde (supplemented with 4% paraformaldehyde if necessary). Cells were then washed with OsO_4 in caco and dehydrated with gradients of ethanol (25%, 50%, 70%, 85%, 95%, 100%) on ice. Before imaging, the cells were dehydrated using the critical point dryer (Leica CPD300) and sputtered with Au/Pu for 180 seconds. Images were captured using the SEM scanning microscope (Zeiss Sigma RESEM) and processed in Adobe Illustrator.

2.7 Transfection

2.7.1 Transient Transfection of siRNA

Cells were cultured in 24-well cell culture plates (VWR 10062-896) using fresh medium supplemented with FBS but contained no antibiotics. When reached70-80 % confluence, cells were rinsed twice with transfection

medium (sc-36868) and ready for use. Transfection mixture contained solution A and solution B. Solution A contained 6-10 μl siRNA duplex and solution B contained 6-10 μl of siRNA transfection reagent (Santa Cruz sc-29528). Solution A and B were gently mixed together and sat at room temperature for 15-30 minutes. Then add the transfection mixture onto the cells drop by drop. After 6-8 hours incubation, add equal volume of fresh medium supplemented with 20% FBS and continue culture for 24-72 hours until ready for use.

WM115 cells were cultured in 24 well plates then transfected using the siRNA transfection reagent (Santa Cruz, sc-29528) per manufacturer's instructions. siRNAs used in the transient transfections were: control scrambled siRNA (Santa cruz, sc-37007) and ATF4 siRNA (Santa cruz, sc-35112). Following siRNA treatment for 24 hr, cells were treated with PZ1225. At 8 hr after PZ1225 treatment, qRT-PCR and Western blot were performed to analyze the effects of siATF4 on PZ1225 killing efficacy.

2.7.2 Transient Transfection of plasmid

Cells are culture in DMEM medium supplemented with 10% FBS and 1% Penicillin-Streptomycin in 6-well plate until 70-90% confluent. Before the day of transfection, replace fresh medium without antibiotics. On the day of transfection, 4 μg of plasmid DNA and 8 μl of lipofectamine 2000 reagent

(Life Technoloties 11668027) are diluted in 250 μl Opti-MEM medium (Life Technologies 31985-070)and incubated for 5min at RT. Then the two solutions were combined and incubated for another 20 minutes at RT and added drop by drop onto the cells. After 24 hours of incubation, cells are treated and processed for further analysis. Plasmids used in this thesis include pSG5-PAD4, pSG5-PAD4^{C645S}, pIRES-PAD2 and ER-dsRed.

2.7.3 Construct of Mammalian Cell Lines that Contain Inducible shRNA sequence in the genome

To construct cell lines with inducible expression of shRNA, the TRIPZ lentiviral inducible shRNAmir system was used. pTRIPZ vector contained ampicillin resistance for plasmid construction and purification, the shRNAmir for knockdown of the target gene, and the puromycin resistance for selection of successful incorporation of the plasmid in the genome of the mammalian cells. The expression of incorporated shRNAmir was designed to be inducible by doxycycline (Tet-On system). After construction, the pTRIPZ vector is transfected into HEK 293T cells using lipofectamine 2000 (life technologies) together with the trans-lentiviral packaging system (GE Healthcare Dharmacon kit, TLP5912). The lentiviral particles are then purified from the medium and transduced into target mammalian cell lines such as WM115 and U2OS cells by spin inoculation. After 48 hours of transduction, select transduced cells with puromycin for 3-10 days. Cell

morphology and proliferation are monitored until most of the transduced cells are selected by puromycin. Survived cells are induced by doxycycline to express the shRNA and knockdown of the target gene is tested by RNA and protein analyses. pTRIPZ shSESN2 vector used in Chapter 3 is designed and constructed in Wang lab.

2.8 Peptide Pull-down Experiment

2.8.1 Making of GST Fusion Protein

pGEX plasmids that contain GST-tagged gene cassette is transfected into *E.coli* BL21 strain and single colony was picked and cultured for 12-15 hours at 37°C with vigorous shaking. On the second day, the culture was diluted at 1:100 with fresh 2 X YT medium and grown at 20-30°C until A_{600}reach 0.6-0.8. IPTG was added into the culture to a final concentration of 0.1 mM and continued to culture for 4 hours. E. coli cells were then pelleted with centrifuge at 4°C, 7700 x g for 10 min. Samples were kept on ice from this step forward. Cell pellets were resuspended in 50 μl PBS per ml of cell culture and sonicated with Bioruptor (Diagenode Inc.) in ice-cold ddH_2O until cells were fully disrupted. Triton X-100 was then added into the cell suspension to a final concentration of 1 % and incubated on a rotor at 4°C for 30 min. Cell debris was excluded by centrifuge at maximum speed (12,000 x g) for 10 min at 4°C.The supernatant contained GST-tagged protein was incubated with Glutathione Agarose beads (Sigma G4510-5ml) for

purification purpose. GST-tagged proteins were then eluted from the glutathione beads and used for peptide pull-down assay.

2.8.2 Peptide Pull-down Assay

Peptide Pull-down Assay was performed as described before[129]. H3 peptides were conjugated with Biotin at C-terminal (ChinaPeptides Co., Ltd). About 10 μg of each peptide was incubated with the streptavidin beads (Pierce, 20349) then washed with IP buffer (10 mM Tris-HCl pH 8.0, 2 mM EDTA, 150mM NaCl, 0.2% Triton X-100, and 0.2% NP-40) supplemented with protease inhibitors cocktail. GST-tagged CBX2 or CBX7 protein is amplified in BL21 bacteria strain and purified with Glutathione beads. GST-tagged proteins are eluted from Glutathione beads before incubation. After incubation, the peptide-conjugated streptavidin beads were washed with IP buffer three times 10 min each. The beads was then boiled and processed for western blot analysis with anti-GST antibody (abm G018).

Chapter 3

Combinatorial treatment of PZ1225, a novel DNA intercalator, and U0126, a MEK kinase inhibitor, significantly induce apoptotic cell death in cancer cells

3.1 Abstract

DNA intercalating has been a widely adopted ideology in chemotherapy reagent design since the discovery of the first chemo-reagent to cure a solid tumor in 1958. However, toxic side effects of these reagents limit their application in the chemotherapy. To overcome this problem, we need to carefully examine cellular mechanisms of the compounds to balance the anti-cancer efficacy with their genomic toxicity and other side effects. Here we report a novel small molecule PZ1225, which intercalates into DNA double helix, distorts DNA and induces DNA double strand breaks. We studied the cellular mechanisms of PZ1225 and found it induces ER stress and unfolded protein response (UPR), inhibits autophagy efflux, and kills cancer cells via apoptosis. Interestingly, PZ1225 activates MAPK signaling pathway and p70S6K phosphorylation with prolonged treatment, suggesting a potential drug resistance mechanism that promotes cell survival. Based on the microarray analyses and mechanism studies, we proposed a combinatorial treatment of PZ1225 and the MEK 1/2 inhibitor U0126 that abolishes ERK and p70S6K phosphorylation. The double treatment

significantly induces DNA damaging signaling and apoptotic cell death in cancer cells but not in the non-tumorigenic cells. These results suggest PZ1225 or a combination of PZ1225 and U0126 as potential chemotherapy approaches. Moreover, in this study, we proposed the methodology to identify combinatorial chemotherapy reagents by incorporating high-throughput gene expression profiling and cellular mechanism analyses into the computing of a compound in relation with the upstream chemical inhibitors.

3.2 Introduction

According to the *Cancer Facts and Figures* published by American Cancer Society, in 2016, 1,685,210 people in the United State are estimated to be newly diagnosed with cancer and 595,690 lives are to be taken away by cancer[130].Human endeavors to fight cancer, the second leading cause of death, dated back to the ancient Greek age[131]. However, not until the mid 20th century did we realize cancer is a genetic disease. Genomic instability, including changes in chromosome numbers and insertion or deletion of nucleotides in the genome, is one of the major characteristics of cancer[16]. Unlike normal cells, cancerous cells replicate much faster but often lack an intricate DNA damage repair system, making them susceptible to DNA damage inducers such as DNA intercalators[132,133]. Efficient intercalators contain at least one planar polycyclic aromatic pharmacophore, and those

containing two to three indole rings are considered the most effectiveintercalators[134,135]. Intercalation results in distortion of DNA topology and impacts on DNA replication, transcription and repair, all of which lead to cell death in fast-proliferating cancer cells more efficiently than normal cells, thereby creating a therapeutic window. However, toxicity remains an obstacle for such reagent in treating tumors. For example, hair loss is a common side effect for chemotherapy reagents due to the fast proliferating nature of follicle cells. Besides hair loss, the side effects of the widely used chemotherapy reagent doxorubicin includes cardiotoxicity, fever and joint pain, which are not directly related to the proliferating rate of the cell[136]. To overcome these side effects, we need to carefully examine the cellular mechanisms of the compound and gain an in depth understanding of the crosstalk between pathways affected by these chemicals[137].

While mutations in crucial driver genes alter cell behavior and initiate tumor development, these mutations also affect response of cell to chemotherapy[138,139]. For example, activating mutations in the mitogen-activated protein kinase (MAPK) pathway are common in melanoma[140-142]. MAPK signaling pathway consists of a kinase cascade including MAPKKK/RAF, MAPKK/MEK and MAPK/ERK. The BRAF V600E mutation makes the gene constantly active, which promotes cell survival and contributes to drug resistance in treatment of cancer[139].Althoughthe inhibitors targeting the mutant activating kinases have made to clinical trials

and the drug market, their drug resistance and long-term therapeutic efficacy need further elucidation[52,143].

Besides genome instability, physiological stress in the endoplasmic reticulum (ER) is also important for cancer cell homeostasis[144]. When unfolded protein accumulates in ER lumen, the ER is stressed and activates unfolded protein response (UPR). UPR attenuates global protein translation, activates chaperon proteins aiding the protein folding, as well as other protective mechanisms, such as autophagy, that promotes cell proliferation and survival[145-147]. Activation of UPR leads to phosphorylation of PERK, alternative splicing of XBP1 and nuclear translocation of ATF6. These three branches of UPR together activate genes involved in ER stress alleviation[148].PERK is a kinase and sensor of the ER stress; upon activation, it auto-phosphorylates and activates eIF2α by phosphorylation. Activation of eIF2α attenuates the translation of most mRNAs, while selectively increases the translation of ATF4. ATF4 trans-locates into nucleus and serves as a transcription factor to activate specific stress response genes such as DDIT3 and SESN2[86,92]. UPR helps cells to cope with stress, while induces cell death when stress cannot be relieved.[73,85,149] In cancer cells, high proliferation rates require a high speed of protein folding, assembly and transport, which creates a pressure in the ER. Thus a mild, physiological UPR promotes proliferation in cancer cells[150]. Constant hypoxia, nutrient deprivation, DNA damage and other metabolic stress also contribute to elevated ER stress in

cancer cells[150]. In fact, it has been found that large solid tumor growth requires eIF2α phosphorylation by PERK[151].However, prolonged ER stress/UPR could potentially lead to cell death[150,152]. The importance of UPR in cancer cells makes it a potential therapeutic target. For instance, inhibitors against the ER-associated degradation (ERAD) process preferentially inhibit cancer cell growth[153].

ER stress affects downstream mammalian target of rapamycin (mTOR)[154] and autophagy signaling[94] to regulate cellular protein metabolism. Deregulation in mTOR signaling is associated with tumorigenesis, metastasis and chemotherapy resistance[155-157]. mTOR signaling is regulated by multiple pathways including but not limited to PI3K-Akt and MAPK pathways. It also plays a central role in regulating cell cycle progression[158], ribosome biogenesis[159], and autophagy[86]. Under physiological conditions, autophagy recycles misfolded proteins by engulfing and degradation with hydrolases in autophagolysosome to produce cellular components and energy[83,84]. Significant changes of autophagy efflux, either activation or inhibition, could both lead to cell death thus makes it a therapeutic target for cancer treatment[90,160].

In order to analyze the cellular effects of a novel DNA intercalator PZ1225, we performed a high-throughput microarray analyses and revealed a profile of genes affected by PZ1225. We found activation of UPR, altered

mTOR and autophagy pathways, and induction of apoptotic cell death in cancer cells upon treatment of PZ1225. Moreover, the upstream regulator analyses based on microarray data prompted us to develop a combinatorial treatment of PZ1225 with a MEK1/2 specific inhibitor U0126. The two molecules dramatically induced apoptotic cell death in cancer cells.

3.3 Results

3.3.1 PZ1225 is a novel small molecule that intercalates into DNA double helix and induces cell death in cancer cells

PZ1225 is a novel small molecule featuring two indole rings with a two-fold symmetry (Fig. 3-1A(a)) and acetoxygroup ([CH3-C(=O)-O-]) side chains. The two-indole-ring structure is reported to be among the most effective intercalators of DNA[135]. Like other indole-containing molecules, PZ1225 is capable of intercalating into the DNA double helix (Fig. 3-1A(b-d)). PZ1225 interacts with the nucleotides in the DNA double helix via hydrogen bonds and π-π interaction (Fig. 3-1A(d)). The intercalation increases distance of two adjacent nucleotides from 3.4 to5.7 Å (Fig. 3-1A(b)) thus distorting (Fig. 3-1A(b-c)) and ultimately breaking DNA, which potentially leads to apoptotic cell death[161].

To evaluate the efficacy of PZ1225 in killing cancer cells, an ATP titer assay was performed to measure the viability of cancer cells under gradient

PZ1225 treatment relative to control groups (Fig. 3-1B). The half maximal inhibitory concentration (IC_{50}) of PZ1225 in non-tumorigenic cell lines such as mouse embryonic fibroblasts (MEFs) and normal human fibroblasts (NHFs) was compared to that in cancerous cells including drug-resistant cancer cell line MES-SA/Dx5 and melanoma cell line WM115(Fig. 3-1B). IC_{50} of PZ1225 in cancer cells ranged from 8to 18μM while less than 20% non-tumorigenic cells died under the same treatment condition. The IC_{50}difference between cancerous cells and non-tumorigenic cells creates a therapeutic window for chemotherapy.

3.3.2 PZ1225 induces ER stress and UPR in cancer cells to mediate cell death

To fully evaluatePZ1225 as a chemotherapy reagent, we investigated the cellular mechanisms of PZ1225. For microarray analyses, osteosarcoma U2OS cells were treated with 30μM PZ1225 for 6 h. We identified 244 genes with more than 2-fold increase and 274 genes with more than 2-fold decrease in gene expression (Fig. 3-2A).The genes changed by more than 2-fold were analyzed based on the pathway. Out of 24 pathways significantly affected by PZ1225 (p-value <0.05) (Table 3-1), gene ratio involved in ER stress ranked the highest (Fig. 3-2B). Key genes in ER stress and UPR such as EIF2AK3 (PERK), XBP1 and DDIT3 increased by roughly 5 folds, 3 folds and 43 folds, respectively (Fig. 3-2C-E).

Following the lead of microarray analyses, we further analyzed the expression of genes involved in ER stress and UPR (Fig. 3-3A). At 6 h after PZ1225 treatment, stress response genes ATF4, SESN2 and DDIT3 were upregulated at the mRNA level detected by RT-qPCR (Fig. 3-3B).Activation of PERK mediated UPR was analyzed with Western blot. After PZ1225 treatment, we detected PERK phosphorylation indicated by an up-shift of the protein band, eIF2α phosphorylation and increased amounts of ATF4, SESN2 and DDIT3 proteins (Fig. 3-3C). XBP1 alternative splicing was also detected following the method described previously[162] (Fig. 3-3I). These results suggest PZ1225 activates UPR in the cancer cells.

Since stressed ER presents a swelling or fragmented morphology[163,164], we also analyzed morphology changes of ER. ER membrane was labeled with an ER targeting sequence fused with a red fluorescence protein. In control cells, a well-organized ER lumen structure was observed; while after PZ1225 treatment, ER becomes swelled and fragmented; supporting ER stress is induced by PZ1225 (Fig. 3-3D).

The role of ER stress and the unfolded protein response in cell fate determination is not clear. Physiological UPR facilitates cancer cells to cope with multiple growth stresses and when the ER stress prolongs, UPR can also commit cells to apoptosis. To evaluate the role of UPR in PZ1225 mediated cell death, we investigated the transcription factor ATF4 that is activated by

PZ1225. ATF4 siRNA was transfected into cancer cells to interfere with ATF4 expression and cell viability was evaluated. Along with a decrease in ATF4 protein level, pro-apoptotic factorDDIT3 and DNA damage marker PARP cleavage were inhibited (Fig. 3-3E). In the cell viability assay, cell survival rate increased by ~2 fold after ATF4 knockdown (Fig. 3-3F). Since ATF4 has been reported to regulate the expression of SESN2 and downstream mTOR signaling (illustrated in Fig. 3-4A) [92,93], the effects of SESN2 in cell death was evaluated in a cell line that expresses SESN2 shRNA upon doxycycline induction. In the cells that express SESN2 shRNA, DNA damage marker γH2A.X decreased concurrently with the inhibition of SESN2 (Fig. 3-3G). Similarly with ATF4 knockdown, cell survival rate was increased ~2 fold in SESN2 shRNA treated cells than control cells upon treatment of PZ1225 (Fig. 3-3H). These results suggest that PZ1225 mediated cell death requires ATF4 and SESN2 activity thus UPR plays a pro-apoptotic role after PZ1225 treatment. Notably, cancer cells with siATF4 or shSESN2 did not grow as well as control groups (Fig. 3-3F & H), indicating a pro-survival role of UPR under physiological conditions.

3.3.3 PZ1225 inhibits mTOR signaling and autophagy in cancer cells

It has been reported that ER stress induced SESN2 expression inhibits mammalian target of rapamycin (mTOR)[86,92,93]. mTOR signaling is at the hub of multiple pathways that converges cell survival and proliferation signaling,

such as autophagy pathway[88] (Fig. 3-4A). At the early stage of autophagy, ER membrane could potentially participate in the membrane isolation process to formautophagosomes[165]. In melanoma WM115 cells, we observed typical autophagic vesicles with double membrane structures over 200nm in diameter enclosing cellular components by Transmission Electron Microscopy (TEM)[166](Fig. 3-4B), suggesting accumulation of autophagic vesicles in these cells. However, accumulation of membrane bound LC3-II protein was detected by Western blot (Fig. 3-4C), suggesting inhibition of autophagy[167]. Interestingly, the amount of p62/SQSTM1, a marker for autophagy protein turnover, was not increased (Fig. 3-4C).

To study how PZ1225 affects autophagy, we studied the process at multiple steps including autophagosome formation and fusing of autophagosome and lysosome. The formation of autophagosome was observed by transfecting the ER-dsRED plasmid into U2OS cells that stably express GFP fused LC3 protein. Live cell imaging was then performed using fluorescent microscope. In control cells, a continuous intact ER lumen structure was observed (Fig. 3-4D).Moderate GFP-LC3 signals indicate autophagy happened at basal level and normal turnover rate(Fig. 3-4D). In contrast, PZ1225 treatment elevated GFP-LC3 signal significantly (Fig. 3-4D). At the same time, swelled and fragmented ER labeled by ER-dsRED co-localized with GFP-LC3, indicating that ER membrane was incorporated into the autophagosome membrane(Fig. 3-4D). To observe autophagolysosome

fusion, a tandem GFP_mcherry_LC3 plasmid was used to indicate pH in the autophagic vesicles (Fig. 3-4E). After fusion of autophagosomes with lysosomes, acidic pH in autophagolysosomes quenches the GFP signal and only red fluorescence signals are detected (Fig. 3-4E). In control cells, we observed a moderate amount of autophagolysosomes indicated with red puncta (Fig. 3-4F). After PZ1225 treatment, however, the occurrence of predominant yellow puncta indicated inhibition of autophagolysosome formation (Fig. 3-4F). These results suggest that PZ1225 inhibits the autophagy efflux at the later steps.

In another aspect, mTOR signaling phosphorylates p70S6K at threonine 389 and 421[168]. p70S6K further phosphorylates S6 ribosomal protein and promotes protein synthesis (Fig. 3-4A). To investigate how PZ1225 affects mTOR signaling and cell growth, we examined p70S6K phosphorylation. At 6 h after PZ1225 treatment, p70S6K phosphorylation decreased along with induction of SESN2 and mTOR inhibition (Fig. 3-4G). To our surprise, after 12 h treatment, the level of p70S6K phosphorylation restored even though SESN2 induction persisted and the p70S6K protein level dropped dramatically (Fig. 3-4G). The discrepancy between p70S6K phosphorylation at the early and later time points led us to consider other kinases/signaling pathways involved in p70S6K phosphorylation.

3.3.4 PZ1225 activates ERK1/2at 12 h and MEK inhibitor U0126 and PZ1225 induced apoptosis synergistically

To analyze possible signals inducing p70S6K phosphorylation after prolonged PZ1225 treatment, we analyzed the correlation between the gene expression profile of PZ1225and that of other inhibitors using the IPA program (Fig. 3-5A). Notably, the strong positive correlation of PZ1225 to ER stress inducer thapsigargin supported our findings about the ER stress induction (Fig. 3-5A). Interestingly, PZ1225 exhibited a significant opposite effect with PI3K-MAPK inhibitors LY294002, PD98059 and U0126 on the expression of the same group of genes (Fig. 3-5A-B, Table3-2 &3-3). The effect of PZ1225 and U0126 on the expression of these genes was further analyzed by RT-qPCR in WM115 cells and we found that the expression of IL8, MCL1, ETV5, EGR1, FOSL1 and MYC genes was induced by PZ1225 but suppressed by U0126 (Fig. 3-5C). To test the effect ofPZ1225 on MEK1/2 kinase activity, we analyzed ERK1/2 phosphorylation by Western blot. As the target protein of MEK 1/2, ERK 1/2 phosphorylation was significantly induced at 12 h after PZ1225 treatment but not at the 6 h time point(Fig. 3-5D), suggesting that PZ1225 activates the MAPK signaling pathway under prolonged treatment conditions. To test if the MAPK kinases are involved in p70S6K phosphorylation, we further analyzed a MEK1/2 inhibitor U0126 together with PZ1225. After treatment with PZ1225 and U0126 for 12 hours, both ERK1/2 and p70S6K phosphorylation were inhibited (Fig. 3-5E). Note

that the p70S6K backbone protein was degraded to an undetectable level (Fig. 3-5E). At the same time, DNA damage markers such as cleaved PARP and γH2A.Xwere dramatically induced (Fig. 3-5F). These results suggest the MAPK signaling pathway is involved in the recovery of p70S6K phosphorylation at the 12 h time point after PZ1225 treatment.

3.3.5 U0126 and PZ1225 inhibit MEK kinase activity and induce apoptotic cell death in cancer cells

The effect of PZ1225 and U0126 in the inhibition of p70s6K phosphorylation prompted us to explore if these two compounds exert synergistic effects in cancer cell killing. The $IC_{50}$was analyzed in WM115 cells with U0126 and/or PZ1225 (Fig. 3-6A-B). The synergistic effect of U0126 and PZ1225 was plotted using an isobologram as described previously by Loewe[169]. The IC_{50} of the combinatorial treatment ((3,3) μM) located within the linear isobole of additivity (Fig. 3-6A-B), suggesting a synergistic effect. To further explore mechanisms of the synergistic inhibition, we measured DNA double strand break with TUNEL assay after 24 h of PZ1225 treatment (Fig. 3-6D). U0126 didn't induce DNA double strand break. In contrast, combinatorial treatment of PZ1225 and U0126 induced 9 folds more DNA double strand break compared to U0126 alone (Fig. 3-6D). Following this lead, we measured apoptosis in WM115 cells (Fig. 3-6C). Compared to U0126 alone, combinatorial treatment significantly increased percentage of early

apoptotic cells (PI negative and annexin V positive) from 9.9% to 36.5% and dead cells (PI and annexin V double positive) from 3.3% to 25.2%. These findings indicate an increase in cell killing efficiency by activation of apoptosis in U0126 and PZ1225 double treated cells. We further evaluated the toxicity of the combinatorial treatmentinWM115 cells and normal human fibroblasts (NHFs) in parallel. After treatment for 15 h with PZ1225 and U0126 at 20μM concentration, only 10% WM115 cells survived but more than 80% of NHF cells remained alive (Fig. 3-6E). Western blot analyses detected PARP cleavage and γH2A.Xin WM115 cells but not in NHF cells (Fig. 3-6F). These results indicate PZ1225 and U0126 in combination makes a promising chemotherapy strategy by inducing DNA damage and cell death particularly in cancer cells.

3.4 Discussion

Overall, our study revealed the cellular mechanisms of the novel DNA intercalator PZ1225 (Fig. 3-7). PZ1225 induces ER stress, activates UPR and prohibits autophagy efflux and finally results in apoptotic cell death in cancer cells. The induction of MAPK pathway after prolonged treatment restores the p70S6K phosphorylation, indicating a crosstalk between the MAPK kinase pathway and the mTOR signaling pathway. The restoration of p70S6K phosphorylation suggests the cells could bypass the programmed cell death by stimulating protein synthesis and cell survival at the late time point after

PZ1225 treatment. As such, MAPK likely serves as a drug resistant signaling pathway in PZ1225 treated cells. Previously, it has been reported that doxorubicin induces MAPK signaling pathway transiently before cell death and the inhibition of the kinases impairs doxorubicin induced apoptosis[170]. In contrast, inhibition of MEK1/2 promotes PZ1225 induced apoptosis. How PZ1225 activates MAPK signaling pathway under prolonged treatment condition remains an open question.

WM115 is a human melanoma cell line that harbors a $BRAF^{V600E}$ mutation. This BRAF point mutation results in constant activation of the MAPK signaling pathway and contributes to tumorigenesis[34].The $BRAF^{V600E}$ mutation also plays a role in the chemotherapy resistance[139]. Inhibition of its downstream kinase MEK1/2 by U0126 is not sufficient to induce significant cell death.

To design a more effective chemotherapy with less toxicity, understanding of the cellular mechanisms is vital. In this study, we untangled the mechanisms of cell death induced by PZ1225 by revealing its effect on several major stress/chemotherapy-responsive pathways. Most importantly, the microarray analysis reveals possible cell signaling that might promote cell survival. Combination of the cellular biology and high-throughput analyses of genes provided the information needed to design a better chemotherapy strategy. Based on the information retrieved, we designed a combination treatment of PZ1225 and U0126.Compared to inhibiting MEK alone or PZ1225 alone, the combination treatment presented a synergistic

effect in cancer cell killing and significantly increased apoptotic cell death. The synergistic effect of PZ1225 and U0126 allows lower dose of each drug to achieve a significant killing, thereby decreasing the toxic side effects.

Future endeavors to study the efficacy of PZ1225 shall include the *in vivo* mouse xenograft model. Based on the *in vitro* studies, we need to focus on the evaluation of toxicity and side effects *in vivo*, such as cardio-toxicity and liver toxicity.

Figure 3-1.

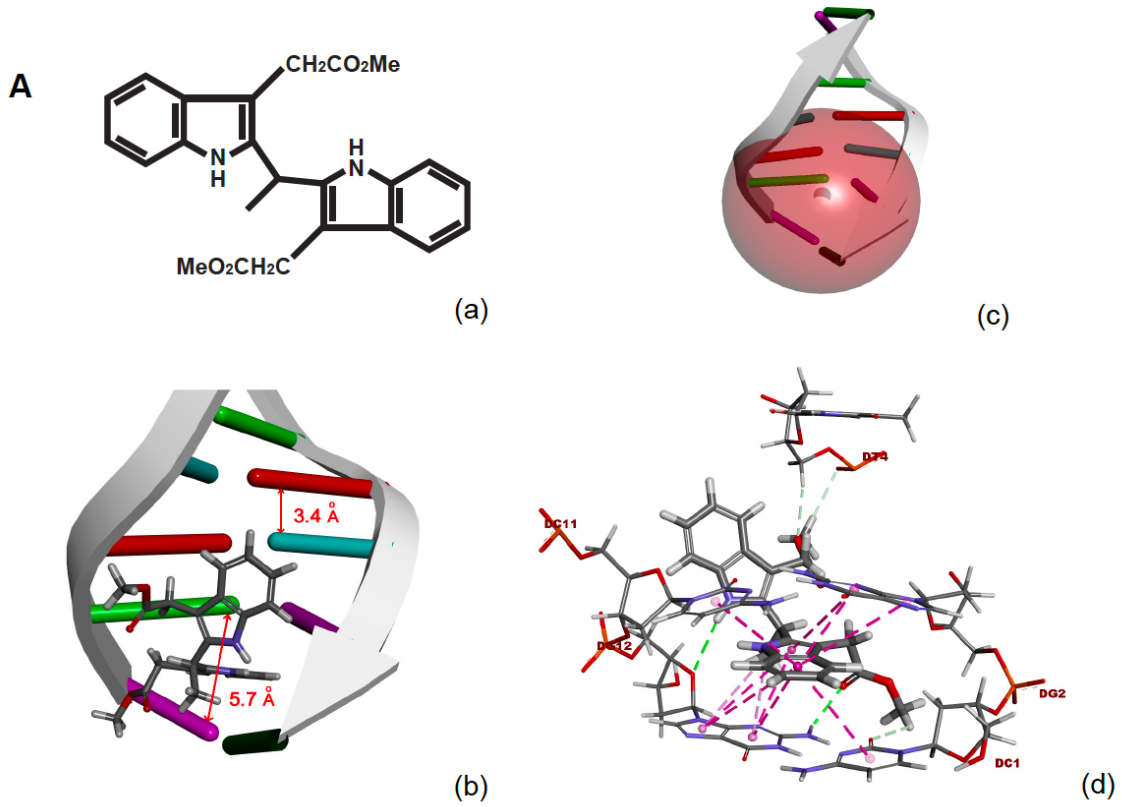

B

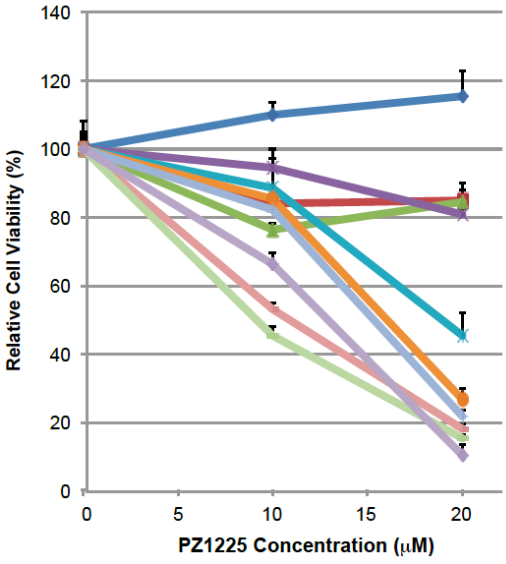

	IC_{50}	Cell line
NHF	N/A	Normal human fibroblast
HacaT	N/A	Immortal human keratinocyte
293T	N/A	Embryonic kidney cell
MEF	N/A	Mouse embryonic fibroblast
WM115	18μM	Melanoma
HepG2	16μM	Liver carcinoma
HL60	15μM	Promyelocytic leukemia
HCT116 p53-/-	10μM	Colon carcinoma
HCT116 p53+/+	8μM	Colon carcinoma
MES-SA/DX5	13μM	Multidrug-resistant sarcoma

Figure **3-1.** PZ1225 is a DNA intercalator that preferentially inhibits cancer cell growth over non-tumorigenic cells.

PZ1225 is a small molecule consist of two indole rings in a 2-fold symmetry structure (A (a)); the indole ring structure enables it to interact with nucleotide acid, intercalate into the DNA double helix and distort DNA double helix (A (b-d)). A cell viability assay measuring ATP level in the cell was used to evaluate killing efficacy of PZ1225 in different cancer cell lines. PZ1225 shows an inhibitory effect to cancer cells selectively (B). IC_{50} of non-tumorigenic and primary cell lines such as NHF is greater than 40 μM (the highest concentration tested). However, in tumor cell lines including multi-drug resistant MES-SA/Dx5 and WM115 $BRAF^{V600E}$ cells, IC_{50} is much lower.

Figure 3-2.

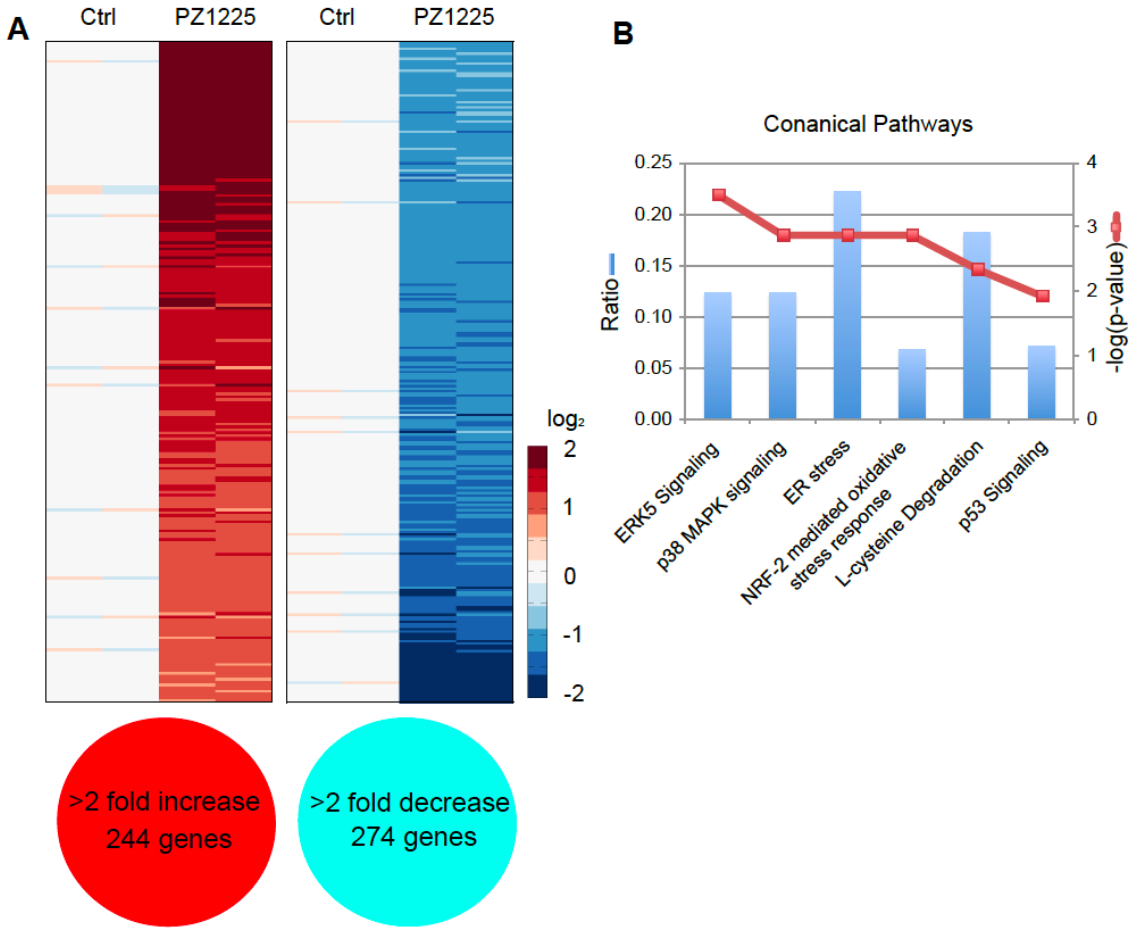

C

Canonical Pathway	Genes (fold of induction)
Unfolded protein response/ ER stress	DDIT3(42.75), DNAJB9(12.36), ERO1LB(11.98), EIF2AK3(5.16), PPP1R15A(5.34), XBP1(2.93), CEBPB(3.22), CEBPG(2.95), INSIG1(2.31), SEL1L(2.23), HSPA6(3.43), DNAJC3(3.71), HSPA5(3.65), SYVN1(2.72)
ERK5 Signaling	FOS(13.93), RPS6KA5(2.38), CREB5(2.26), NGF(2.67), FOSL1(2.58), MEF2C(2.14), MEF2A(2.19)
p38 MAPK Signaling	DUSP10(2.83), RPS6KA5(2.38), MYC(2.10), DUSP1(2.29), CREB5(2.26), IL1A(17.12), TIFA(2.01), MEF2C(2.14), MEF2A(2.19)
NRF2-mediated Oxidative Stress Response	SQSTM1(2.76), DNAJC10(2.01), BACH1(2.10), HMOX1(4.20), MAFF(3.89), FOS(13.93), SOD2(2.06), DNAJC3(3.71), FOSL1(2.58), HERPUD1(4.20)
p53 Signaling	JMY(2.20), CDKN1A(2.02), GADD45A(3.02), HDAC9(5.26), PMAIP1(3.86), SIRT1(2.35), TNFRSF10B(3.25)

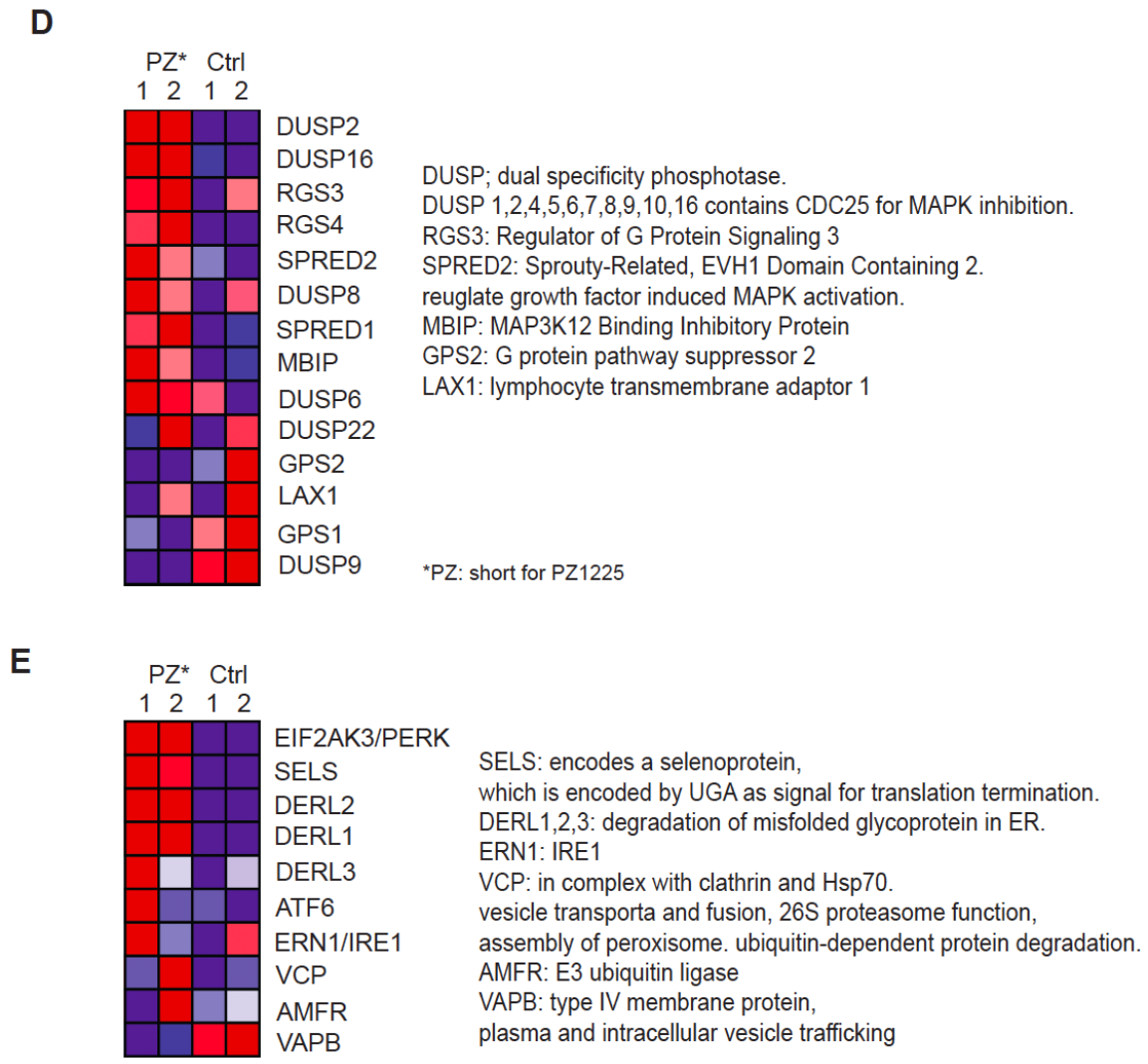

Figure **3-2.** Microarray analysis reveals genes affected by PZ1225.

PZ1225 affects cancer cell transcriptome significantly. Transcription of 518 genes is altered by more than 2 fold, with 244 genes activated by PZ1225 and 274 genes inhibited (A). PZ1225 affected genes belong to different stress response pathways, including ER stress response and MAPK signaling (analyzed with IPA-ingenuity program in B). Genes in ER stress/UPR signaling such as DDIT3 and EIF2AK3, in MAPK signaling such as DUSP10 and FOSL1 and in autophagy such as SQSTM1 are induced by PZ1225 (shown in C). Heatmaps shown genes in the MAPK signaling and unfolded responses were significantly affected by PZ1225 (D-E).

Figure 3-3.

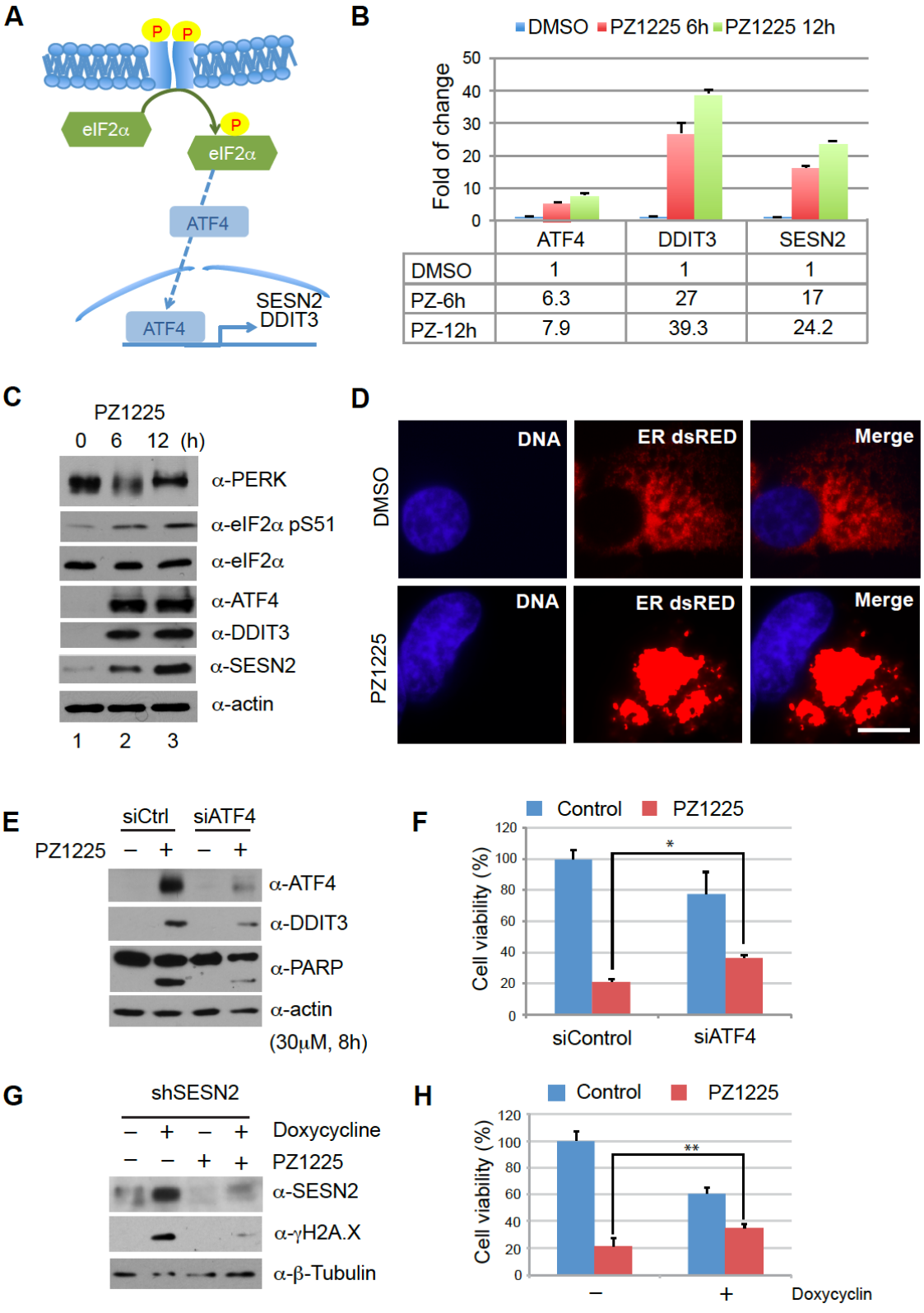
A
P
P
eIF2α
P
eIF2α
ATF4
ATF4
SESN2
DDIT3
B
DMSO
PZ1225 6h
PZ1225 12h
Fold of change
50
40
30
20
10
0
ATF4
DDIT3
SESN2
DMSO 1 1 1
PZ-6h 6.3 27 17
PZ-12h 7.9 39.3 24.2
C
PZ1225
0 6 12 (h)
α-PERK
α-eIF2α pS51
α-eIF2α
α-ATF4
α-DDIT3
α-SESN2
α-actin
1 2 3
D
DMSO
PZ1225
DNA
ER dsRED
Merge
E
siCtrl
siATF4
PZ1225 – + – +
α-ATF4
α-DDIT3
α-PARP
α-actin
(30μM, 8h)
F
Control
PZ1225
Cell viability (%)
120
100
80
60
40
20
0
*
siControl
siATF4
G
shSESN2
– + – + Doxycycline
– – + + PZ1225
α-SESN2
α-γH2A.X
α-β-Tubulin
H
Control
PZ1225
Cell viability (%)
120
100
80
60
40
20
0
**
–
+
Doxycyclin

I

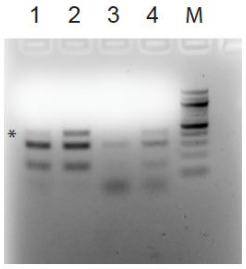

Figure**3-3.** PZ1225 molecules induce ER stress response in cancer cells.

A model figure of ER stress signaling pathway includes auto-phosphorylation of PERK, activation of eIF2α and ATF4. Transcription factor ATF4 further activates stress response genes such as DDIT3 and SESN2 (A). Induction of genes in the ER stress signaling is confirmed on reverse transcription real time PCR analyses (B) and Western blot (C). Morphology of ER swelling and fragmentation was observed by labeling ER with ER-dsRED (D). ATF4 knockdown affects expression of DDIT3, PARP cleavage (E), and cell viability (F).XBP1 splicing was observed following the protocol described previously. The band highlighted by star denotes XBP1 alternative splicing (I). Scale bar, 10 μm.

Figure 3-4.

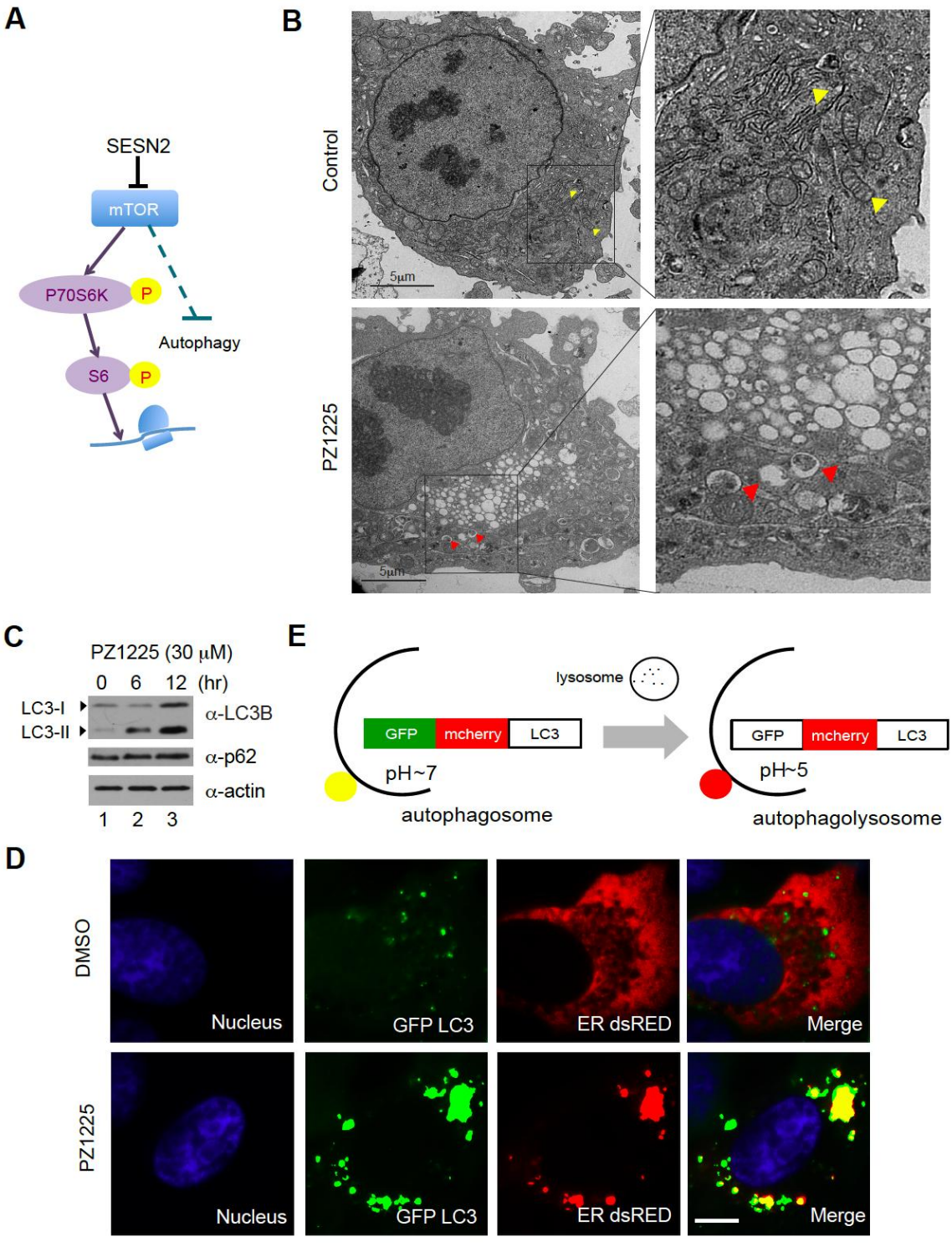
A
SESN2
mTOR
P70S6K
P
Autophagy
S6
P
B
Control
PZ1225
5μm
5μm
C
PZ1225 (30 μM)
0 6 12 (hr)
LC3-I
LC3-II
α-LC3B
α-p62
α-actin
1 2 3
E
lysosome
GFP
mcherry
LC3
pH~7
autophagosome
GFP
mcherry
LC3
pH~5
autophagolysosome
D
DMSO
PZ1225
Nucleus
GFP LC3
ER dsRED
Merge
Nucleus
GFP LC3
ER dsRED
Merge

F

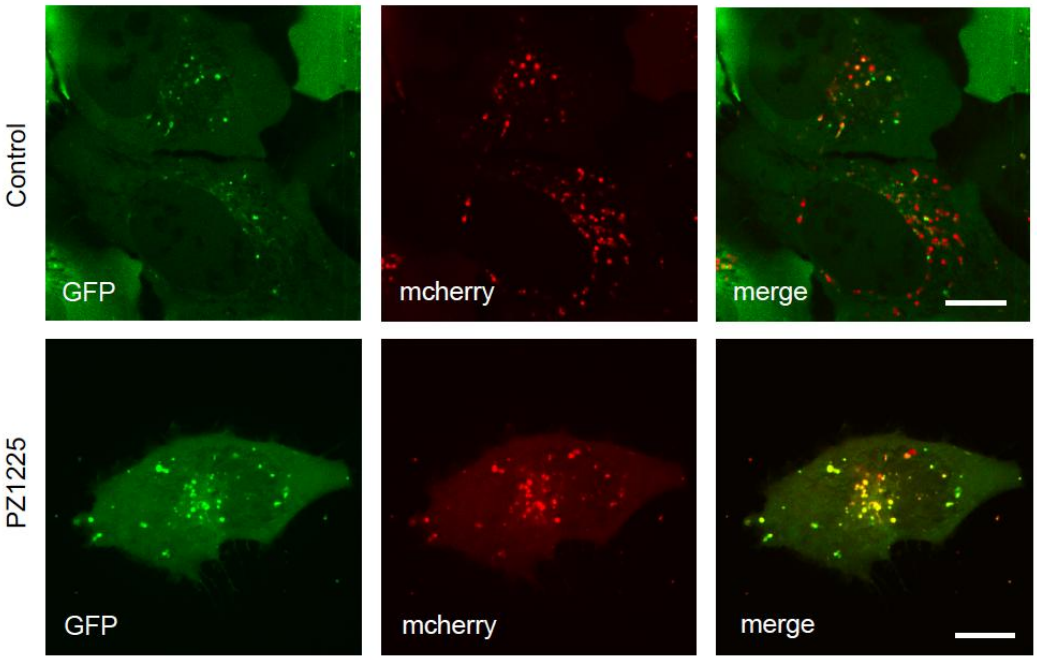
Control
PZ1225
GFP
mcherry
merge
GFP
mcherry
merge

G

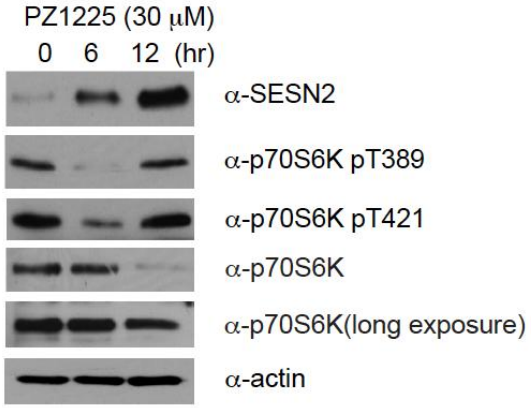
PZ1225 (30 μM)
0 6 12 (hr)
α-SESN2
α-p70S6K pT389
α-p70S6K pT421
α-p70S6K
α-p70S6K(long exposure)
α-actin

Figure**3-4.** PZ1225 alters mTOR signaling and autophagy efflux in cancer cells.
A, diagram illustrating ER stress induces SESN2 and further alters mTOR signaling and autophagy. B, autophagic vesicles were observed by transmission electron microscopy. Yellow arrows denote normal ER/Golgi membrane structure and mitochondria in the control cells. Red arrows denote signature double membrane autophagic vesicles after PZ1225 treatment. C, accumulation of LC3-II protein measured by Western blot. Note that p62 accumulation was not observed. D, autophagic vesicles were visualized by GFP-LC3 and ER membrane was visualized by ER-dsRED in fluorescent microscopy assays. E-F, a GFP-mcherry-LC3 tandem plasmid was used to measure pH in the autophagic vesicles (E). Yellow puncta in live image denote neutral pH in autophagic vesicles. G, the effects of PZ1225 on p70S6K phosphorylation and SESN2 expression were measured by Western blot. Note the decrease of p70S6K phosphorylation at 6 h after PZ1225 treatment and the recovery at 12 h. Scale bar, 10μm.

Figure 3-5.

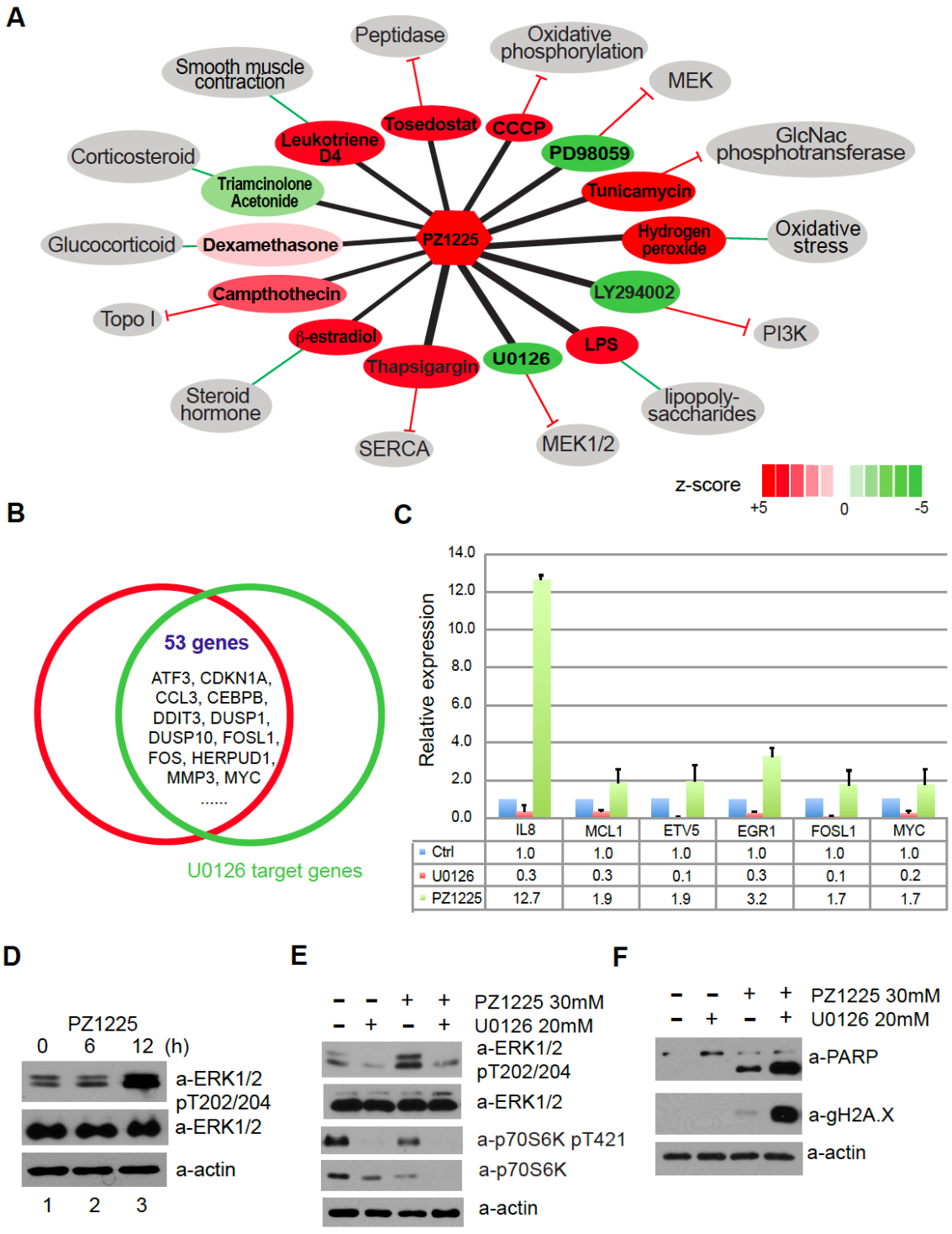
A
Peptidase
Oxidative phosphorylation
Smooth muscle contraction
MEK
Tosedostat
CCCP
Leukotriene D4
PD98059
GlcNac phosphotransferase
Corticosteroid
Triamcinolone Acetonide
Tunicamycin
Glucocorticoid
Dexamethasone
PZ1225
Hydrogen peroxide
Oxidative stress
Campthothecin
LY294002
Topo I
β-estradiol
PI3K
LPS
Thapsigargin
U0126
Steroid hormone
lipopoly-saccharides
SERCA
MEK1/2
z-score
+5
0
-5
B
53 genes
ATF3, CDKN1A, CCL3, CEBPB, DDIT3, DUSP1, DUSP10, FOSL1, FOS, HERPUD1, MMP3, MYC
.....
U0126 target genes
C
Relative expression
14.0
12.0
10.0
8.0
6.0
4.0
2.0
0.0
IL8 MCL1 ETV5 EGR1 FOSL1 MYC
Ctrl 1.0 1.0 1.0 1.0 1.0 1.0
U0126 0.3 0.3 0.1 0.3 0.1 0.2
PZ1225 12.7 1.9 1.9 3.2 1.7 1.7
D
PZ1225
0 6 12 (h)
a-ERK1/2 pT202/204
a-ERK1/2
a-actin
1 2 3
E
PZ1225 30mM
U0126 20mM
a-ERK1/2 pT202/204
a-ERK1/2
a-p70S6K pT421
a-p70S6K
a-actin
F
PZ1225 30mM
U0126 20mM
a-PARP
a-gH2A.X
a-actin

Figure **3-5.** The effects of PZ1225 on ER and autophagy.

A, correlation of PZ1225 and other inhibitors was analyzed by IPA upstream regulator analysis (A). Oval colors reflect the z-score of each chemical. A green oval color indicates a negative z-score and an opposite effect of PZ1225 and the corresponding chemical such as U0126. A positive z-score is indicated with red color. The weight of the connecting lines was assigned according to the p-value of each chemical. Thicker streak indicates a smaller p-value and a stronger correlation. z-score and p-value for each chemical were listed in Table 3-3. B, a set of genes affected by U0126 and PZ1225 was reported by the IPA upstream regulator analysis. C, U0126 and PZ1225 showed opposite trend on the expression of genes such as IL8, MCL1, and FOSL1 measured with RT-qPCR. n=3. D, the effects of PZ1225 on ERK1/2 phosphorylation at 6 and 12 h after treatment were analyzed by Western blot. E-F, the effects of combinatorial PZ1225 and U0126 treatment on ERK1/2 and p70S6K phosphorylation (E), PARP cleavage, and □ H2A.X (F) were analyzed by Western blot.

Figure 3-6.

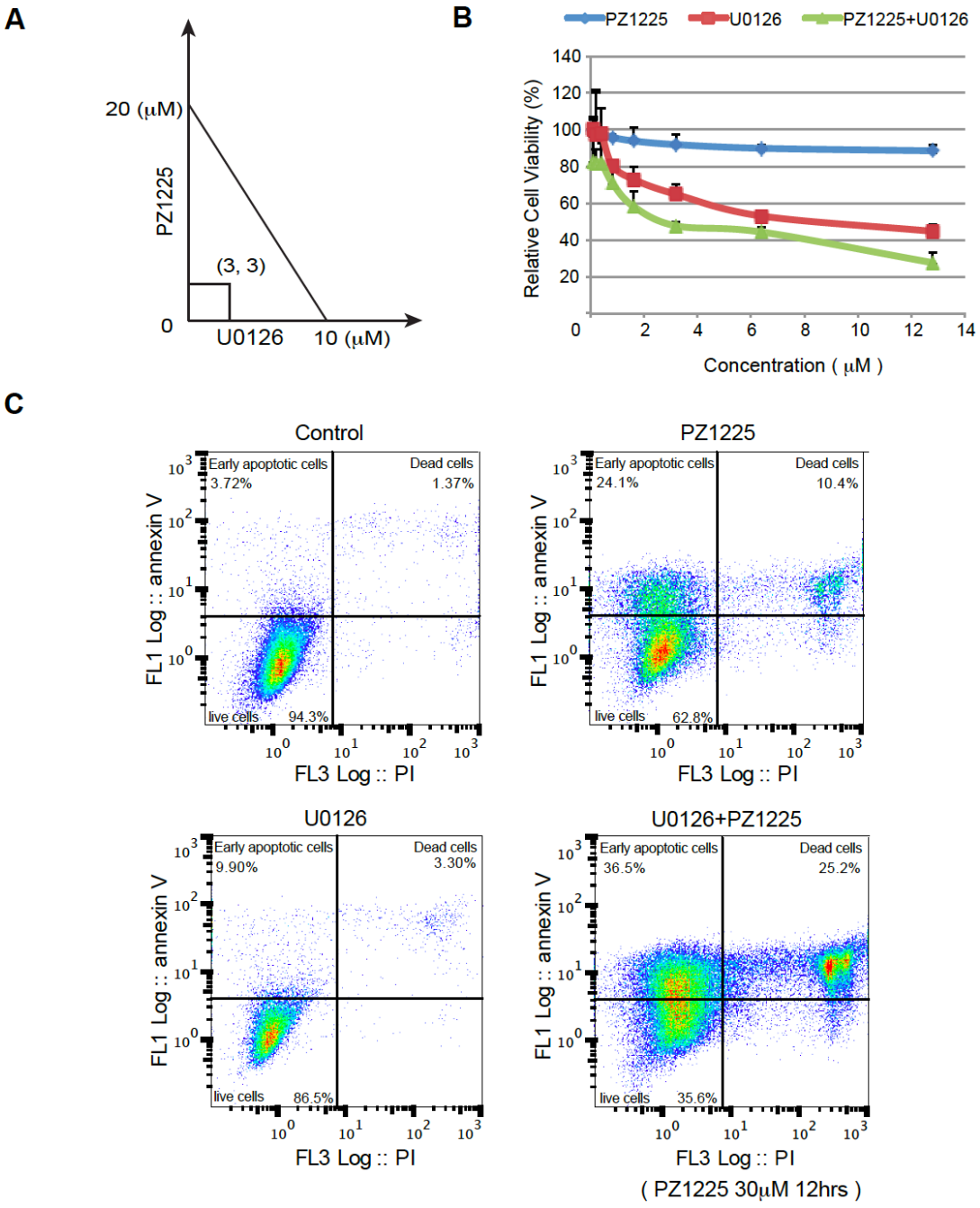
A
20 (μM)
PZ1225
(3, 3)
0
U0126
10 (μM)
B
PZ1225
U0126
PZ1225+U0126
Relative Cell Viability (%)
Concentration (μM)
C
Control
Early apoptotic cells
3.72%
Dead cells
1.37%
live cells
94.3%
PZ1225
Early apoptotic cells
24.1%
Dead cells
10.4%
live cells
62.8%
U0126
Early apoptotic cells
9.90%
Dead cells
3.30%
live cells
86.5%
U0126+PZ1225
Early apoptotic cells
36.5%
Dead cells
25.2%
live cells
35.6%
FL1 Log :: annexin V
FL3 Log :: PI
(PZ1225 30μM 12hrs)

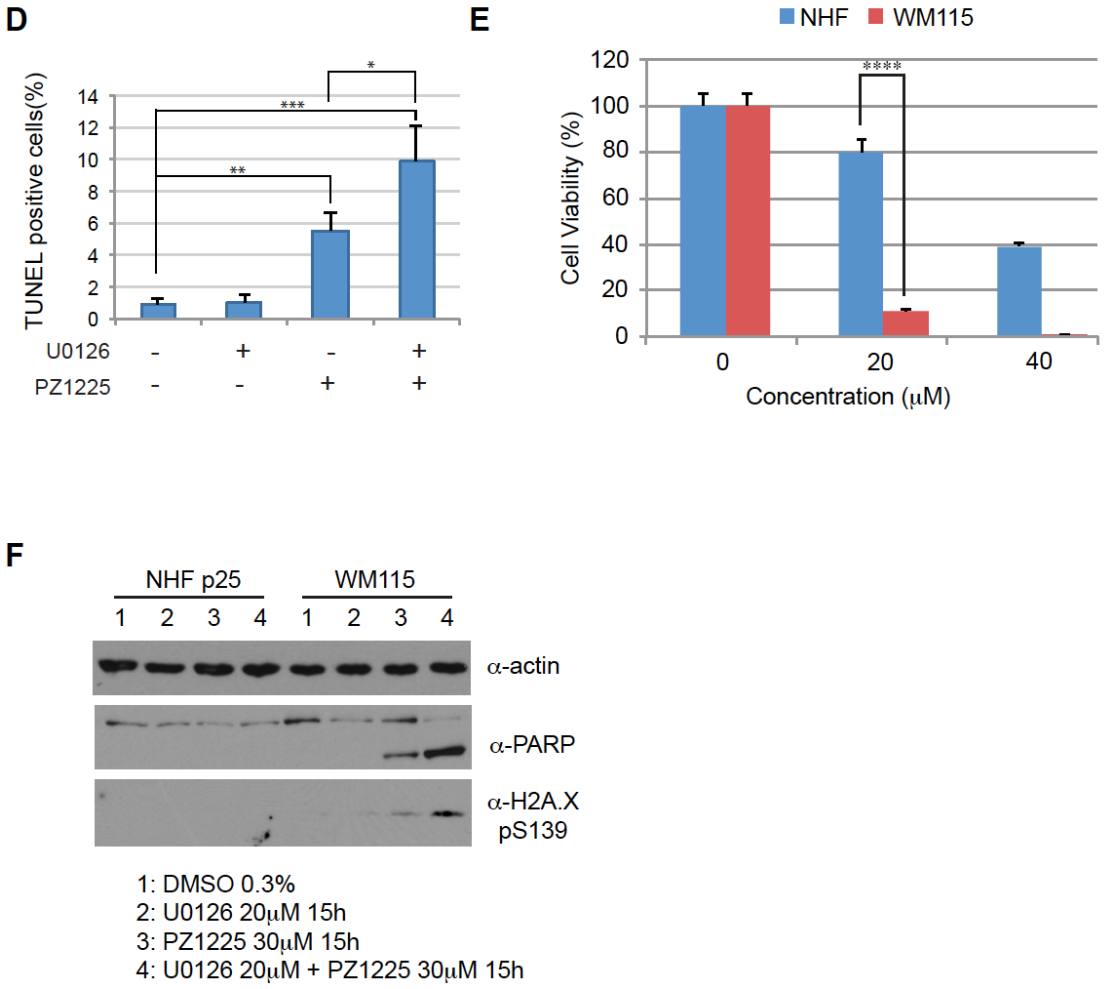

Figure **3-6.** Combinatorial U0126 and PZ1225 treatment significantly increased DNA damage and cell death in cancer cells.

A, an isobologram graph illustrating synergistic effect of U0126 and PZ1225 in cell death induction. B-C, TUNEL assay (B) and flow cytometry analyses (C) showed a combination of U0126 and PZ1225 significantly increased DNA double strand breaks (B) and apoptotic cell death (C). n=4, *p-value<0.05, **p-value<0.005, ***p-value<0.005. D-E, a combination of PZ1225 (20 μM, 15h) and U0126 (20 μM, 15h) induced significant cell death in cancerous WM115 cells but not in non-tumorigenic NHF cells (D). n=3, ****p-value<0.005. Concurrently, more PARP cleavage and H2A.X were observed in WM115 cells but was not detectable in NHF cells (E).

Figure 3-7.

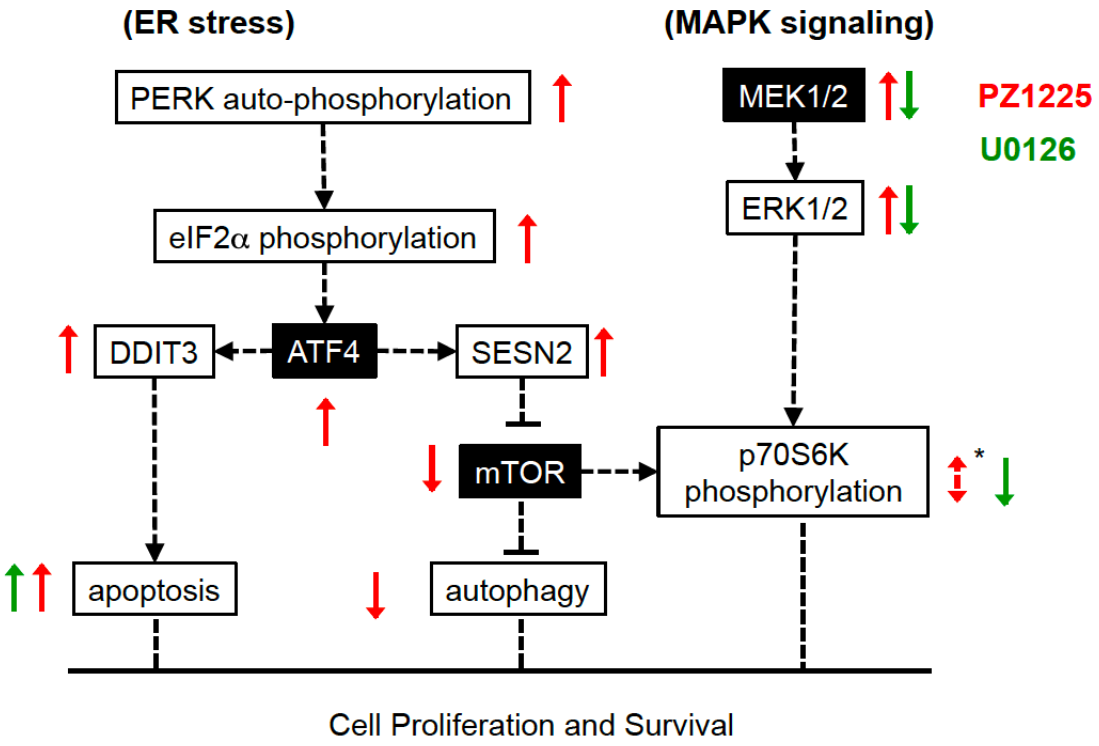

Figure **3-7**. Model figure of cell pathways affected by PZ1225 in cancer cells. PZ1225 induces ER stress indicated by PERK and eIF2 phosphorylation ATF4 induction. ER stress signals inhibition of mTOR by SESN2 induction, which activates autophagy. However, efflux of autophagy is inhibited at later stage by PZ1225. In another aspect, PZ1225 activates MAPK signaling pathway. The kinase cascade regulates p70S6K activation by phosphorylation and further affects transcription from S6 ribosome. Most importantly, PZ1225 intercalates into DNA and results in significant apoptotic cell death. In the combinational treatment, U0126 inhibits MAPK signaling and sensitizes cancer cells to DNA damage.

Table 3-1. p-value of canonical pathways regulated by PZ1225.

Ingenuity Canonical Pathways	p-value
Circadian Rhythm Signaling	2.29E-04
ERK5 Signaling	3.16E-04
Bladder Cancer Signaling	6.03E-04
p38 MAPK Signaling	1.35E-03
Endoplasmic Reticulum Stress Pathway	1.35E-03
NRF2-mediated Oxidative Stress Response	1.38E-03
L-cysteine Degradation I	4.57E-03
UDP-N-acetyl-D-glucosamine Biosynthesis II	1.10E-02
ILK Signaling	1.26E-02
Airway Pathology in Chronic Obstructive Pulmonary Disease	1.95E-02
Cholecystokinin/Gastrin-mediated Signaling	2.24E-02
Polyamine Regulation in Colon Cancer	2.24E-02
Pathogenesis of Multiple Sclerosis	2.45E-02
Thio-molybdenum Cofactor Biosynthesis	2.82E-02
L-cysteine Degradation II	2.82E-02
IL-17A Signaling in Gastric Cells	3.16E-02
Corticotropin Releasing Hormone Signaling	3.24E-02
Superpathway of Cholesterol Biosynthesis	3.89E-02
TNFR2 Signaling	4.27E-02
Mevalonate Pathway I	4.27E-02
IL-6 Signaling	4.47E-02
p53 Signaling	4.68E-02
Role of IL-17A in Psoriasis	5.01E-02
Superpathway of Methionine Degradation	5.01E-02

Table 3-2. Categories of PZ1225 and U0126 overlapping genes.

Genes up-regulated by PZ1225 and down-regulated by U0126*

Transcription	Cell signaling	Cell proliferation & cell death	Others
ATF3 20.9	AREG/ARE 5.6	CDKN1A 2.0	ARC 3.3
BHLHE40 4.0	DUSP1 2.8	MCL1 2.4	ABCB1 2.1
CCNL1 2.2	DUSP5 3.3	PHLDA1 3.2	HSPA5 3.6
DDIT3 42.8	EREG 4.7		HMOX1 3.4
EGR1 18.5	ERRFI1 4.0	**Cytokine**	HERPUD1 9.7
FOS 3.4	FGF2 3.4	CCL3 2.2	PER1 2.8
FOSL1 2.6	IER2 2.5	CXCL3 3.8	PER2 2.1
KLF10 2.4	PTGS2 34.8	CXCL11 3.1	LDLR 2.3
MYC 2.1	RND3 4.0	IL1A 17.1	MMP3 8.8
NR4A1 2.8	TRIB1 2.7	IL8 2.7	TAC1 2.5
NR4A2 7.3	VEGFA 2.6		
NR4A3 2.2			
ZFP36 2.9			

*PZ1225 data from two biological repeats of microarray. U0126 data is retrieved by IPA from published datasets. Numbers represent fold of induction by PZ1225.

Table 3-3. The Z-score and p-value of chemicals in the upstream regulator analysis by IPA.

Chemicals	Z-score	p-value
Thapsigargin	5.163	1.33E-28
U0126	-5.877	3.01E-24
Lipopolysaccharide (LPS)	8.101	4.24E-23
Tunicamycin	4.751	9.82E-22
Hydrogen Peroxide	5.786	6.85E-20
LY294002	-6.17	7.80E-19
PD98059	-6.417	2.16E-18
Carbonyl cyanide m-chlorophenyl hydrazone (CCCP)	4.32	1.12E-17
Dexamethasone	1.183	8.34E-17
Tosedostat	3.86	9.76E-17
Triamcinolone acetonide	-1.866	6.85E-16
β-estradiol	4.587	6.57E-15
Leukotriene D4	4.035	7.46E-15
Camptothecin	3.104	5.60E-14

Chapter 4

PAD4 is required for the formation of macrophage extracellular traps in murine peritoneal cavity macrophage

4.1 Abstract

Since the discovery of the neutrophil extracellular traps (NETs)in bacteria killing in 2004, ETs have been reported in other types of immune cells such as eosinophil[114] and mast cells[115]. Although the studies of ETs have been mainly focused on NETs, the structures of NETs and its function still needs further elucidation, especially for its function in the disease pathologies besides bacteria killing. Macrophage is one of the major cell types in the immune system and was regarded as the first defense of pathogens together with neutrophils. In one aspect, macrophages exert a phagocytosis function to swallow and kill pathogens. In another aspect, macrophages play an important role to activate or suppress inflammation by secretion of different cytokines/chemokines. Besides their known functions in the defense of pathogens, whether macrophages release ETs and the possible mechanisms of release is an interesting yet poorly studied area. Here I report the capability of mice peritoneal cavity macrophages to release the decondensed chromatin into the extracellular space. Most importantly, my studies suggest PAD4, but not PAD2, is required for histone citrullination

and extracellular trap formation in murine macrophages extracted from peritoneal cavity and in macrophage cell lines RAW 264.7 and J774A.1. In addition, the extracellular trap structure form independently of bacteria but with calcium ionophore treatment or by serum starvation.

4.2 Introduction

Macrophages and neutrophils are both white blood cells that serve important functions in the immune system and considered the first defenders against pathogens[171-173]. Neutrophils mature in the bone marrow and circulate in the blood stream. During inflammation, neutrophils are attracted by chemokines, migrate to the site of inflammation through blood vessel and infiltrate into the infected tissue[174]. Beside their function in innate immunity, in 2004, neutrophil extracellular traps (NETs) were firstly reported to help trap and kill bacteria[113].NETs contain antimicrobial proteins such as neutrophil elastase, myeloperoxidase and cathespin G, which help to kill invading bacterias[175,176]. Histones in the NETs structure bind bacteria DNA and aid the bacteria killing as well[177,178].Recently, more and more studies reported the role of NETs in chronic and acute diseases, such as atherosclerosis[117], thrombosis[120,123], and ischemic injury[179,180]. Tissue resident macrophages are highly heterogeneous and fulfill a tissue specific function. One of the most important functions of macrophage is phagocytosis, which digests invading pathogens and unhealthy cells[181]. Some studies

reported that macrophage phagocytosis activity helps clear NETs and cell debris[182]. However, whether macrophages form extracellular traps via the similar mechanism as neutrophils and the functions of such a structure are largely unknown.

Peptidylarginine deiminase 4 (PAD4) is an enzyme that catalyzes the conversion of arginine/monomethyl-arginine to citrulline on histone H3[183], H4[183,184], H2A[184,185]and H1[186]. In 2009, Yanming Wang reported that hypercitrullination of histones results in chromatin decondensation and release of chromatin into extracellular space in HL60 cells[124]. Later on, the requirement of PAD4 in NET formation is reported in multiple diseases such as atherosclerosis[118,119] and thrombosis[122]. More recently, PAD4 inhibitor was found to inhibit cancer metastasis after clinical surgery[121].

Studies on macrophage extracellular traps-like (ETL) structures have reported the release of chromatin by macrophage with stimulation of different types of microorganisms, including *S. aureus, H. Somni, M. Haemolytica, E. coli, C. albicans* and *M. tuberculosis*[187-193]. By examination of diffused DNA with immunostaining or with scanning electron microscope (SEM), extracellular traps in the extracellular space are detected. But the involvement of PAD4 and citrullination in ETLs are unknown.

Here I report the formation of macrophage extracellular traps by murine peritoneal macrophages under the stimuli of calcium ionophore or serum starvation. In addition, I also find hypercitrullination of chromatin mediated by PAD4 is required for formation of METs under both conditions.

4.3 Results

4.3.1 Peritoneal cavity macrophages (PCMs) become hypercitrullinated and form macrophage extracellular traps (METs)

To investigate whether macrophages are capable of forming extracellular traps, we extracted macrophages from peritoneal cavity of wild type C57BL/6J mice. After stimulation with calcium ionophore and lipopolysaccharide (LPS), hypercitrullination on histone H3 arginine 2, 8 and 17 was detected with immunostaining (Fig. 4-1A). Chromatin labeled by the histone H3 citrullination was decondensed and presented in the extracellular space, indicated by irregular shaped and trap-like chromatin structure viewed by immunostaining and scanning electron microscope (SEM) (Fig. 4-1A & E). The decondensed chromatin was also indicated by diffused DNA labeled with Hoechst dye (Fig.4-1A). These imaging results suggest formation of extracellular traps by macrophages and the involvement of hypercitrullination in the process. Compared to NETs, however, myeloperoxidase—a key component in NETs—was not observed on METs

(Fig. 4-1B). The composition difference of METs and NETs may provide important information in distinguishing the two structures *in vivo*.

4.3.2 PAD4 is required for hypercitrullination and extracellular trap formation in PCM.

To evaluate how peptidyle deiminase proteins affect extracellular trap formation in macrophages, we treated the macrophages with a PAD inhibitor YW3-56. The inhibitor significantly decreased hypercitrullination and MET formation shown by immunostaining (Fig. 4-1C). The percentage of METs decreased from 6% to 1% upon the application of YW3-56 (Fig. 4-1D). The result suggested a role of PAD proteins in this process. To further identify which PAD is involved, we adopted a PAD4 knockout mice model and extracted peritoneal macrophages without PAD4 expression[125].The expression of PAD4 in both wild type and knockout mice were tested with RT-qPCR and Western blot (Fig. 4-2A&B). Notably, PAD4 expression at both RNA and protein levels showed haploid insufficiency.

In macrophages extracted from PAD4 wild type mice, hypercitrullination and MET formation were induced by calcium ionophore and LPS for 3.5 hours and serum starvation for 24 hours (Fig. 4-2C-F); while in PAD4 knockout mice, both hypercitrullination and METs were not observed under the same conditions (Fig. 4-2C-F). To have a better view of

the METs fibers, we observed the structure under the Scanning Electron Microscope (Fig. 4-1E). In wild-type macrophages, we observed extracellular chromatin fibers with a diameter around 10-20 nm but not in the PAD4 knockout macrophages (Fig. 4-1E). The hypercitrullination was also not detectable in the Western blot analyses with different histone H3 citrullination antibodies (Fig. 4-2D). Moreover, citrullination on histone H3 arginine 2, 8, 17 and 26 all decreased in mice containing a single copy of the PAD4 gene (Fig. 4-2D). At the same time, percentage of cells that forms METs dropped by as much as 4 folds in PAD4 heterozygous macrophages (Fig.4-2E). These results suggest that histone hypercitrullination and MET formation are dependent on PAD4 expression.

Since macrophages are highly plastic and versatile, we further explored MET formation using macrophages derived from bone marrow L929 medium. In these cells, hypercitrullination could barely be observed and no MET formation was induced even under prolonged treatment of calcium ionophore and/or LPS. At the same time, in the bone marrow derived macrophages, PAD4 expression is relatively low while PAD2 protein is abundant, which further suggests PAD4 is involved in the regulation of METs (Fig. 4-2G).

4.3.3 PAD4 but not PAD2 overexpression induces extracellular traps formation in RAW 264.7 and J774A.1 macrophage cell lines

Out of 5 PAD proteins in mammalian cells, PAD4 is the only one that contains a bona fide nuclear localization signal[194]. However, it has been reported that PAD2 mediated H3R26 citrullination facilitates binding of estrogen receptor to DNA in the breast cancer cell MCF-7[195,196]. In peritoneal cavity macrophages extracted from PAD4 knockout mice, we detected expression of PAD2 protein (Fig. 4-3A). The expression of PAD2 and the non-detectable level of H3Cit26 in PAD4 knockout macrophages (Fig. 4-3B) suggest the requirement of PAD4 for histone hypercitrullination.

To study how PAD2 and PAD4 regulate hypercitrullination respectively, we tested expression of PAD2 and PAD4 protein in macrophage cell lines RAW 264.7 and J774A.1 that are established from tumor bearing mice. Compared to peritoneal macrophages, the cell lines express higher level of PAD2 but PAD4 expression is non-detectable compared to that in peritoneal cavity macrophages (Fig.4-3A). Under the stimulation of calcium ionophore and/or LPS, hypercitrullination on histone H3 was not detected in these cell lines (Fig. 4-3B). At the same time, MET formation is absence in these cells even under prolonged treatment up to 15 hours (Fig. 4-3C). Notably, after stimulation, citrullination level on histone H3 Cit 2, 8 and 17

was slightly increased compared to basal level (Fig. 4-3B), suggesting a facultative role of PAD2 in histone citrullination.

The cells were then used for transient transfection with plasmids containing PAD4 expressing cassette. In both cells lines, PAD4 overexpression induced hypercitrullination and ET formation (Fig. 4-3F), suggesting PAD4 protein is sufficient to induce hypercitrullination. To further evaluate the requirement of PADs in ET induction, we overexpressed PAD4, PAD2 and PAD4^{C645S} proteins in the osteosarcoma cell line U2OS respectively. As shown before[129], overexpression of PAD4 significantly induced hypercitrullination and formation of ETs. However, we newly observed PAD2 and PAD^{C645S} were not able to produce a comparable level of histone hypercitrullination (Fig. 4-3D) and formation of ETs (Fig. 4-3E). The results indicate a correlation between PAD4 and ET formation in different cells including primary macrophages, macrophage cell lines and mammalian cancer cells.

4.3.4 Histone H3R26 citrullination interferes with polycomb protein binding to methylated lysine 27 and promotes chromatin decondensation.

To investigate the mechanisms behind PAD4 mediated hypercitrullination, we investigated the binding activity of polycomb group (PcG) proteins at lysine 27. PcG proteins CBX2 and CBX7bind to methylated

lysine 27via their chromodomain and mediate silencing of target genes[197]. The chromodomain of PcG protein CBX2 and CBX7 was fused with GST tag, cloned into the pGEX vector and purified from the BL21 *E.coli* strain. Expression of GST and GST tagged proteins were verified using SDS-PAGE (Fig. 4-4A). Coomassie brilliant blue staining revealed equal amount of proteins used in the peptide pull-down experiment. Three histone H3 peptides were included in the study—histone H3 peptide without modifications, histone H3 peptide with citrullinated arginine 26, and histone H3 peptide with citrullinated arginine 26 and methylated lysine 27. The peptide pull-down assay revealed efficient binding to the histone H3 peptide with methylated lysine 27, but not the unmethylated control, by CBX2 and CBX7 chromodomain. When citrullinated at arginine 26, PcG binding to histones decreased significantly (Fig.4-4B). The result suggests citrullination at arginine 26 interferes with the binding of polycomb proteins to lysine 27 methylation, which potentially prohibited heterochromatin formation mediated by PcG protein and promotes chromatin decondensation.

4.4 Discussion

In Chapter 4, I reported that (1) macrophage forms extracellular traps under stimuli such as calcium ionophore treatment and serum starvation; and (2) the formation of METs is dependent on PAD4-mediated chromatin hypercitrullination and decondensation; (3) PAD4 but not PAD2

overexpression in macrophage cells and cancer cells induces hypercitrullination and release of chromatin; and (4) citrullination of histone H3arginine 26 can potentially affect the binding of polycomb proteins to the adjacent lysine 27 methylation sites and interferes with condensation of chromatin.

Previously, researchers mainly focused on microorganisms as stimuli for METs. Here we used calcium ionophore, LPS and serum starvation as the stimuli. Calcium ionophore is amobile ion-carrier that promotes penetration of calcium ions across the cell membrane. While LPS (lipopolysaccharide) is an endotoxin found in the outer membrane of Gram-negative bacteria. Both reagents were used to induce NET formation in neutrophils. When used to induce hypercitrullination in macrophages, calcium ionophore is significantly more effective than LPS. Indeed, in macrophages treated with LPS alone, I did not observe significant hypercitrullination or more MET formation compared to the control group. This observation suggests either METs are not a major mechanism in fighting microorganism infection or it is not LPS but other components of microbes that induce METs. When macrophages are cultured in serum depleted medium, METs were released from the cell after 9 hours of culture, suggesting that starvation stimulates the formation of METs. Based on the studies in neutrophils, we could propose couple mechanisms that might be involved in this process. Reactive oxygen species (ROS) have been reported to play an important role in releasing of

chromatin by neutrophils. Studies have linked ROS stimulated NET formation with autophagy and some even consider NET-mediated cell death as a result of autophagy because autophagy inhibition suppresses NET formation[198]. Considering the fact that serum starvation is one of inducers for oxidative stress and autophagy in cells, MET formation induced by starvation could be address by autophagy. To test the hypothesis, we could apply the methods used in Chapter 3 to study the activation and efflux of autophagy in macrophages. We could also test how autophagy inhibitors affect METs formation in starved macrophages.

Although other research groups reported macrophage extracellular traps-like structures, the existence of such structure was mainly illustrated by DNA/histone staining and/or SEM. Here I reported hypercitrullination on histone H3 at arginine 2, 8, 17 and 26 as the component of METs, suggesting that hypercitrullination on histone H3 isa novel marker for METs. We also reported here that induction of H3cit26 is dependent on PAD4 enzyme activity. The requirement for PAD4 in MET formation provides a powerful tool in the functional study of METs.

In the studies of extracellular traps, Dr. Scott Coonrod's group has reported that PAD2 protein promotes expression of estrogen receptor target genes by citrullinating histone H3 at arginine 26[195,196]. It is indeed a surprising discovery since PAD2 does not contain a nuclear localization

signal. To shed light on the function of PADs in MET formation, I also evaluated function of PAD2 and found PAD2 expression is not sufficient to induce hypercitrullination and METs (Figure 4-3). However, in RAW 264.7 and J774A.1 cells that express a higher level of PAD2 compared to PCM, I observed elevated level of H3 citrullination at arginine 2, 8, 17 after combined treatment of calcium ionophore and LPS. This result indicates a facultative role of PAD2 in histone citrullination at specific sites on histones but not in the induction of genome-wide hypercitrullination.

It is noteworthy that METs induced by calcium ionophore or serum starvation in PCM is at a low percentage—equal to or lower than10%. MET formation is a suicidal process. When chromatin is released, proteins contained in the nucleus, cytoplasm or cellular vesicles are projected into the extracellular space along with the chromatin. Components such as ROS and hydrolases will attract other immune cells to the location. When this happens *in vivo*, it will potentially trigger the sterile inflammation and stimulate a systematic reaction of the animal body. Thus functions of METs *in vivo* raise many open questions to be answered.

Figure 4-1.

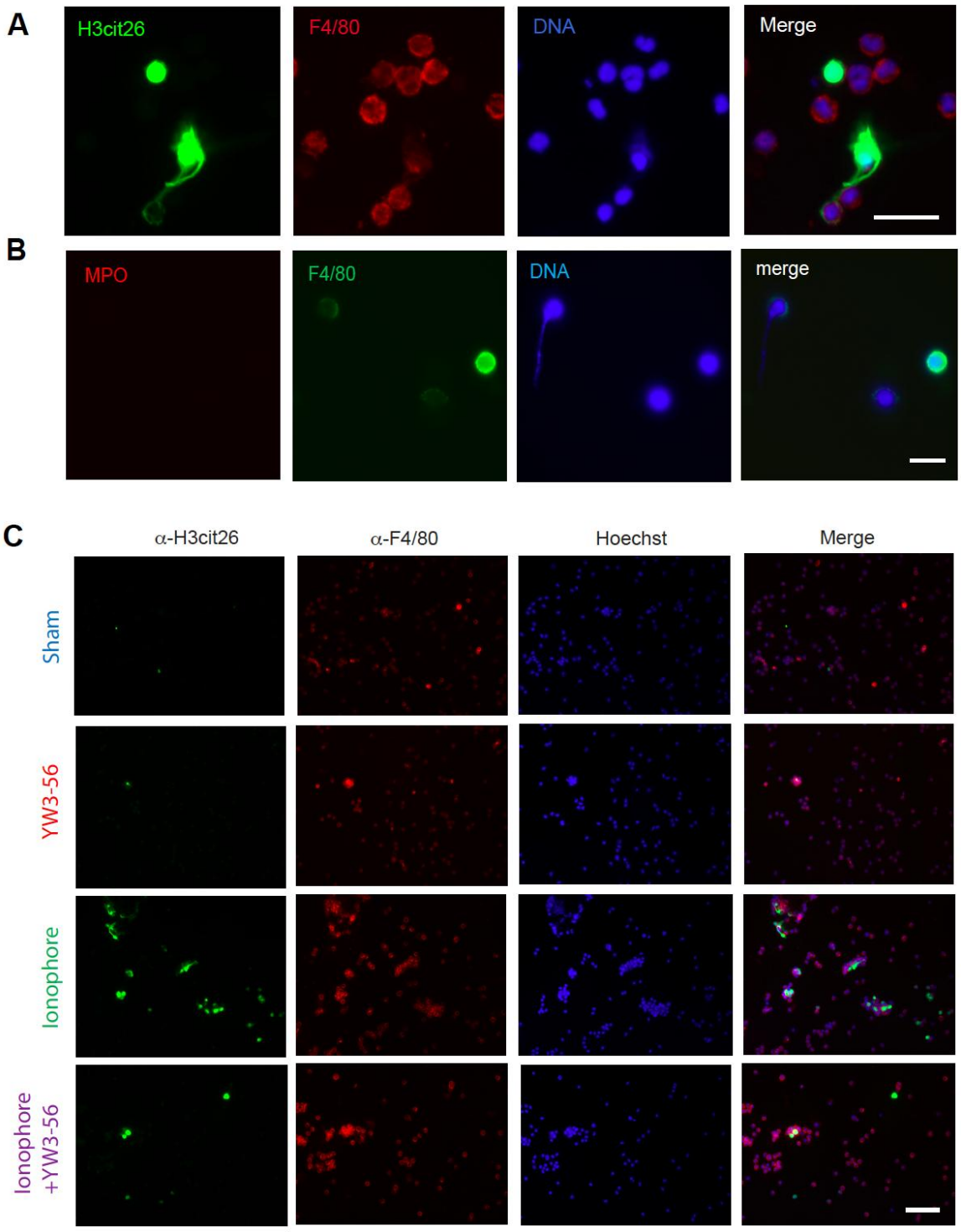
A
H3cit26
F4/80
DNA
Merge
B
MPO
F4/80
DNA
merge
C
α-H3cit26
α-F4/80
Hoechst
Merge
Sham
YW3-56
Ionophore
Ionophore +YW3-56

D

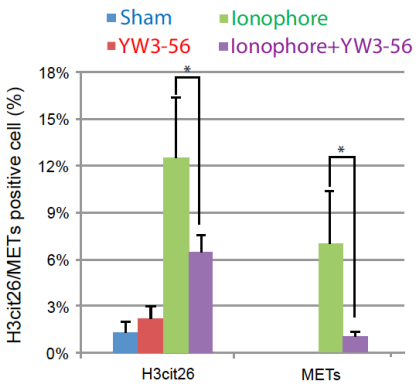
Sham
Ionophore
YW3-56
Ionophore+YW3-56
H3cit26/METs positive cell (%)
18%
15%
12%
9%
6%
3%
0%
*
*
H3cit26
METs

E

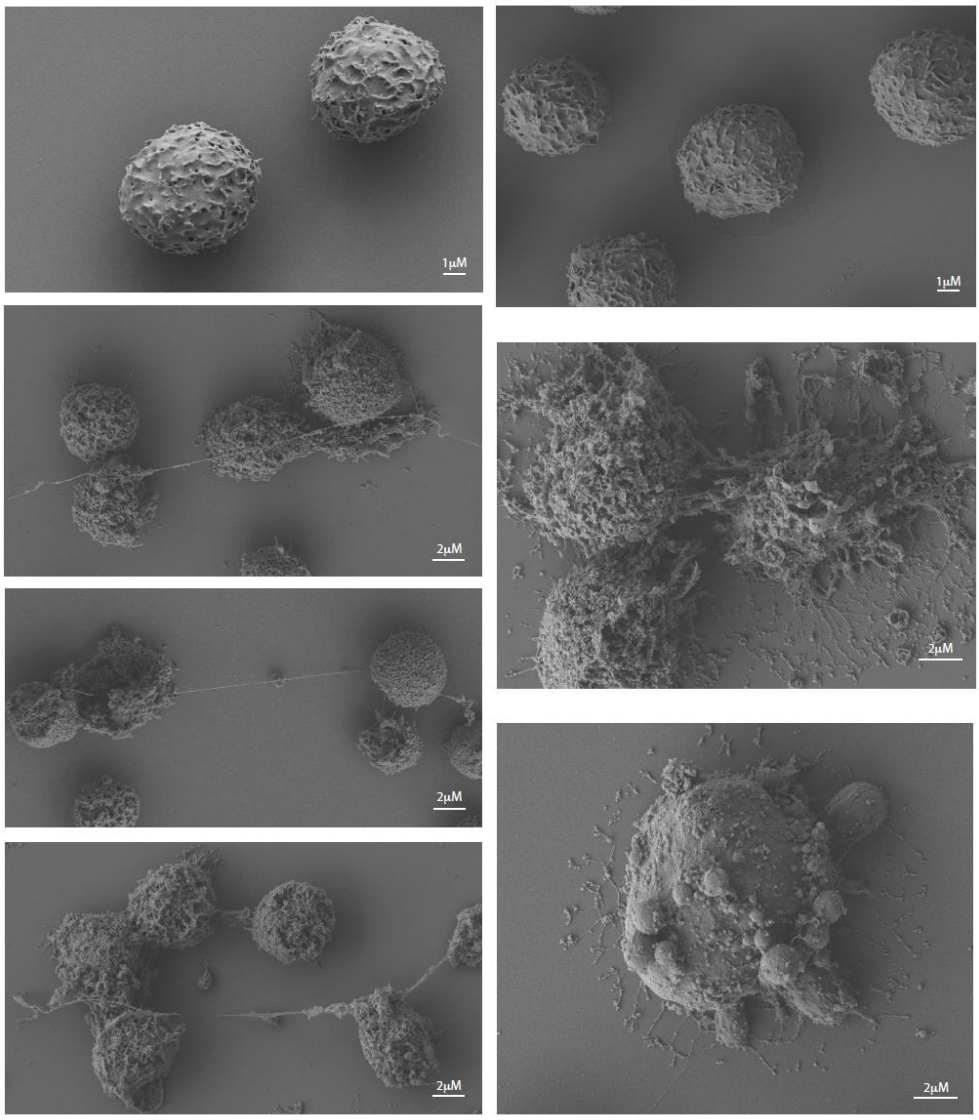
1μM
1μM
2μM
2μM
2μM
2μM
2μM

Figure **4-1.** Peritoneal cavity macrophages form extracellular traps.
A, Calcium ionophore and LPS treatment induced macrophage extracellular trap formation in peritoneal cavity macrophages. Citrullination on histone H3 at arginine 26 was detected on the MET structure. B, MPO was not detected on the structure. C, PAD inhibitor YW3-56 inhibited MET formation. D, quantification showing the percentage of cells forming METs out of the macrophage population. *n=3, $p<0.05$. E, SEM image of extracellular trap fibrous structure. Scale bar is 20 μm(A), 10 μm(B), and 50 μm(C) respectively.

Figure 4-2.

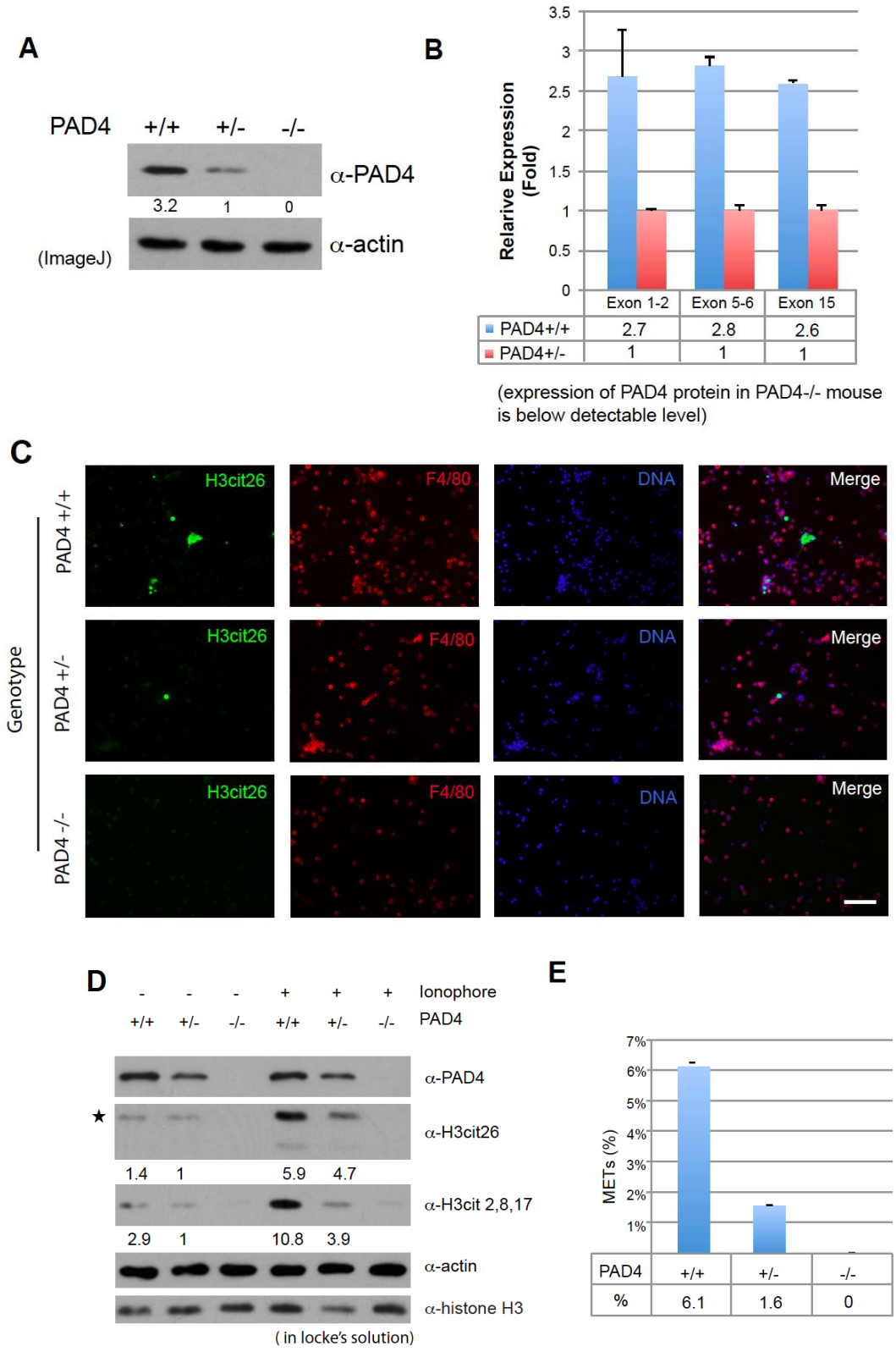
A
PAD4 +/+ +/- -/-
α-PAD4
3.2 1 0
(ImageJ)
α-actin
B
Relarive Expression (Fold)
3.5
3
2.5
2
1.5
1
0.5
0
Exon 1-2 Exon 5-6 Exon 15
PAD4+/+ 2.7 2.8 2.6
PAD4+/- 1 1 1
(expression of PAD4 protein in PAD4-/- mouse is below detectable level)
C
Genotype
PAD4 +/+
PAD4 +/-
PAD4 -/-
H3cit26
F4/80
DNA
Merge
D
- - - + + + Ionophore
+/+ +/- -/- +/+ +/- -/- PAD4
α-PAD4
α-H3cit26
1.4 1 5.9 4.7
α-H3cit 2,8,17
2.9 1 10.8 3.9
α-actin
α-histone H3
(in locke's solution)
E
METs (%)
7%
6%
5%
4%
3%
2%
1%
PAD4 +/+ +/- -/-
% 6.1 1.6 0

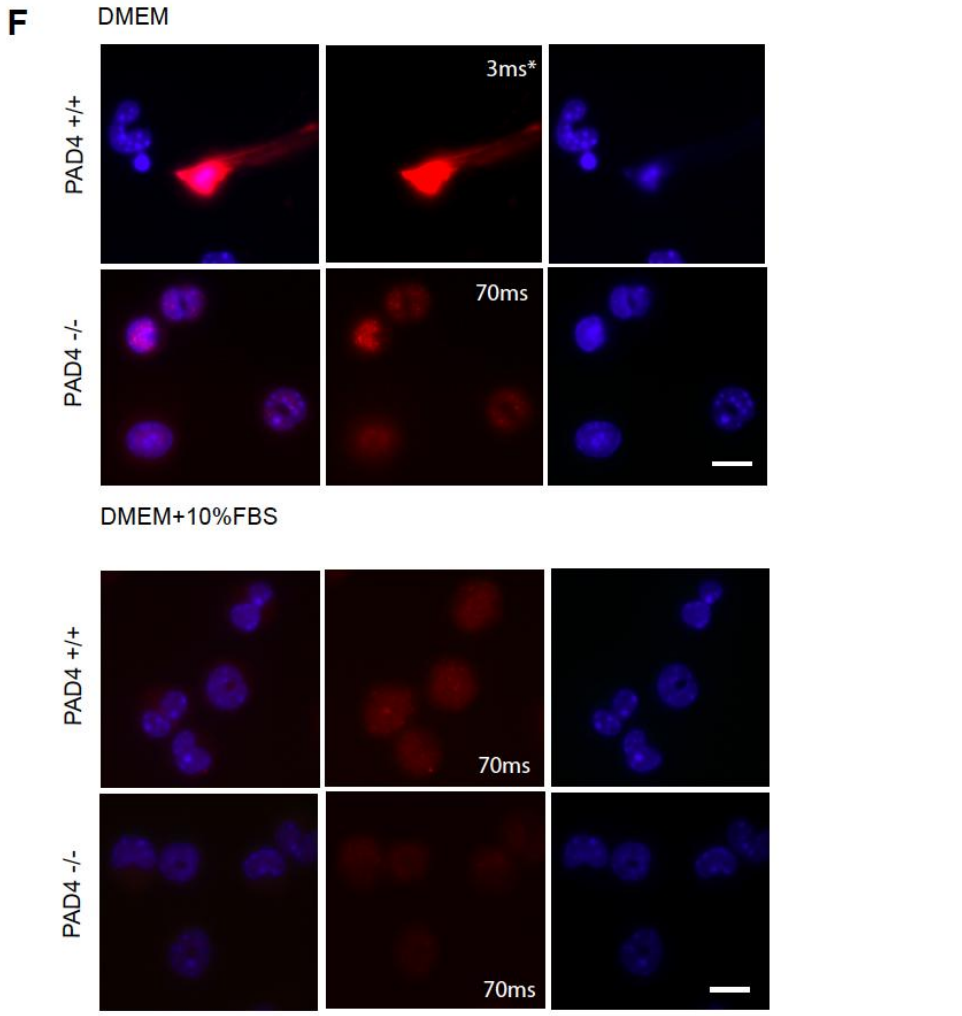
F
DMEM
PAD4 +/+
PAD4 -/-
3ms*
70ms
DMEM+10%FBS
PAD4 +/+
PAD4 -/-
70ms
70ms

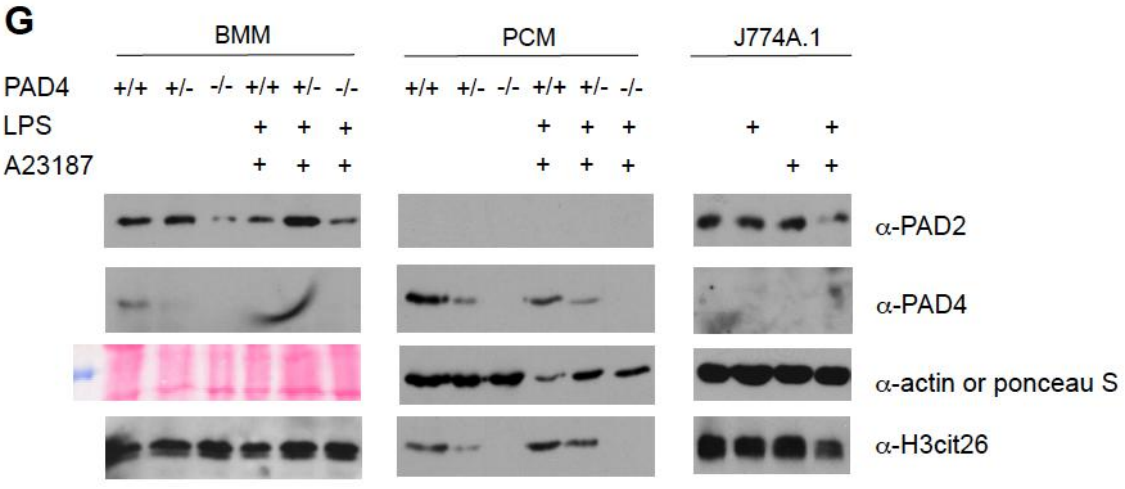
G
BMM
PCM
J774A.1
PAD4 +/+ +/- -/- +/+ +/- -/- +/+ +/- -/- +/+ +/- -/-
LPS + + + + + + + + + + + +
A23187 + + + + + + + + + + + +
α-PAD2
α-PAD4
α-actin or ponceau S
α-H3cit26

Figure **4-2.** PAD4 is required for calcium ionophore induced extracellular trap formation and histone H3 hypercitrullination in murine peritoneal cavity macrophage.

A-B, PAD4 expression was tested at transcriptional level (A) and translational level (B). C, calciumionophore induces extracellular traps and histone H3 hypercitrullination in peritoneal cavity macrophages extracted from wild type C57BL/6J mice but decreased in PAD heterozygous mice and non-detectable in PAD4 knockout mice. D, both H3Cit26 and H3Cit 2, 8,17 were induced by calcium ionophore and the induction depends on PAD4 expression. E, 6.1% of macrophages extracted from PAD4wild type mice formed extracellular traps after 3.5 hours induction while in PAD4 knockout mice, no ETs structure was formed. Scale bar, 50 μm (C) and 10 μm (F). * Exposure time is indicated on the figures.

Figure 4-3.

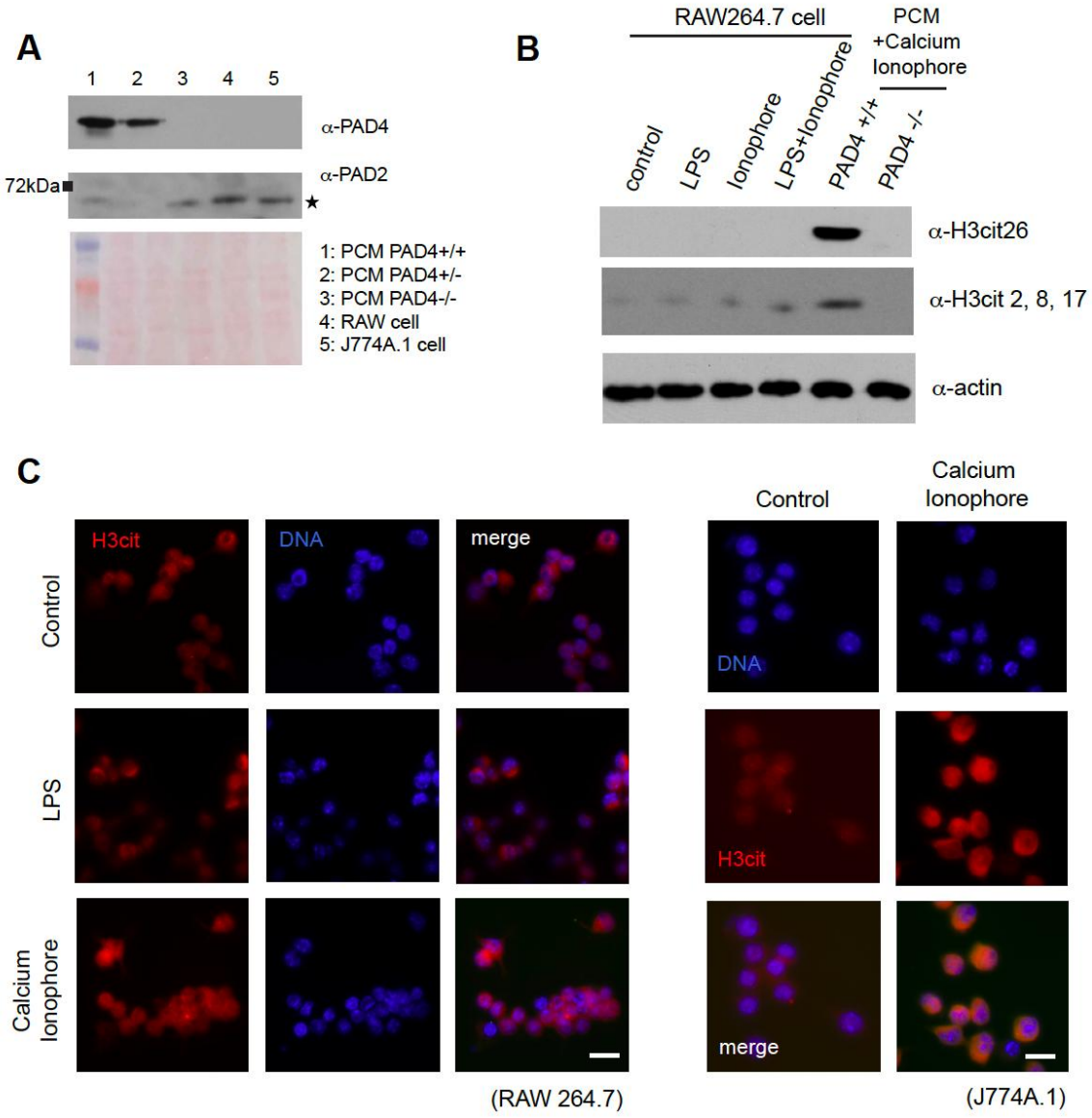
A
1 2 3 4 5
α-PAD4
72kDa
α-PAD2
1: PCM PAD4+/+
2: PCM PAD4+/-
3: PCM PAD4-/-
4: RAW cell
5: J774A.1 cell
B
RAW264.7 cell
PCM +Calcium Ionophore
control
LPS
Ionophore
LPS+Ionophore
PAD4 +/+
PAD4 -/-
α-H3cit26
α-H3cit 2, 8, 17
α-actin
C
H3cit
DNA
merge
Control
LPS
Calcium Ionophore
Control
Calcium Ionophore
DNA
H3cit
merge
(RAW 264.7)
(J774A.1)

D

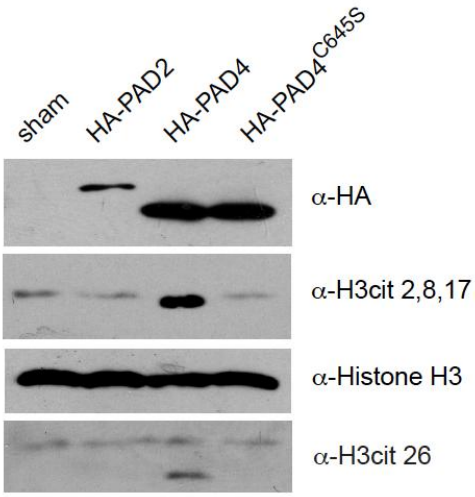
sham
HA-PAD2
HA-PAD4
HA-PAD4C645S
α-HA
α-H3cit 2,8,17
α-Histone H3
α-H3cit 26

E

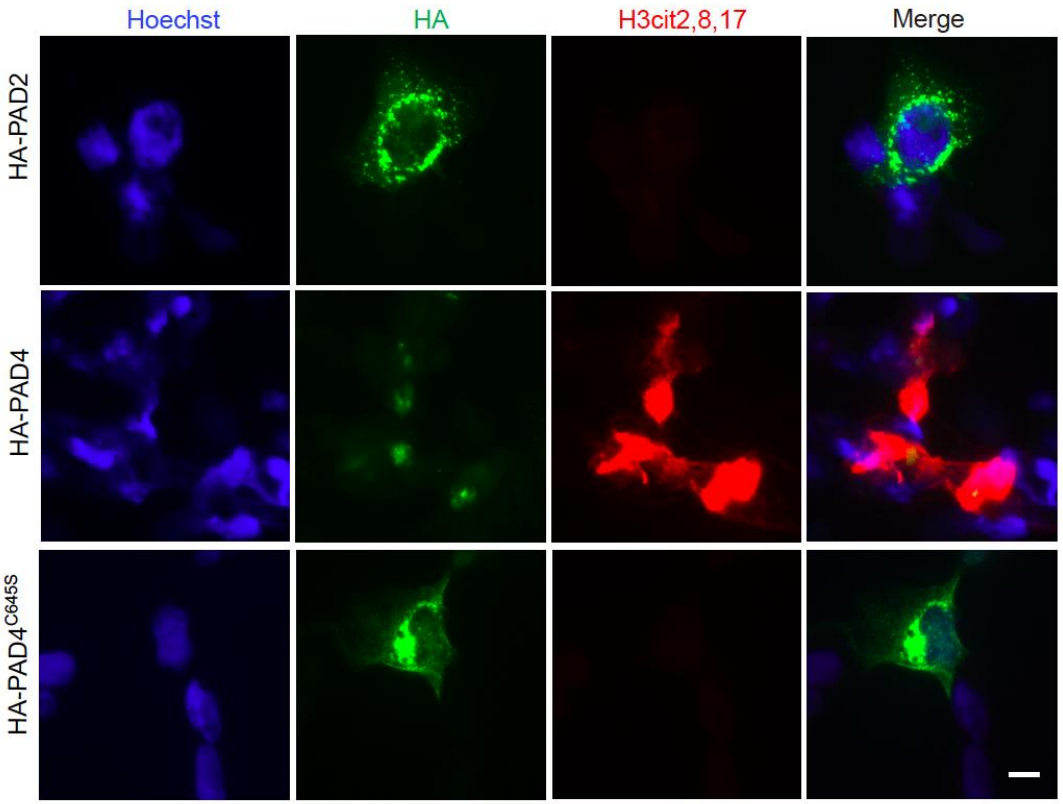
Hoechst
HA
H3cit2,8,17
Merge
HA-PAD2
HA-PAD4
HA-PAD4C645S

Figure **4-3.** Overexpression of PAD4 induces MET formation in macrophage cell lines and cancer cells.

PAD4 expression was analyzed in macrophage cell lines J774A.1 and RAW264.7. Both cell lines did not express PAD4 at a comparable level with murine PCM. Instead, PAD2 expression was detected in both cell lines but not detectable in PCM (A). LPS or ionophore or both cannot induce either histone H3 citrullination (B) or extracellular traps structure (C) in both cell lines. At the same time, overexpression of PAD4, but not PAD2 or PAD4 with C645S mutation, induced histone H3 citrullination (D) and extracellular traps structure (E) in both cell lines. Scale bar in C & E, 10 μm

Figure 4-4.

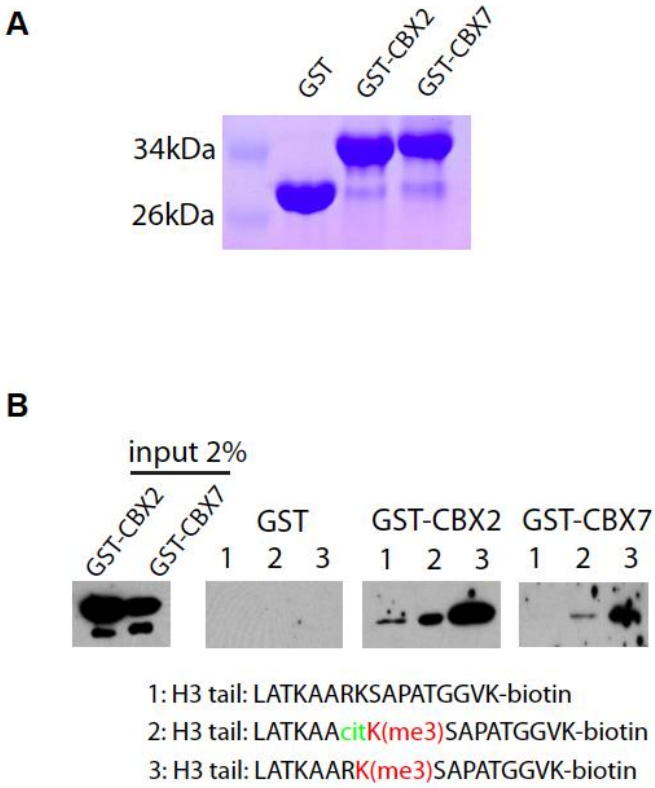

Figure **4-4.** Citrullination on histone H3 arginine 26 interferes with binding of chromodomain protein to methylated lysine 27.

Chromodomain of CBX 2 and CBX 7 are amplified from residues (6-69) and (1-71) of the proteins respectively. The GST or GST tagged chromodomain proteins are purified from BL21 *E.coli* strain (A). Histone H3 peptides with no modification, cit26, or cit26K27me3 were labeled with biotin and used in the peptide pull down assay. Binding efficiency of chromodomain proteins to different peptides are evaluated by western blotting (B).

Chapter 5

Summary and Future Directions

5.1 Summary

In my thesis, I have explored different biology aspects that are involved in the development and treatment of tumor. I have tested the systematic effects of a small molecule PZ1225 on cancer cells. The small molecule induced DNA damage, activated ER stress/UPR, inhibited autophagy and resulted in apoptotic cell death in tumor cells. A combinatorial therapy is also developed based on the mechanism study of PZ1225. At the same time, I explored the mechanism of macrophage extracellular trap formation, which may shed light on the studies of tumor associated macrophages.

With the advantage of microarray analyses, we are able to obtain a comprehensive perspective and study the cellular pathways affected by PZ1225 in a network. The network consists of ER stress, mTOR, autophagy, apoptosis and MAPK pathway. In PZ1225 treated cells, inhibition of mTOR signaling pathway potentially leads to inhibition of autophagy and MAPK kinase cascade[89,199-201]. The interconnection of top signaling pathways affected by PZ1225 is taken into consideration in the design of the combination therapy.

To reach an accurate evaluation, high-throughput analyses need to be supplemented with biochemistry and molecular biology methods. For example, in the microarray analysis, we cannot draw a conclusion on regulation of autophagy since the diagnosis markers used for autophagy is not detectable at the transcriptional level. However, when autophagy was investigated using tandem GFP-mcherry-LC3 system and double staining of Lamp1 and LC3, imaging tools revealed inhibition of autophagy at later stages.

Similarly, in the study of macrophage extracellular traps, we cannot adapt an isolated view to interpret the result. In fact, the highly plastic and versatile nature of macrophage population requires us to pay special attention to the lineage and maturity status of the cell. My study in the peritoneal cavity macrophages presents a simple yet important mechanism of MET formation, i.e., the correlation of METs and PAD4 expression. The study also clarifies a facultative role of PAD2 in histone citrullination, if not dispensable.

5.2 Combinatorial therapy is a highly promising approach to overcome drug resistance in chemotherapy

Resistance to chemotherapy develops under different mechanisms. At cellular level, cancer cells detoxify chemotherapy agents by drug inactivation, decreased drug intake, increased drug efflux, alteration of the target pathway, etc. At the genomic level, cancer genome acquires mutations that escape targeting of specific inhibitors, activates additional cell survival signaling pathways and DNA damage repair machineries, disrupts programmed cell death pathways such as apoptosis, etc[31,32,202]. Most importantly, tumor tissue is intrinsically heterogeneous. In the tumor tissue, a small group of cells acquire the properties similar to the stem cells and are more resistant to certain chemotherapy[44,203-205]. When cancer cells are challenged by chemotherapy, the drug resistant cells are selected and further develop into multi-drug resistant malignant tumor.

To overcome drug resistance, combination therapy is one of the most effective strategies[50,51,202,206]. Combination therapy is not a totally novel strategy. It has been applied to the treatment of HIV and achieved certain successes. The first combination therapy in cancer treatment dated back to the 1980s. Back then, the rationale for drug combination is indeed extremely poor. With the development of sequencing techniques and high-throughput analyses nowadays, design of combinatorial therapy is much more reliable than decades ago. However, current combination strategies consisting of targeted drugs and chemotherapy agents are still rather pragmatic than following a compelling rationale. Examples include the combination of

monoclonal antibodies trastuzumab with chemotherapy agent paclitaxel and rituximab with doxorubicin[207,208]. In these cases, targeted drugs are the major player that results in the cancer-killing efficacy and chemotherapy agents are added to induce an overall non-targeted cytotoxicity.

In the last decades, we have reached many achievements in the treatment of cancer. A large number of inhibitors are designed and many have been approved by FDA, which creates a huge pool of possible combinations. Thus a reliable and rational strategy is in need. Most of the computational methods currently lack a comprehensive view of the cell protein networks[51]. Indeed, an in-depth study into the protein networks will be powerful in predicting the efficacy of therapy.

Here we developed a network modeling method to design combinatorial therapy. Firstly, the cells are processed for microarray analyses and genes with more than 2 fold change in expression level are used as the pool for all the analyses. In our study, we used molecular and cellular biology means to supplement for the high throughput study and developed a network model of PZ1225. Based on this network, possible combinatorial inhibitors are explored by their effects in correlation with genes affected by PZ1225. We then studied the genes targeted by both PZ1225 and possible combinatorial inhibitors and analyzed the gene function. That is when we found the MAPK inhibitors U0126, PD98059 and PI3K inhibitors LY294002

decrease a group of genes that are induced by PZ1225. Many genes in this group regulate transcription and cell proliferation, suggesting that up-regulation of these genes after PZ1225 treatment is an attempt of cancer cells to restore the homeostasis and resist the killing. Thus we inhibited the possible drug resistant signaling pathways and achieved significant increase in killing efficacy. This in-depth network modeling method could be applied to the therapy design in the personalized medicine. Together with the information on genomic background of patient, the prediction on drug effects will be more precise and specific.

Although we adapted in-depth high throughput analyses and supplemented it with other experiments, there are still genes affected in the network that we do not fully understand. For example, the WM115 cells already contain the constitutively active MAPK signaling. But PZ1225 treatment further activated the MEK 1/2 kinase and the mechanism remains unclear. Studies of the mechanism will potentially add to the current combination therapy and even creates better combinations.

5.3 Studies on the MET formation will shed light on study of cancer microenvironment

In cancer biology, discussion on the immune cells has been focused on T cells, natural killer (NK) cells and dendritic cells (DCs) while a large

amount of tumor-associate neutrophils (TANs) and tumor-associated macrophages (TAMs) is also found in the tumor tissue[105,209-211]. As the first line of defenders during the infection of pathogens, reports on TANs and TAMs present both beneficial and deleterious roles in the tumor development and in the cancer chemotherapy.

The function of NETs in tumor is newly discovered and poorly defined. So far, it is considered more of a beneficial mechanism to the cancer cell proliferation and metastasis. In 2013, Zychlinsky group is among the first to show TANs in Ewing sarcoma (ES) form NETs using the patient specimen sections[127]. They proposed the possibility of roles played by NETs could be both pro-cancer and anti-cancer. Later, Lorenzo Ferri group published their study on NETs formation after surgical resection of tumor. In a murine infection model, they demonstrated induction of microvascular NETs deposition and trapping of circulating lung carcinoma cells under the webbed structure. Concurrently, they observed an increase in hepatic micrometastases at 48 hours and a heavier metastases burden at 2 weeks[128]. Similarly, Allan Tsung group reported a correlation of NETs and liver cancer metastasis after surgical resection of tumor in patients. In a murine model, they showed local inhibition of NETs formation or DNase digestion of NETs reduces the metastatic propensity[121]. These data in murine model and in human patients suggest a pro-cancer role of NETs *in vivo*. With proteins such as neutrophil elastase and myeloperoxidase being components of NETs, the

roles NETs play in tumor progression extend beyond the chromatin fibers *per se*.

Compared to NETs, METs remains a poorly studied field. The challenge in macrophage studies is partly created by the plasticity of these cells. In human body, large numbers of macrophages remain resident in the tissue while additional monocyte in the bone marrow will be recruited to inflammation site and differentiate into more macrophages[212,213]. Macrophages from different organs present slightly different morphology and express different surface markers. Researchers try tocategorize mature macrophages mainly into two lineages—the M1 macrophages and M2 macrophages. M1 macrophages are pro-inflammatory and are induced in response to Th1 cytokines such as IFN-γ . In contrast, M2 macrophages are anti-inflammatory and are induced by cytokines such as IL-4 and IL-13[214]. They secret a high level of IL-10 and exert an immune-repressive function. TAMs in the tumor tissue are more likely to present an M2-like phenotype and promote cancer cell growth, progression and metastasis[214]. But the definition of M1 and M2 macrophages is oversimplified and not applicable in many occasions[215].

The PCM used in the METs study is extracted from unstimulated C57BL/6J mice. According to the studies of cell surface markers and maturity of cells, PCM consists of two groups of cells—large peritoneal macrophages

(F4/80 ^{high} CD11b ^{high} MHC-II^{-}) and small peritoneal macrophages (F4/80 ^{high} CD11b ^{high} MHC-II ^{high}). Under physiological condition, 90% of macrophages in the peritoneal cavity belong to the more mature LPM group[216,217]. In our study, the percentage of cells form METs is around 6%. With the data obtained so far, we have little clue on the correlation of macrophage subpopulation and METs formation. However, studies on the subpopulation of macrophages and their functions will be important in the understanding of macrophage function. Flow cytometry is a powerful tool to isolate macrophage cells into different lineage but it relies on selection of surface markers to define the lineages.

In this thesis, I reported the requirement for PAD4 but not PAD2 in METs formation. The function of PADs in mediating histone citrullination has been focused on PAD4 and PAD2. In multiple tumor types, elevated PAD4 expression has been reported[218]. When treated with PAD inhibitors, tumor size shrunk in a mouse xenograft model[92]. These data together suggest a role of PAD4 in tumor tissue. Inhibitors of PADs like Cl-amidine and YW3-56 are both pan-PAD inhibitors thus exploration on PAD4 could be done using the PAD4 transgenic mice.

Notably, PAD4 expression is required for extracellular trap formation in neutrophils[125] and macrophages (chapter 4 of the thesis). In cancer cells, overexpression of PAD4 also induces hypercitrullination on histones and

release of decondensed chromatin[129]Studies into the ET components will be important to distinguish different ETs in the tumor tissue. At the same time, whether cancer cell produces ETs in vivo and possible functions of the structure need further investigation.

On the METs structures, Iidentified histone hypercitrullination at histone H3 arginine 2, 8, 17 and 26 in the PAD4 wild type macrophages. In the macrophage cell lines express abundant PAD2 protein, although hypercitrullination is not observed, an elevation of histone H3 citrullination suggests a role of other PADs in the mediation of local citrullination. Considering the fact that citrullination at arginine 26 interferes with recognition of methylated lysine 27, citrullination of histone in the gene promoter may regulate expression of genes directly.

Appendix

PADA4 exacerbates the brain damage after stroke in C57BL/6J mice.

Appendix A presents my work for a collaboration project with my colleague Yuchen Chen in Dr. Gong Chen lab in the Biology department at Pennsylvania State University (University Park). Yuchen Chen performed all the surgery work on mice to induce stroke and I maintained the mice colonies and performed analyses of the mice samples.

A.1 Introduction

Stroke is the leading cause of disability[219,220]. In the United States, stroke happens to someone every 40 seconds. Ischemic stroke makes up about 80% of all types of stroke (data from Centers for Disease Control and Prevention and American Stroke Association). Up to now, the only FDA approved medicine for ischemic stroke is tissue plasminogen activator (tPA). tPA works by dissolving blood vessel clots and restoring blood flow back to the stroke site. However, to avoid neuronal death, the medicine needs to be administered within 4.5 hours of stroke onset[221,222]. In addition, one potential risk of tPA is bleeding in the brain and other tissues, which results in hemorrhage that is life threatening. Several studies already showed that clot-dissolving reagents indeed increased the number of patients died following stroke[223,224].

The damage of stroke mainly resulted from neuronal death[225,226]. In the cerebral cortex, different types of neurons control the movement, sensation, vision, emotion, memory, speech and the ability to reason and think. Stroke induces irreversible damage to neurons, which impair the function of human body permanently. During and after stroke, systematic immune responses play important yet complicated roles, beneficial and deleterious. The immune response isinduced by resident glial cells, astrocytes and neurons in the brain as well as infiltrated monocytes and neutrophils from the blood stream[227-231]. For example, activation of microglia and astrocytes induce a cascade of immune responses after stroke and potentially exacerbate the damage to neuronal cells[231]. Intervention of the immune responses has been explored as potential therapeutic strategy[232,233].

As mentioned previously in Chapter 4, PAD4 was reported to be involved in the pathology of diseases. Most recently (2014-2016), several papers reported that PAD4 exacerbated the ischemia/reperfusion stress pathology in myocardial[180], kidney[212] and liver[234] tissues. Either knockout of PAD4 gene or administration of PAD4 inhibitor could rescue the stress pathology. Interestingly, DNase I, which digests extracellular DNA, could also rescue the stress pathology[180], suggesting a function of ETs in the ischemia/reperfusion stress.

To explore the function of PAD4 in ischemia/reperfusion injury, a murine stroke model is constructed by injection of endothelin-1 into the forelimb motor cortex. As a result, stroke is induced and fine movements of mice forelimbs are impaired, which could be detected by behavior analyses such as staircase test and grid walking test. Endothelin-1 (ET-1) is a vasoconstrictor produced by vascular endothelial cells. Once delivered into the cerebral cortex, ET-1 results in contraction of blood vessel and focal ischemia. After couple hours, ET-1 become inactive, blood stream flows back into the ischemic tissue, which results in reperfusion injury.

Here I present the preliminary results obtained in the murine stroke model. I have observed neuronal protection in PAD4 knockout mice and decrease in the tissue loss. Concurrently, less cytokine/chemokine expression is observed in the PAD knockout mice brain.

A.2 Results

In the 4 sets of preliminary experiments, I have observed reduced neuronal damage and tissue loss in the mice brain (Figure A-1).Neuronal marker NeuN reduced significantly in the PAD4 wild type mice. NeuN is a nuclear antigen that expresses specifically in the neuronal cells. NeuN expresses abundantly in mature neurons but not in unhealthy or dying neurons. Loss of NeuN signal at the stroke site suggests the damage of

neurons after stroke. Interestingly, in PAD4 knockout mice, less damage of neuron (denoted by more healthy NeuN staining) is observed at the stroke site, suggesting knockout of PAD4 either helped the recovery of damaged neurons or protected neurons from the ischemia/reperfusion injury from the beginning.

Glial fibrillary acidic protein (GFAP) is an intermediate filament protein expressed by astrocytes. In brain damage, GFAP highly expresses in the reactive astrocytes, which is the major components in the glial scare around the damaged site. The glial scar prevents the spreading of the stress signals and protected tissues around the damaged site. At the same time, astrocytes extend their plasma membrane to fill the empty space generated by dead neurons, which potentially impair the regeneration of neuron[235]. In PAD4 wild type stroke brain, I observed thickened and elongated processes of astrocytes denoted by GFAP staining (Figure A-1). Notably, the GFAP signal also denotes a glial scar surrounding the tissue damage site. In the PAD4 knockout mice, however, the glial scare is much smaller and less GFAP process extension and thickening are observed, suggesting that PAD4 promotes reactive astrocyte and formation of glial scar.

Iba1 is a 17 kDa protein in the cytoplasm of microglia and macrophages. Its expression is upregulated in the reactive microglia after brain injury such as ischemic stroke. The reactive microglia presents a

"deramified" morphology with enlarged soma and shortened processes[236]. This is exactly the morphology of microglia in the PAD4 wild type brain after stroke, denoted by Iba1 staining (Figure A-1). Again, in the PAD4 knockout mice, the number of reactive microglia is significantly less than that in the wild type (Figure A-1), suggesting decreased inflammation in the injured brain.

From the microarray data obtained from PAD4 knockout neutrophils (data from lab member Dr. Pingxin Li), we identified several cytokine/chemokine whose expression is affected by PAD4. I tested the expression of the same group of factors in the damage brain tissue and in the blood stream of the stroke mice. Interestingly, in the brain tissue extracted from the damaged site, I detected decreased cytokine/chemokine expression in PAD4 knockout mice; while in the blood serum, a higher level of IL-6 protein is detected in the same group of mice. The results suggest circulating immune cells and the resident immune cells may be regulated by different mechanisms in the ischemic injury.

A.3 Summary and future direction

The preliminary results clearly suggest a role of PAD4 in the ischemia/reperfusion injury induced by stroke in the mouse brain. The difference of cytokine/chemokine expression in PAD4 wild type and

knockout mice further suggests a role of PAD4 in the immune system. In future explorations, I will test the detailed mechanism behind the protective role of PAD4 suppression. The exacerbation of ischemia/reperfusion damage induced by PAD4 could be due to several reasons. First of all, the ischemia/reperfusion injury in the tissue inevitably induces inflammation. It has been reported that in rheumatoid arthritis patient, inflammation induced antibodies are directed specifically to citrullinated proteins, which is one of the mechanisms that initiate the pain in the joint and promote development of advanced disease[237,238]. Secondly, the discovery of NETs at the tissue damage site suggests a function of extracellular trap in the disease pathology. Notably, when NETs or other ETs were released, cellular contents were projected to the extracellular space as well, which further triggers local inflammation. Last but not least, PAD4 contains a nucleus localization signaling and citrullinates histones. Considering the binary code I proposed in Chapter 4, PAD4 may directly affect gene expression by altering activating/suppressing markers on the histones.

Notably, PAD4 inhibitor YW3-56 was not able to induce a significant protective effect in the preliminary tests (Figure A-2). It worth mention that in these test, YW3-56 is delivered by intraperitoneal injection at the same time and after the stroke onset. Whether the inhibitor could penetrate the blood brain barrier is an open question. I will explore different delivery methods in the later experiment design.

Figure A-1.

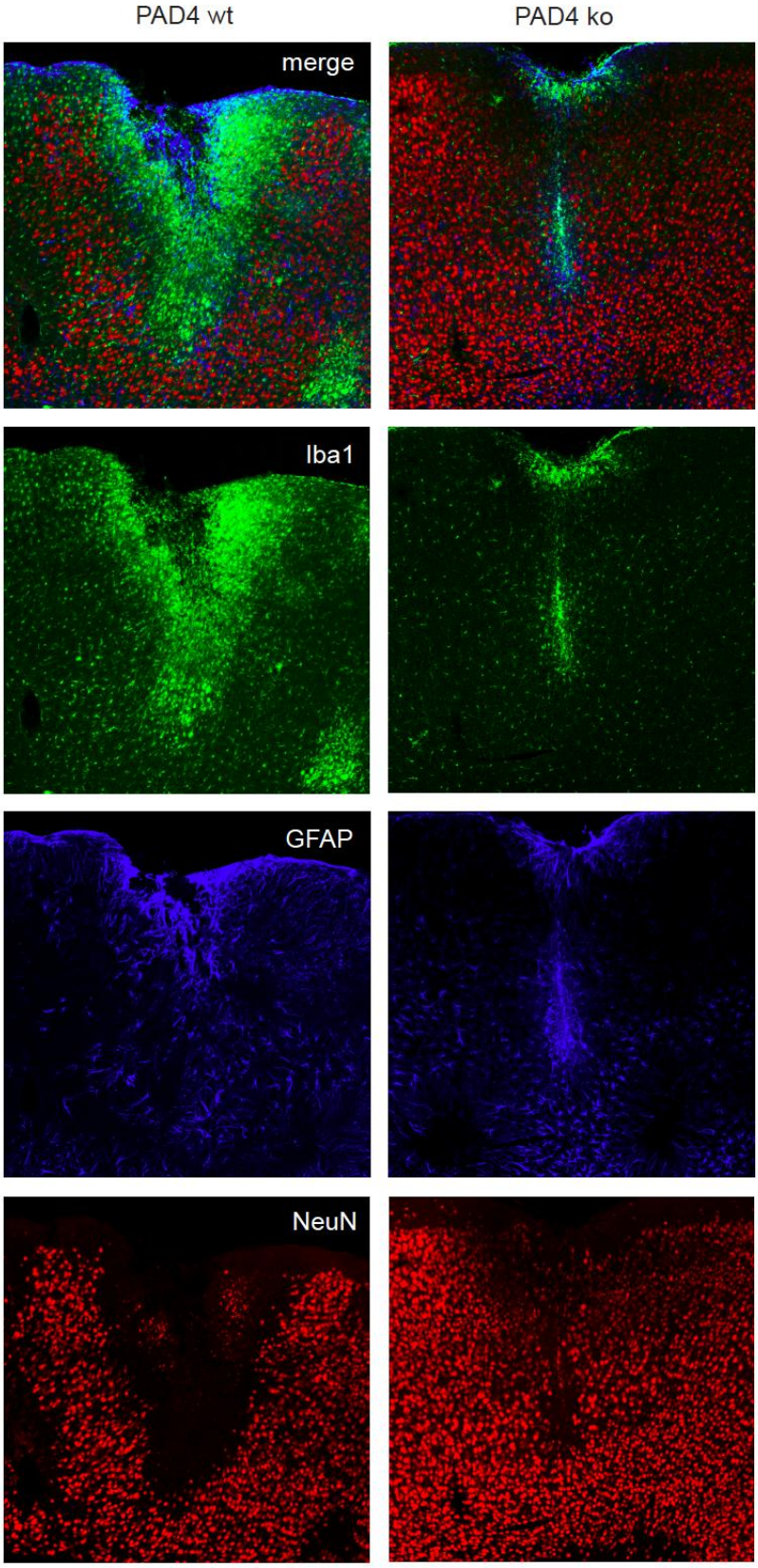

Figure **A-1**. Immunostaining of NeuN, Iba1, GFAP in the mice brain following stroke induction.

Both PAD4 wild type and knockout mice in the C57Bl/6J background are used for the induction of stroke. The surgeries are administered as described in the method. 14 days after stroke, mice are euthanized and perfused before extraction of brain. Following 15 h to 24 h fixation, mice brains are sliced and preceded to IHC analyses. NeuN is used as neuron marker, Iba1 as microglia marker and GFAP as astrocyte marker. In the PAD4 knockout mice, neurons are protected and less glial scar and inflammation are observed.

Figure A-2.

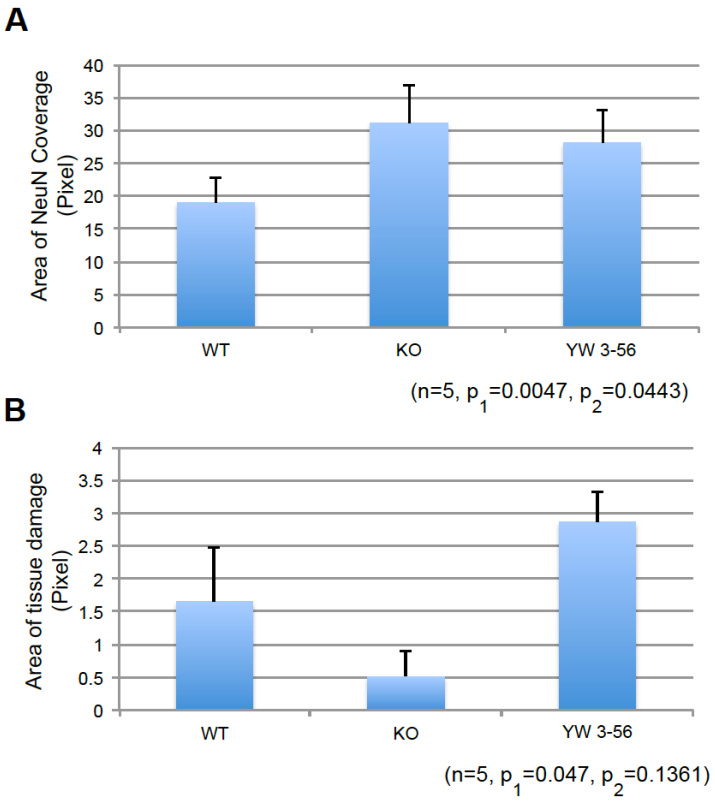

Figure **A-2**. Result observed in figure A-1 is quantified with Image J.
The areas of NeuN coverage (A) and tissue loss (B) are quantified. PAD4 knockout presented a significant increase in NeuN coverage (p-value=0.0047) and decrease in tissue loss (p-value=0.047). However, the PAD4 inhibitor YW3-56 delivered by i.p. injection did not show a significant difference compared to wild type in both NeuN coverage and tissue loss (p-value=0.0443 and 0.1361 respectively).

Figure A-3.

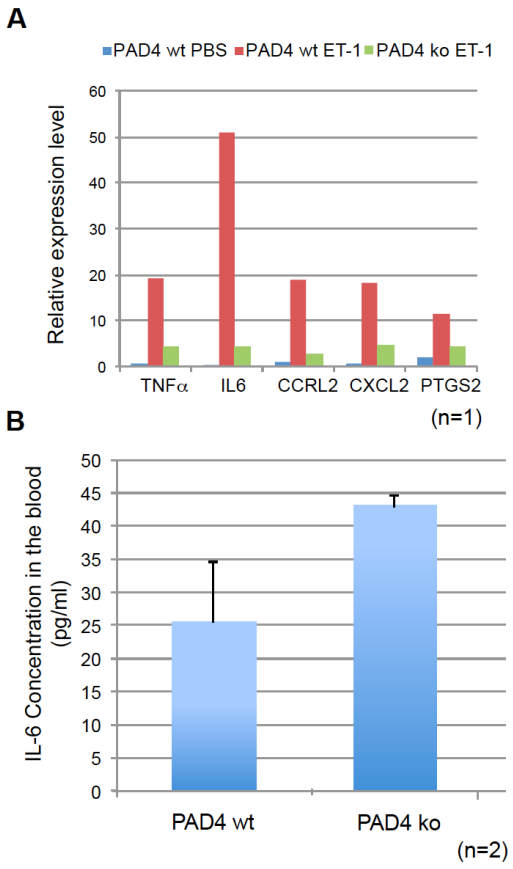

Figure **A-3**. Preliminary data shows cytokine/chemokine expression differs in the brain tissue (A) and in the blood stream (B) of PAD4 knockout mice.
Key cytokines and chemokine that are hypothesized to be affected by PAD4 are tested in the brain tissue extracted specifically from the damage site. In knockout mice, decreased expression of the factors is observed. Blood are extracted from heart before perfusion of the brain and IL-6 in the blood serum is detected using ELISA. Increased IL-6 in the circulating blood is observed in PAD4 knockout mice.

Bibliography

1. Douglas Hanahan RAW. The Hallmarks of Cancer. *Cell* 2000; **100**: 14.
2. Hanahan D, Weinberg RA. Hallmarks of cancer: the next generation. *Cell* 2011; **144**(5): 646-74.
3. Cheung-Ong K, Giaever G, Nislow C. DNA-damaging agents in cancer chemotherapy: serendipity and chemical biology. *Chem Biol* 2013; **20**(5): 648-59.
4. Society AC. Cancer Facts & Figures 2016. 2016.
5. Hansemann VDD. Ueber asymmetrische Zelltheilung in epithel Krebsen und deren biologische Bedeutung. *Virchow's Arch Path Anat* 1890; **119**.
6. Boveri T. Zur Frage der Entstehung Maligner Tumoren. *Science* 1914; **40**(1041): 3.
7. Nowell PC, Hungerford DA. A minute chromosome in human chronic granulocytic leukemia. *Science* 1960; (132): 14.
8. A dK, AG vK, G G, et al. A cellular oncogene is translocated to the Philadelphia chromosome in chronic myelocytic leukaemia. . *Nature* 1982; (300): 3.
9. ROWLEY JD. A New Consistent Chromosomal Abnormality in Chronic Myelogenous Leukaemia identified by Quinacrine Fluorescence and Giemsa Staining. *Nature* 1973; (243): 4.
10. Shih C, Shilo BZ, Goldfarb MP, Dannenberg A, Weinberg RA. Passage of phenotypes of chemically transformed cells via transfection of DNA and chromatin. *Proc Natl Acad Sci* 1979; (76): 5.
11. Pulciani S, Santos E, Lauver AV, Long LK, Robbins KC, Barbacid M. Oncogenes in human tumor cell lines: molecular cloning of a transforming gene from human bladder carcinoma cells. *Proc Natl Acad Sci* 1982; (79): 5.
12. Parada LF, Shih CJ, Weinberg RA. Human EJ bladder carcinoma oncogene is homologue of Harvey sarcoma virus ras gene. *Nature* 1982; (297): 5.
13. Goldfarb M, Shimizu K, Perucho M, Wigler M. Isolation and preliminary characterization of a human transforming gene from T24 bladder carcinoma cells. *Nature* 1982; (296): 5.
14. Knudson AG. Mutation and cancer: statistical study of retinoblastoma. *Proc Natl Acad Sci* 1971; (68): 4.
15. O'Connor MJ. Targeting the DNA Damage Response in Cancer. *Mol Cell* 2015; **60**(4): 547-60.
16. Negrini S, Gorgoulis VG, Halazonetis TD. Genomic instability--an evolving hallmark of cancer. *Nat Rev Mol Cell Biol* 2010; **11**(3): 220-8.
17. Lord CJ, Ashworth A. The DNA damage response and cancer therapy. *Nature* 2012; **481**(7381): 287-94.
18. Jackson SP, Bartek J. The DNA-damage response in human biology and disease. *Nature* 2009; **461**(7267): 1071-8.
19. R F, MK L, MR R, et al. The human mutator gene homolog MSH2 and its association with hereditary nonpolyposis colon cancer. *Cell* 1993; **75**: 12.
20. CE B, SM B, PT M, et al. Mutation in the DNA mismatch repair gene homologue hMLH1 is associated with hereditary non-polyposis colon cancer. *Nature* 1994; **368**: 4.

21. Vilar E, Gruber SB. Microsatellite instability in colorectal cancer—the stable evidence. *Nature Reviews Clinical Oncology* 2010: 10.
22. CR B, A G. Microsatellite instability in colorectal cancer. *Gastroenterology* 2010; **138**: 15.
23. EB K, HD K. The blood and bone marrow in yellow cross gas (mustard gas) poisoning: changes produced in the bone marrow of fatal cases. *J Med Res* 1919; **40**: 12.
24. LS G, MM W, W D, MJ G, A G, MT M. Nitrogen mustard therapy; use of methyl-bis (beta-chloroethyl) amine hydrochloride and tris (beta-chloroethyl) amine hydrochloride for Hodgkin's disease, lymphosarcoma, leukemia and certain allied and miscellaneous disorders. *J Am Med Assoc* 1946; **132**: 7.
25. S F. Some observations on the effect of folic acid antagonists on acute leukemia and other forms of incurable cancer. *Blood* 1949; **4**: 7.
26. S F, LK D. Temporary remissions in acute leukemia in children produced by folic acid antagonist, 4-aminopteroyl-glutamic acid. *N Engl J Med* 1948; **238**: 7.
27. Li MC, Hertz R, Bergenstal DM. Therapy of choriocarcinoma and related trophoblastic tumors with folic acid and purine antagonists. *N Engl J Med* 1958; **259**: 9.
28. Rosenberg B, Camp LV, Krigas T. Inhibition of Cell Division in Escherichia coli by Electrolysis Products from a Platinum Electrode. *Nature* 1965.
29. C T, H T, KP Y, ML M, DA K. Daunomycin, an antitumor antibiotic, in the treatment of neoplastic disease: Clinical evaluation with special reference to childhood leukemia. *Cancer* 1967; **20**: 21.
30. Theologides A, Yarbro JW, Kennedy BJ. Daunomycin inhibition of DNA and RNA synthesis. *Cancer* 1968; **21**(1): 6.
31. Sun Y-L, Patel A, Kumar P, Chen Z-S. Role of ABC transporters in cancer chemotherapy. *Chinese Journal of Cancer* 2012; **31**(2): 7.
32. Eckford PDW, Sharom FJ. ABC Efflux Pump-Based Resistance to Chemotherapy Drugs. *Chem Rev* 2009; **109**(7): 23.
33. Choi CH. ABC transporters as multidrug resistance mechanisms and the development of chemosensitizers for their reversal. *Cancer Cell Int* 2005; **5**: 30.
34. Rad R, Cadinanos J, Rad L, et al. A genetic progression model of Braf(V600E)-induced intestinal tumorigenesis reveals targets for therapeutic intervention. *Cancer Cell* 2013; **24**(1): 15-29.
35. Fenaux EWCPBHMVBQIDPMP. p53 Mutations Are Associated With Resistance to Chemotherapy and Short Survival in Hematologic Malignancies. *Blood* 1994; **84**(9).
36. Reles A, Wen WH, Schmider A, et al. Correlation of p53 Mutations with Resistance to Platinum-based Chemotherapy and Shortened Survival in Ovarian Cancer. *Clinical Cancer Research* 2001; **7**: 14.
37. Do PM, Varanasi L, Fan S, et al. Mutant p53 cooperates with ETS2 to promote etoposide resistance. *Genes & Development* 2012; **26**(8): 830-45.
38. Guo X, Ma N, Wang J, et al. Increased p38-MAPK is responsible for chemotherapy resistance in human gastric cancer cells. *BMC Cancer* 2008; **8**(375): 9.
39. Lee JM, Bernstein A. Apoptosis, cancer and the p53 tumour suppressor gene. *Cancer and Metastasis Reviews* 1995.

40. Fridman JS, Lowe SW. Control of apoptosis by p53. *Oncogene* 2003; **22**(56): 9030-40.
41. Wu GS. The functional interactions between the p53 and MAPK signaling pathways. *Cancer Biol Ther* 2004; **3**(2): 6.
42. BUSH JA, LI G. CANCER CHEMORESISTANCE: THE RELATIONSHIP BETWEEN P53 AND MULTIDRUG TRANSPORTERS. *Int J Cancer* 2002; **98**: 8.
43. V M, P W, M M, et al. Inhibition of mitogen-activated protein kinase Erk1/2 promotes protein degradation of ATP binding cassette transporters A1 and G1 in CHO and HuH7 cells. *PLoS One* 2013; **8**(4).
44. Navin N, Krasnitz A, Rodgers L, et al. Inferring tumor progression from genomic heterogeneity. *Genome Res* 2010; **20**: 13.
45. Parkin B, Ouillette P, Li Y, et al. Clonal evolution and devolution after chemotherapy in adult acute myelogenous leukemia. *Blood* 2013; **121**: 9.
46. Yao X, Panichpisal K, Kurtzman N, nugent K. Cisplatin Nephrotoxicity: A Review. *Am J Med Sci* 2007; **334**(2): 115-24.
47. Miller RP, Tadagavadi RK, Ramesh G, Reeves WB. Mechanisms of Cisplatin nephrotoxicity. *Toxins (Basel)* 2010; **2**(11): 2490-518.
48. Minotti G, Menna P, Salvatorelli E, Cairo G, Gianni L. Anthracyclines: molecular advances and pharmacologic developments in antitumor activity and cardiotoxicity. *Pharmacol Rev* 2004; **56**(2): 185-229.
49. Chatterjee K, Zhang J, Honbo N, Karliner JS. Doxorubicin cardiomyopathy. *Cardiology* 2010; **115**(2): 155-62.
50. Yardley DA. Drug resistance and the role of combination chemotherapy in improving patient outcomes. *Int J Breast Cancer* 2013; **2013**: 137414.
51. Al-Lazikani B, Banerji U, Workman P. Combinatorial drug therapy for cancer in the post-genomic era. *Nat Biotechnol* 2012; **30**(7): 679-92.
52. Inamdar GS, Madhunapantula SV, Robertson GP. Targeting the MAPK pathway in melanoma: why some approaches succeed and other fail. *Biochem Pharmacol* 2010; **80**(5): 624-37.
53. Cobb JMEMH. Pharmacological inhibitors of MAPK pathways. *TRENDS in Pharmacological Sciences* 2002; **23**(1): 6.
54. G.V. Long DS, H. Gogas, E. Levchenko, F. de Braud, J. Larkin, C. Garbe, T. Jouary, A. Hauschild, J.J. Grob, VP. Mohr, V. Probachai, D. Schadendorf, P. Nathan, C. Robert, A. Ribas, D.J. DeMarini, J.G. Irani, M. Casey, K. Flaherty. Combined BRAF and MEK Inhibition versus BRAF Inhibition Alone in Melanoma. *The New England Journal of Medicine* 2014; **371**: 12.
55. Eroglu Z, Ribas A. Combination therapy with BRAF and MEK inhibitors for melanoma: latest evidence and place in therapy. *Ther Adv Med Oncol* 2016; **8**: 9.
56. Ayers D, Nasti A. Utilisation of nanoparticle technology in cancer chemoresistance. *J Drug Deliv* 2012; **2012**: 265691.
57. Sturm I, Bosanquet A, Hermann S, Guner D, Dorken B, Daniel P. Mutation of p53 and consecutive selective drug resistance in B-CLL occurs as a consequence of prior DNA-damaging chemotherapy. *Cell Death and Differentiation* 2003; **10**: 8.
58. Jiricny J. The multifaceted mismatch-repair system. *Nat Rev Mol Cell Biol* 2006; **7**(5): 335-46.

59. Chaabane W, User SD, El-Gazzah M, et al. Autophagy, apoptosis, mitoptosis and necrosis: interdependence between those pathways and effects on cancer. *Arch Immunol Ther Exp (Warsz)* 2013; **61**(1): 43-58.
60. Ambrosini G, Adida C, Altieri DC. A novel anti-apoptosis gene, survivin, expressed in cancer and lymphoma. *Nature Medicine* 1997; **3**(8): 917-21.
61. Ouyang L, Shi Z, Zhao S, et al. Programmed cell death pathways in cancer: a review of apoptosis, autophagy and programmed necrosis. *Cell Prolif* 2012; **45**(6): 487-98.
62. Proskuryakov SY, Gabai VL. Mechanisms of Tumor Cell Necrosis. *Current Pharmaceutical Design* 2010; **16**: 14.
63. Skalka M, Matyasova J, Cejkova M. DNA IN CHROMATIN OF IRRADIATED LYMPHOID TISSUES DEGRADES IN VIVO INTO REGULAR FRAGMENTS. *FEBS LETTERS* 1976; **72**: 4.
64. Wong RS. Apoptosis in cancer: from pathogenesis to treatment. *J Exp Clin Cancer Res* 2011; **30**: 87.
65. B. Nelson Chau T-TC, Yisong Y. Wan, James DeGregori, Jean Y. J. Wang. Tumor Necrosis Factor Alpha-Induced Apoptosis Requires p73 and c-ABL Activation Downstream of RB Degradation. *Molecular and cellular biology* 2004; **24**: 10.
66. Aizawa T KT, Einhorn TA, Gerstenfeld LC. Induction of apoptosis in chondrocytes by tumor necrosis factor-alpha. *J Orthop Res* 2001; **19**: 12.
67. Jack Hutcheson JCS, Emily Bickel, Nathaniel J. Brown, Philippe Bouillet, Andreas Strasser, Harris Perlman. Combined loss of proapoptotic genes Bak or Bax with Bim synergizes to cause defects in hematopoiesis and in thymocyte apoptosis. *The Journal of experimental medicine* 2005; **201**: 12.
68. Feng Dong MP, Yangming Xiao, Youmin Zhong, Yimou Wu, Guangming Zhong. Degradation of the Proapoptotic Proteins Bik, Puma, and Bim with Bcl-2 Domain 3 Homology in Chlamydia trachomatis-Infected Cells. *Infect Immun* 2005; **73**: 4.
69. Hearps AC BJ, Connor CE, Woods GM, Lowenthal RM, Ragg SJ. Mitochondrial cytochrome c release precedes transmembrane depolarisation and caspase-3 activation during ceramide-induced apoptosis of Jurkat T cells. *Apoptosis* 2002; **7**: 8.
70. E Bossy-Wetzel DDN, D R Green. Mitochondrial cytochrome c release in apoptosis occurs upstream of DEVD-specific caspase activation and independently of mitochondrial transmembrane depolarization. *EMBO Journal* 1998; **17**: 13.
71. Chaitanya GV, Alexander JS, Babu PP. PARP-1 cleavage fragments- signatures of cell-death proteases in neurodegeneration. *Cell Communication and Signaling* 2010; **8**(31): 11.
72. Casares N, Pequignot MO, Tesniere A, et al. Caspase-dependent immunogenicity of doxorubicin-induced tumor cell death. *J Exp Med* 2005; **202**(12): 1691-701.
73. Breckenridge DG, Germain M, Mathai JP, Nguyen M, Shore GC. Regulation of apoptosis by endoplasmic reticulum pathways. *Oncogene* 2003; **22**(53): 8608-18.
74. Emmy P. Rogakou WN-N, Chye Boon, Yves Pommier, William M. Bonner. Initiation of DNA Fragmentation during Apoptosis Induces Phosphorylation of H2AX Histone at Serine 139. *The Journal of biological chemistry* 2000; **275**: 6.
75. Solier S, Pommier Y. The nuclear gamma-H2AX apoptotic ring: implications for cancers and autoimmune diseases. *Cell Mol Life Sci* 2014; **71**(12): 2289-97.

76. Yousefi S, Simon HU. Autophagy in cancer and chemotherapy. *Results Probl Cell Differ* 2009; **49**: 183-90.
77. Sui X, Chen R, Wang Z, et al. Autophagy and chemotherapy resistance: a promising therapeutic target for cancer treatment. *Cell Death Dis* 2013; **4**: e838.
78. Lee JG, Shin JH, Shim HS, et al. Autophagy contributes to the chemo-resistance of non-small cell lung cancer in hypoxic conditions. *Respir Res* 2015; **16**: 138.
79. Duran A, Linares JF, Galvez AS, et al. The signaling adaptor p62 is an important NF-kappaB mediator in tumorigenesis. *Cancer Cell* 2008; **13**(4): 343-54.
80. Qu X. Promotion of tumorigenesis by heterozygous disruption of the beclin 1 autophagy gene. *Journal of Clinical Investigation* 2003; **112**(12): 1809-20.
81. Tanida I UT, Kominami E. LC3 and Autophagy. *Methods Mol Biol* 2008; **445**: 12.
82. Salvatore J. Cherra III SMK, Guy Uechi, Manimalha Balasubramani, John Mountzouris, Billy W. Day, Charleen T. Chu. Regulation of the autophagy protein LC3 by phosphorylation. *The Journal of cell biology* 2010; **190**: 7.
83. Ogata M, Hino S, Saito A, et al. Autophagy is activated for cell survival after endoplasmic reticulum stress. *Mol Cell Biol* 2006; **26**(24): 9220-31.
84. Khaminets A, Heinrich T, Mari M, et al. Regulation of endoplasmic reticulum turnover by selective autophagy. *Nature* 2015; **522**(7556): 354-8.
85. Zhang X, Yuan Y, Jiang L, et al. Endoplasmic reticulum stress induced by tunicamycin and thapsigargin protects against transient ischemic brain injury: Involvement of PARK2-dependent mitophagy. *Autophagy* 2014; **10**(10): 1801-13.
86. Wang Y, Li P, Wang S, et al. Anticancer peptidylarginine deiminase (PAD) inhibitors regulate the autophagy flux and the mammalian target of rapamycin complex 1 activity. *J Biol Chem* 2012; **287**(31): 25941-53.
87. Senft D, Ronai ZA. UPR, autophagy, and mitochondria crosstalk underlies the ER stress response. *Trends Biochem Sci* 2015; **40**(3): 141-8.
88. Kim YC, Guan KL. mTOR: a pharmacologic target for autophagy regulation. *J Clin Invest* 2015; **125**(1): 25-32.
89. Jung CH, Ro SH, Cao J, Otto NM, Kim DH. mTOR regulation of autophagy. *FEBS Lett* 2010; **584**(7): 1287-95.
90. Yang ZJ, Chee CE, Huang S, Sinicrope FA. The role of autophagy in cancer: therapeutic implications. *Mol Cancer Ther* 2011; **10**(9): 1533-41.
91. Padmaja Gadea GR, Uday B. Maachania, Mark A. Rizzoc, Tetsuya Okadad, Ron Prywese, Alan S. Crossb, Kazutoshi Morid, and Dhananjaya V. Kalvakolanu. An IFN-γ–stimulated ATF6–C/EBP-β–signaling pathway critical for the expression of Death Associated Protein Kinase 1 and induction of autophagy. *PNAS* 2012; **109**: 6.
92. Wang S, Chen XA, Hu J, et al. ATF4 Gene Network Mediates Cellular Response to the Anticancer PAD Inhibitor YW3-56 in Triple-Negative Breast Cancer Cells. *Mol Cancer Ther* 2015; **14**(4): 877-88.
93. Bruning A, Rahmeh M, Friese K. Nelfinavir and bortezomib inhibit mTOR activity via ATF4-mediated sestrin-2 regulation. *Mol Oncol* 2013; **7**(6): 1012-8.
94. B'Chir W, Maurin AC, Carraro V, et al. The eIF2alpha/ATF4 pathway is essential for stress-induced autophagy gene expression. *Nucleic Acids Res* 2013; **41**(16): 7683-99.

95. Hettman J, Movva NR, Hall MN. Targets for cell cycle arrest by the immunosuppressant rapamycin in yeast. *Science* 1991; **253**: 5.
96. Matsushita M, Suzuki NN, Obara K, Fujioka Y, Ohsumi Y, Inagaki F. Structure of Atg5.Atg16, a complex essential for autophagy. *J Biol Chem* 2007; **282**(9): 6763-72.
97. Komatsu M, Waguri S, Ueno T, et al. Impairment of starvation-induced and constitutive autophagy in Atg7-deficient mice. *J Cell Biol* 2005; **169**(3): 425-34.
98. Zheng Q, Su H, Ranek MJ, Wang X. Autophagy and p62 in cardiac proteinopathy. *Circulation research* 2011; **109**(3): 296-308.
99. Komatsu M, Ichimura Y. Physiological significance of selective degradation of p62 by autophagy. *FEBS Lett* 2010; **584**(7): 1374-8.
100. Susann Voigt SP, Parvin Davarnia, Supandi Winoto-Morbach, Christian Röder, Christoph Arenz, Anna Trauzold, Dieter Kabelitz, Stefan Schütze, Holger Kalthoff and Dieter Adam. TRAIL-induced programmed necrosis as a novel approach to eliminate tumor cells. *BMC Cancer* 2014; **14**: 14.
101. Peter Vandenabeele WD, Franky Van Herreweghe, and Tom Vanden Berghe. The Role of the Kinases RIP1 and RIP3 in TNF-Induced Necrosis. *Science Signaling* 2010; **3**(115): 9.
102. Fiers W BR, Boone E , Cornelis S , Declercq W , Decoster E , Denecker G , Depuydt B , De Valck D , De Wilde G , Goossens V , Vandevoorde V , Vercammen D, et al. TNF-induced intracellular signaling leading to gene induction or to cytotoxicity by necrosis or by apoptosis. *Europe PMC* 1995; **47**: 9.
103. Dinnen RD DL, Petrylak DP, Mao Y, Cassai N, Szmulewicz J, et al. Activation of targeted necrosis by a p53 peptide: a novel death pathway that circumvents apoptotic resistance. *J Biol Chem* 2007; **282**(37): 12.
104. Srivastava P. Roles of heat-shock proteins in innate and adaptive immunity. *Nat Rev Immunol* 2002; **2**(3): 185-94.
105. Gajewski TF, Schreiber H, Fu YX. Innate and adaptive immune cells in the tumor microenvironment. *Nat Immunol* 2013; **14**(10): 1014-22.
106. Sauter B, Albert ML, Francisco L, Larsson M, Somersan S, Bhardwaj N. Consequences of Cell Death: Exposure to Necrotic Tumor Cells, but Not Primary Tissue Cells or Apoptotic Cells, Induces the Maturation of Immunostimulatory Dendritic Cells. *J Exp Med* 2000; **191**: 11.
107. Orsini F, Pavelic Z, Mihich E. Increased Primary Cell-mediated Immunity in Culture Subsequent to Adriamycin or Daunorubicin Treatment of Spleen Donor Mice. *Cancer Research* 1977; **37**: 8.
108. Arinaga S, Akiyoshi T, Tsuji H. Augmentation of the Generation of Cell-mediated Cytotoxicity after a Single Dose of Adriamycin in Cancer Patients. *Cancer Research* 1986; **46**: 4.
109. Obeid M, Tesniere A, Ghiringhelli F, et al. Calreticulin exposure dictates the immunogenicity of cancer cell death. *Nat Med* 2007; **13**(1): 54-61.
110. Correale P, Del Vecchio MT, Di Genova G, et al. 5-fluorouracil-based chemotherapy enhances the antitumor activity of a thymidylate synthase-directed polyepitopic peptide vaccine. *J Natl Cancer Inst* 2005; **97**(19): 1437-45.

111. Galetto A, Buttiglieri S, Forno S, Moro F, Mussa A, Matera L. Drug- and cell-mediated antitumor cytotoxicities modulate cross-presentation of tumor antigens by myeloid dendritic cells. *Anticancer Drugs* 2003; **14**(10): 833-43.
112. Gasser S, Orsulic S, Brown EJ, Raulet DH. The DNA damage pathway regulates innate immune system ligands of the NKG2D receptor. *Nature* 2005; **436**(7054): 1186-90.
113. Brinkmann V, Reichard U, Goosmann C, et al. Neutrophil Extracellular Traps Kill Bacteria. 2004.
114. Shigeharu Ueki RCNM, Ionita Ghiran, Lisa A. Spencer, Ann M. Dvorak, and Peter F. Weller. Shigeharu Ueki-Eosinophil extracellular DNA trap cell death mediates lytic release of free secretion-competent eosinophil granules in humans. 2013.
115. von Kockritz-Blickwede M, Goldmann O, Thulin P, et al. Phagocytosis-independent antimicrobial activity of mast cells by means of extracellular trap formation. *Blood* 2008; **111**(6): 3070-80.
116. Papayannopoulos V MK, Hakkim A, Zychlinsky A. Neutrophil elastase and myeloperoxidase regulate the formation of neutrophil extracellular traps. *The Journal of cell biology* 2010; **191**(3): 15.
117. Warnatsch A, Ioannou M, Wang Q, Papayannopoulos V. Neutrophil extracellular traps license macrophages for cytokine production in atherosclerosis. 2015.
118. Sokolove J, Brennan MJ, Sharpe O, et al. Brief report: citrullination within the atherosclerotic plaque: a potential target for the anti-citrullinated protein antibody response in rheumatoid arthritis. *Arthritis and rheumatism* 2013; **65**(7): 1719-24.
119. Knight JS, Luo W, O'Dell AA, et al. Peptidylarginine deiminase inhibition reduces vascular damage and modulates innate immune responses in murine models of atherosclerosis. *Circulation research* 2014; **114**(6): 947-56.
120. Gould TJ, Vu TT, Swystun LL, et al. Neutrophil extracellular traps promote thrombin generation through platelet-dependent and platelet-independent mechanisms. *Arteriosclerosis, thrombosis, and vascular biology* 2014; **34**(9): 1977-84.
121. Tohme S, Yazdani HO, Al-Khafaji AB, et al. Neutrophil Extracellular Traps Promote the Development and Progression of Liver Metastases after Surgical Stress. 2016.
122. Martinod K, Demers M, Fuchs TA, et al. Neutrophil histone modification by peptidylarginine deiminase 4 is critical for deep vein thrombosis in mice. *PNAS* 2013; **110**.
123. Fuchs TA, Brill A, Wagner DD. Neutrophil extracellular trap (NET) impact on deep vein thrombosis. *Arteriosclerosis, thrombosis, and vascular biology* 2012; **32**(8): 1777-83.
124. Wang Y, Li M, Stadler S, et al. Histone hypercitrullination mediates chromatin decondensation and neutrophil extracellular trap formation. *The Journal of cell biology* 2009; **184**(2): 205-13.
125. Li P, Li M, Lindberg MR, Kennett MJ, Xiong N, Wang Y. PAD4 is essential for antibacterial innate immunity mediated by neutrophil extracellular traps. *The Journal of experimental medicine* 2010; **207**(9): 1853-62.

126. Ravi S. Keshari AJ, Megha Dubey, Nikhil Kothari, Monica Kohli, Jaishri Bogra, Manoj K. Barthwal, Madhu Dikshit. Cytokines Induced Neutrophil Extracellular Traps Formation: Implication for the Inflammatory Disease Condition. *PloS one* 2012; **7**(10): 8.
127. Berger-Achituv S, Brinkmann V, Abed UA, et al. A proposed role for neutrophil extracellular traps in cancer immunoediting. *Front Immunol* 2013; **4**: 48.
128. Cools-Lartigue J, Spicer J, McDonald B, et al. Neutrophil extracellular traps sequester circulating tumor cells and promote metastasis. *J Clin Invest* 2013.
129. Leshner M, Wang S, Lewis C, et al. PAD4 mediated histone hypercitrullination induces heterochromatin decondensation and chromatin unfolding to form neutrophil extracellular trap-like structures. *Frontiers in immunology* 2012; **3**: 307.
130. Society AC. Cancer Facts and Figures. 2015: 56.
131. A. Rosalie David MRZ. Cancer: an old disease, a new disease or something in between? *Nature Revies Cancer* 2010; **10**: 6.
132. Darkin RKRBMS. Anti-cancer drugs which intercalate into DNA: How do they act? *TIBS* 1983.
133. Ferguson LR, Chen H, Collins AR, et al. Genomic instability in human cancer: Molecular insights and opportunities for therapeutic attack and prevention through diet and nutrition. *Semin Cancer Biol* 2015; **35** S5-S24.
134. Kaushik NK, Kaushik N, Attri P, et al. Biomedical importance of indoles. *Molecules* 2013; **18**(6): 6620-62.
135. Wang W, Zhao M, Wang Y, et al. {2-[1-(3-Methoxycarbonylmethyl-1H-indol-2-yl)-1-methyl-ethyl]-1H-indol-3-yl}-acet ic acid methyl ester (MIAM): its anti-cancer efficacy and intercalation mechanism identified via multi-model systems. *Mol Biosyst* 2011; **7**(3): 766-72.
136. Ichikawa Y, Ghanefar M, Bayeva M, et al. Cardiotoxicity of doxorubicin is mediated through mitochondrial iron accumulation. *J Clin Invest* 2014; **124**(2): 617-30.
137. Alshabanah OA, Hafez MM, Al-Harbi MM, et al. Doxorubicin Toxicity can be Ameliorated during Antioxidant L-Carnitine Supplementation. *Oxidative Medicine and Cellular Longevity* 2010; **3**(6): 428-33.
138. Eric Wattel CP, Bernard Hecquet, Michael Vanrumbeke, Bruno Quesnel, Isabelle Dervite, Pierre Morel, Pierre Fenaux. p53 Mutations Are Associated With Resistance to Chemotherapy and Short Survival in Hematologic Malignancies. *Blood* 1994; **84**(9).
139. Sun C, Wang L, Huang S, et al. Reversible and adaptive resistance to BRAF(V600E) inhibition in melanoma. *Nature* 2014; **508**(7494): 118-22.
140. Haluska FG, Tsao H, Wu H, Haluska FS, Lazar A, Goel V. Genetic alterations in signaling pathways in melanoma. *Clin Cancer Res* 2006; **12**(7 Pt 2): 2301s-7s.
141. Kumar SM, Dai J, Li S, et al. Human skin neural crest progenitor cells are susceptible to BRAF(V600E)-induced transformation. *Oncogene* 2014; **33**(7): 832-41.
142. Li B, Yuan M, Kim IA, Chang CM, Bernhard EJ, Shu HK. Mutant epidermal growth factor receptor displays increased signaling through the phosphatidylinositol-3 kinase/AKT pathway and promotes radioresistance in cells of astrocytic origin. *Oncogene* 2004; **23**(26): 4594-602.

143. Pritchard AL, Hayward NK. Molecular pathways: mitogen-activated protein kinase pathway mutations and drug resistance. *Clin Cancer Res* 2013; **19**(9): 2301-9.
144. Clarke HJ, Chambers JE, Liniker E, Marciniak SJ. Endoplasmic reticulum stress in malignancy. *Cancer Cell* 2014; **25**(5): 563-73.
145. Han D, Lerner AG, Vande Walle L, et al. IRE1alpha kinase activation modes control alternate endoribonuclease outputs to determine divergent cell fates. *Cell* 2009; **138**(3): 562-75.
146. Hollien J, Lin JH, Li H, Stevens N, Walter P, Weissman JS. Regulated Ire1-dependent decay of messenger RNAs in mammalian cells. *J Cell Biol* 2009; **186**(3): 323-31.
147. Harding HP, Novoa I, Zhang Y, et al. Regulated Translation Initiation Controls Stress-Induced Gene Expression in Mammalian Cell. *Molecular cell* 2000; **6**.
148. Hetz C. The unfolded protein response: controlling cell fate decisions under ER stress and beyond. *Nat Rev Mol Cell Biol* 2012; **13**(2): 89-102.
149. SteFan J. Marciniak CYY, Seiichi Oyadomari, Isabel Novoa, Yuhong Zhang, Rivka Jungreis, Kazuhiro Nagata, Heather P. Harding, David Ron. CHOP induces death by promoting protein synthesis and oxidation in the stressed endoplasmic reticulum. *Genes & Development* 2004; **18**: 13.
150. Wang M, Kaufman RJ. The impact of the endoplasmic reticulum protein-folding environment on cancer development. *Nat Rev Cancer* 2014; **14**(9): 581-97.
151. Bi M, Naczki C, Koritzinsky M, Fels D, Blais J, Koumenis C. ER stress - regulated translation increases tolerance to extreme hypoxia and promotes tumor growth. *The EMBO Journal* 2005.
152. Wielenga MC, Colak S, Heijmans J, et al. ER-Stress-Induced Differentiation Sensitizes Colon Cancer Stem Cells to Chemotherapy. *Cell Rep* 2015; **13**(3): 490-4.
153. Wang Q, Mora-Jensen H, Weniger MA, et al. ERAD inhibitors integrate ER stress with an epigenetic mechanism to activate BH3-only protein NOXA in cancer cells. *Proc Natl Acad Sci U S A* 2009; **106**(7): 2200-5.
154. Guan BJ, Krokowski D, Majumder M, et al. Translational control during endoplasmic reticulum stress beyond phosphorylation of the translation initiation factor eIF2alpha. *J Biol Chem* 2014; **289**(18): 12593-611.
155. Jiang B-H, Liu L-Z. Role of mTOR in anticancer drug resistance. *Drug Resist Updat* 2008; **11**(3).
156. Jun Sunayama K-IM, Atsushi Sato, Ken Tachibana, Kaori Suzuki, Yoshitaka Narita, Soichiro Shibui, Kaori Sakurada, Takamasa Kayama, Arata Tomiyama, Chifumi Kitanaka. Crosstalk Between the PI3K/mTOR and MEK/ERK Pathways Involved in the Maintenance of Self-Renewal and Tumorigenicity of Glioblastoma Stem-Like Cells. *Stem Cells* 2010; **28**: 10.
157. Yardley DA. Combining mTOR Inhibitors with Chemotherapy and Other Targeted Therapies in Advanced Breast Cancer: Rationale, Clinical Experience, and Future Directions. *Breast Cancer (Auckl)* 2013; **7**: 7-22.
158. Diane C. Fingar CJR, Andrew R. Tee, Lynn Cheatham, Christina Tsou, John Blenis. mTOR Controls Cell Cycle Progression through Its Cell Growth Effectors S6K1 and 4E-BP1/Eukaryotic Translation Initiation Factor 4E. *Molecular Cell Biology* 2004; **24**: 17.

159. Magnuson B, Ekim B, Fingar DC. Regulation and function of ribosomal protein S6 kinase (S6K) within mTOR signalling networks. *Biochem J* 2012; **441**(1): 1-21.
160. Cheong H, Lu C, Lindsten T, Thompson CB. Therapeutic targets in cancer cell metabolism and autophagy. *Nat Biotechnol* 2012; **30**(7): 671-8.
161. Wang FQ, Tong QY, Ma HR, et al. Indole diketopiperazines from endophytic Chaetomium sp 88194 induce breast cancer cell apoptotic death. *Sci Rep* 2015; **5**: 9294.
162. Hiderou Yoshida TM, Akira Yamamoto,Tetsuya Okada, Kazutoshi Mori. XBP1 mRNA Is Induced by ATF6 and Spliced by IRE1 in Response to ER Stress to Produce a Highly Active Transcription Factor. *Cell* 2001; **107**: 11.
163. Urra H, Hetz C. The ER in 4D: a novel stress pathway controlling endoplasmic reticulum membrane remodeling. *Cell Death Differ* 2012; **19**(12): 1893-5.
164. Klee M, Pimentel-Muinos FX. Bcl-X(L) specifically activates Bak to induce swelling and restructuring of the endoplasmic reticulum. *J Cell Biol* 2005; **168**(5): 723-34.
165. Tooze SA, Yoshimori T. The origin of the autophagosomal membrane. *Nat Cell Biol* 2010; **12**(9): 831-5.
166. Martinet W, Timmermans JP, De Meyer GR. Methods to assess autophagy in situ--transmission electron microscopy versus immunohistochemistry. *Methods Enzymol* 2014; **543**: 89-114.
167. Klionsky DJ, Abdelmohsen K, Abe A, et al. Guidelines for the use and interpretation of assays for monitoring autophagy (3rd edition). *Autophagy* 2016; **12**(1): 1-222.
168. Nelo Eidy Zanchi AHLJ. Mechanical stimuli of skeletal muscle: implications on mTOR/p70s6k and protein synthesis. *European Journal of Applied Physiology* 2008; **102**(3): 11.
169. S L. Die Mischiarnei. *Klin Wochenschr* 1927; **6**: 9.
170. Eung-Ryoung Lee J-YK, Yong-Jin Kang, Jae-Yeon Ahn, Jung-Hyun Kim, Bong-Woo Kim, Hye-Yeon Choi, Mi-Young Jeong, Ssang-Goo Cho Interplay between PI3K/Akt and MAPK signaling pathways in DNA-damaging drug-induced apoptosis. *Molecular Cell Research* 2006; **1763**(9): 11.
171. Tan BH, Meinken C, Bastian M, et al. Macrophages Acquire Neutrophil Granules for Antimicrobial Activity against Intracellular Pathogens. *The Journal of Immunology* 2006; **177**(3): 1864-71.
172. Laskay T, van Zandbergen G, Solbach W. Neutrophil granulocytes as host cells and transport vehicles for intracellular pathogens: apoptosis as infection-promoting factor. *Immunobiology* 2008; **213**(3-4): 183-91.
173. Faldt J, Dahlgren C, Ridell M. Difference in neutrophil cytokine production induced bypathogenic and non-pathogenic mycobacteria. *APMIS*; **110**.
174. Cassatella MA. The production of cytokines by polymorphonuclear neutrophils. *Immunology Today* 1995; **16**(1): 6.
175. Papayannopoulos V, Metzler KD, Hakkim A, Zychlinsky A. Neutrophil elastase and myeloperoxidase regulate the formation of neutrophil extracellular traps. *The Journal of cell biology* 2010; **191**(3): 677-91.

176. Metzler KD, Fuchs TA, Nauseef WM, et al. Myeloperoxidase is required for neutrophil extracellular trap formation: implications for innate immunity. *Blood* 2011; **117**(3): 953-9.
177. Xu J, Zhang X, Pelayo R, et al. Extracellular histones are major mediators of death in sepsis. *Nature medicine* 2009; **15**(11): 1318-21.
178. Kutcher ME, Xu J, Vilardi RF, Ho C, Esmon CT, Cohen MJ. Extracellular histone release in response to traumatic injury: implications for a compensatory role of activated protein C. *The journal of trauma and acute care surgery* 2012; **73**(6): 1389-94.
179. Ham A, Rabadi M, Kim M, et al. Peptidyl arginine deiminase-4 activation exacerbates kidney ischemia-reperfusion injury. *American journal of physiology Renal physiology* 2014; **307**(9): F1052-62.
180. Alexander S. Savchenko JIB, Kimberly Martinod, Simon F. De Meyer, Maureen Gallant, Luise Erpenbeck, Alexander Brill, Yanming Wang, Denisa D. Wagner. VWF-mediated leukocyte recruitment with chromatin decondensation by PAD4 increases myocardial ischemia/reperfusion injury in mice. *Blood* 2014; **123**: 8.
181. Aderem A, Underhill DM. MECHANISMS OF PHAGOCYTOSIS IN MACROPHAGES. *Annal Review of Immunology* 1999; **17**: 33.
182. Farrera C, Fadeel B. Macrophage clearance of neutrophil extracellular traps is a silent process. *Journal of immunology* 2013; **191**(5): 2647-56.
183. Wang Y, Wysocka J, Sayegh J, et al. Human PAD4 Regulates Histone Arginine Methylation Levels via Demethylimination. 2004.
184. Hagiwara T, Hidaka Y, Yamada M. Deimination of Histone H2A and H4 at Arginine 3 in HL-60 Granulocytes. 2005.
185. Mohanan S, Cherrington BD, Horibata S, McElwee JL, Thompson PR, Coonrod SA. Potential role of peptidylarginine deiminase enzymes and protein citrullination in cancer pathogenesis. *Biochem Res Int* 2012; **2012**: 895343.
186. Christophorou MA, Castelo-Branco G, Halley-Stott RP, et al. Citrullination regulates pluripotency and histone H1 binding to chromatin. *Nature* 2014; **507**(7490): 104-8.
187. Aulik NA, Hellenbrand KM, Czuprynski CJ. Mannheimia haemolytica and its leukotoxin cause macrophage extracellular trap formation by bovine macrophages. *Infection and immunity* 2012; **80**(5): 1923-33.
188. Bonne-Annee S, Kerepesi LA, Hess JA, et al. Extracellular traps are associated with human and mouse neutrophil and macrophage mediated killing of larval Strongyloides stercoralis. *Microbes and infection / Institut Pasteur* 2014; **16**(6): 502-11.
189. Doster R, Rogers L, Aronoff D, Gaddy J. Doster-Macrophages Produce Extracellular Traps in Response to Streptococcus agalactiae Infection. 2015.
190. Hellenbrand KM, Forsythe KM, Rivera-Rivas JJ, Czuprynski CJ, Aulik NA. Histophilus somni causes extracellular trap formation by bovine neutrophils and macrophages. *Microbial pathogenesis* 2013; **54**: 67-75.
191. Je S, Quan H, Yoon Y, Na Y, Kim B-J, Seok SH. Mycobacterium massiliense Induces Macrophage Extracellular Traps with Facilitating Bacterial Growth. 2016.

192. Liu P, Wu X, Liao C, et al. Escherichia coli and Candida albicans induced macrophage extracellular trap-like structures with limited microbicidal activity. *PloS one* 2014; **9**(2): e90042.
193. Wong KW, Jacobs WR, Jr. Mycobacterium tuberculosis exploits human interferon gamma to stimulate macrophage extracellular trap formation and necrosis. *The Journal of infectious diseases* 2013; **208**(1): 109-19.
194. Vossenaar ER, Zendman AJ, van Venrooij WJ, Pruijn GJ. PAD, a growing family of citrullinating enzymes: genes, features and involvement in disease. *BioEssays : news and reviews in molecular, cellular and developmental biology* 2003; **25**(11): 1106-18.
195. Guertin MJ, Zhang X, Anguish L, et al. Targeted H3R26 deimination specifically facilitates estrogen receptor binding by modifying nucleosome structure. *PLoS genetics* 2014; **10**(9): e1004613.
196. Xuesen Zhanga MB, Michael J. Guertinc, Wei Chend, Sheng Zhangd, Brian D. Cherringtona, Daniel J. Sladee, Christina J. Dreytone, Venkataraman Subramaniane, Kevin L. Bickere, Paul Thompsone, Michael A. Mancinib, John T. Lisc, Scott A. Coonroda. Peptidylarginine deiminase 2-catalyzed histone H3 arginine 26 citrullination facilitates estrogen receptor α target gene activation. *PNAS* 2012; **109**(33): 6.
197. Cao R WL, Wang H, Xia L, Erdjument-Bromage H, Tempst P, Jones RS, Zhang Y. Role of histone H3 lysine 27 methylation in Polycomb-group silencing. *Science* 2002; **298**(5595): 5.
198. Quinten Remijsen TVB, Ellen Wirawan, Bob Asselbergh, Eef Parthoens, Riet De Rycke, Sam Noppen, Michel Delforge, Jean Willems, Peter Vandenabeele. Neutrophil extracellular trap cell death requires both autophagy and superoxide generation. *Cell Research* 2011; **21**(2): 15.
199. Sabatini DDSDAGSMADM. Phosphorylation and Regulation of Akt/PKB by the Rictor-mTOR Complex. *Science* 2005; **307**: 5.
200. Kitanaka JSK-IMASKTKSYNSSKSTKATC. Crosstalk Between the PI3K/mTOR and MEK/ERK Pathways Involved in the Maintenance of Self-Renewal and Tumorigenicity of Glioblastoma Stem-Like Cells. *Stem Cells* 2010; **28**: 10.
201. Babchia N, Calipel A, Mouriaux F, Faussat AM, Mascarelli F. The PI3K/Akt and mTOR/P70S6K signaling pathways in human uveal melanoma cells: interaction with B-Raf/ERK. *Invest Ophthalmol Vis Sci* 2010; **51**(1): 421-9.
202. Luqmani YA. Mechanisms of drug resistance in cancer chemotherapy. *Med Princ Pract* 2005; **14 Suppl 1**: 35-48.
203. Rebecca A. Burrella CS. Tumour heterogeneity and the evolution of polyclonal drug resistance. *Molecular Oncology* 2014; **8**(6): 17.
204. Nicholas A Saunders FS, Erik W Thompson, Michelle M Hill, Liliana Endo-Munoz, Graham Leggatt, Rodney F Minchin, Alexander Guminski. Role of intratumoural heterogeneity in cancer drug resistance: molecular and clinical perspectives. *EMBO Molecular Medicine* 2012; **4**(8): 10.
205. Housman G, Byler S, Heerboth S, et al. Drug resistance in cancer: an overview. *Cancers (Basel)* 2014; **6**(3): 1769-92.

206. Sarkar S, Goldgar S, Byler S, Rosenthal S, Heerboth S. Demethylation and re-expression of epigenetically silenced tumor suppressor genes: sensitization of cancer cells by combination therapy. *Epigenomics* 2013; **5**.
207. Dennis J. Slamon BL-J, Steven Shak, Hank Fuchs, Virginia Paton, Alex Bajamonde, Thomas Fleming, Wolfgang Eiermann, Janet Wolter, Mark Pegram, Jose Baselga, Larry Norton. Use of Chemotherapy plus a Monoclonal Antibody against HER2 for Metastatic Breast Cancer That Overexpresses HER2. *The New England Journal of Medicine* 2001; **344**: 10.
208. Bertrand Coiffier EL, Josette Brière, Raoul Herbrecht, Hervé Tilly, Reda Bouabdallah, Pierre Morel, Eric Van Den Neste, Gilles Salles, Philippe Gaulard, Felix Reyes, Pierre Lederlin, Pierre Lederlin, Christian Gisselbrecht. CHOP Chemotherapy plus Rituximab Compared with CHOP Alone in Elderly Patients with Diffuse Large-B-Cell Lymphoma. *The New England Journal of Medicine* 2002; **346**: 8.
209. Powell DR, Huttenlocher A. Neutrophils in the Tumor Microenvironment. *Trends Immunol* 2016; **37**(1): 41-52.
210. Mantovani A, Sica A. Macrophages, innate immunity and cancer: balance, tolerance, and diversity. *Curr Opin Immunol* 2010; **22**(2): 231-7.
211. Gasser S, Raulet D. The DNA damage response, immunity and cancer. *Semin Cancer Biol* 2006; **16**(5): 344-7.
212. Slava Epelman KJL, Gwendalyn J. Randolph. Origin and Functions of Tissue Macrophages. *Immunity* 2014; **41**(1): 15.
213. Mitchem JB BD, Knolhoff BL, Belt BA, Zhu Y, Sanford DE, Belaygorod L, Carpenter D, Collins L, Piwnica-Worms D, Hewitt S, Udupi GM, Gallagher WM, Wegner C, West BL, Wang-Gillam A, Goedegebuure P, Linehan DC, DeNardo DG. Targeting tumor-infiltrating macrophages decreases tumor-initiating cells, relieves immunosuppression, and improves chemotherapeutic responses. *Cancer Research* 2013; **73**(3): 14.
214. Galdiero MR, Bonavita E, Barajon I, Garlanda C, Mantovani A, Jaillon S. Tumor associated macrophages and neutrophils in cancer. *Immunobiology* 2013; **218**(11): 1402-10.
215. David M. Richards JH, Markus Feuerer. Monocytes and Macrophages in Cancer: Development and Functions. *Cancer Microenvironment* 2012; **6**(2): 13.
216. Eliver Eid Bou Ghosn AAC, Gregory R. Govoni, Takeshi Fukuhara, Yang Yang, Denise M. Monack, Karina R. Bortoluci, Sandro R. Almeida, Leonard A. Herzenberg, Leonore A. Herzenberg Two physically, functionally, and developmentally distinct peritoneal macrophage subsets. *PNAS* 2009; **107**: 6.
217. Alexandra dos Anjos Cassado MRDIL, Karina Ramalho Bortoluci. Revisiting Mouse Peritoneal Macrophages: Heterogeneity, Development, and Function. *Frontiers in immunology* 2015; **6**: 9.
218. Lin Wang XCCa, Guangying Yuan, Yan Zhao, Pengcheng Wang. Expression of Peptidylarginine Deiminase Type 4 in Ovarian Tumors. *Int J Biol Sci* 2010; **6**(5): 11.
219. Dariush Mozaffarian EJB, Alan S. Go, Donna K. Arnett, Michael J. Blaha, Mary Cushman, Sandeep R. Das, Sarah de Ferranti, and on behalf of the American Heart Association Statistics Committee and Stroke Statistics Subcommittee. Heart Disease and Stroke Statistics—2016 Update A Report From the American Heart Association. *Circulation* 2016; **133**(4).

220. Amytis Towfighi JLS. Stroke Declines From Third to Fourth Leading Cause of Death in the United States. *Stroke* 2011; **42**(8): 6.
221. Gregory J. del Zoppo JLS, Edward C. Jauch, Harold P. Adams, on behalf of the American Heart Association Stroke Council. Expansion of the Time Window for Treatment of Acute Ischemic Stroke With Intravenous Tissue Plasminogen Activator. *Stroke* 2009; **40**(8): 6.
222. Davis SM DG. 4.5 hours: the new time window for tissue plasminogen activator in stroke. *Stroke* 2009; **40**(6): 2.
223. Hacke W KM, Fieschi C, von Kummer R, Davalos A, Meier D, Larrue V, Bluhmki E, Davis S, Donnan G, Schneider D, Diez-Tejedor E, Trouillas P. Randomised double-blind placebo-controlled trial of thrombolytic therapy with intravenous alteplase in acute ischaemic stroke (ECASS II). Second European-Australasian Acute Stroke Study Investigators. *THE LANCET* 1998; **352**(9136): 7.
224. group TI-c. The benefits and harms of intravenous thrombolysis with recombinant tissue plasminogen activator within 6 h of acute ischaemic stroke (the third international stroke trial [IST-3]): a randomised controlled trial. *THE LANCET* 2012; **379**(9834): 12.
225. Saver JL. Time Is Brain—Quantified. *Stroke* 2006; **37**(1): 5.
226. Taoufik E PL. Ischemic neuronal damage. *Current Pharmaceutical Design* 2008; **14**(33): 9.
227. Rong Jin GY, Guohong Li. Inflammatory mechanisms in ischemic stroke: role of inflammatory cells. *J Leukoc Biol* 2010; **87**(5): 11.
228. Qing Wang XNT, Midori A. Yenari. THE INFLAMMATORY RESPONSE IN STROKE. *J Neuroimmunol* 2006; **184**(1-2): 16.
229. Takahiro Takano NO, Maria Luisa Cotrina， Maiken Nedergaard. Astrocytes and Ischemic Injury. *Stroke* 2009; **40**(3).
230. George Barreto REW, Yibing Ouyang, Lijun Xu, Rona G. Giffard. Astrocytes: Targets for Neuroprotection in Stroke. *Cent Nerv Syst Agents Med Chem* 2011; **11**(2): 10.
231. Anita R Patel RR, Louise D McCullough, Fudong Liu. Microglia and ischemic stroke: a double-edged sword. *Int J Physiol Pathophysiol Pharmacol* 2013; **5**(2): 18.
232. Ying Fu QL, Josef Anrather, Fu-Dong Shi. Immune interventions in stroke. *Nature Reviews Neurology* 2015; **11**: 12.
233. Richard Macrez CA, Olivier Toutirais, Brigitte Le Mauff, Gilles Defer, Ulrich Dirnagl, Prof Denis Vivien. Stroke and the immune system: from pathophysiology to new therapeutic strategies. *The LANCET Neurology* 2011; **10**(5): 10.
234. Rabadi M, Kim M, D'Agati V, Lee HT. Peptidyl arginine deiminase-4-deficient mice are protected against kidney and liver injury after renal ischemia and reperfusion. *American journal of physiology Renal physiology* 2016; **311**(2): F437-49.
235. Jerry S. Regeneration beyond the glial scar. *Nature Reviews Neuroscience* 2004; **5**(2): 11.
236. Helena W Morrison JAF. A quantitative spatiotemporal analysis of microglia morphology during ischemic stroke and reperfusion. *Journal of Neuroinflammation* 2012; **10**(4): 20.

237. Wigerblad G, Bas DB, Fernades-Cerqueira C, et al. Autoantibodies to citrullinated proteins induce joint pain independent of inflammation via a chemokine-dependent mechanism. *Ann Rheum Dis* 2016; **75**(4): 730-8.
238. Vossenaar ER, van Venrooij WJ. Citrullinated proteins: sparks that may ignite the fire in rheumatoid arthritis. *Arthritis research & therapy* 2004; **6**(3): 107-11.

VITA

Jinquan Sun

197 Amberleigh Ln, Bellefonte, PA16823; jinquansun@gmail.com

Education

Ph.D in MCIBS, GPA 3.85/4.0 Aug 2011-Dec 2016
MICBS program, The Huck Institutes of the Life Sciences,
Pennsylvania State University, University Park, PA, USA

B.S. in Biochemistry, GPA 3.8/4.0 Sept 2007-June 2011
Honor program
China Agricultural University, Beijing, P.R. China

Representative Publications and Poster Presentations

Jinquan Sun*, Xiangyun Chen* and Yanming Wang. *Epigenetic Technological Applications*. ***Elsevier.*** (* authors of equal contribution)
Xiaolin Li, Ye Shen, **Jinquan Sun**, Bin Wang, Qun He.*A reporter for dsRNA response in Neurospora crassa.* ***FEBS Letters****.*
Jinquan Sun and Yanming Wang. PAD4 is required for Macrophage Extracellular Traps (METs) formation in mice peritoneal macrophage cells. ***34th summer symposium: chromatin and Epigenetic Regulation of Transcription.*** (July, 2015; State College, PA)
Jinquan Sun, Wenjing Wang, Yuji Wang, Shiqi Peng and Yanming Wang. Small molecule PZ1225 nanoparticles inhibit cancers via the unfolded protein response and autophagy pathways. ***32nd summer symposium: Sensing and Signaling Across the Mucosa: From Homeostasis to Pathogenesis****.* (June 2013; State College, PA)

Honors and Awards

J. Lloyd Huck Graduate Fellowship June 2014-July 2016
The Huck Institutes of the Life Sciences, Pennsylvania State University

Additional Courses and Experience

IP pipeline Student Intern **Fall 2016**
Office for Innovation, Eberly College of Science, Pennsylvania State University.
Business Bootcamp for Science Entrepreneurs **Certificate, May 2016**
Smeal college of Business,Pennsylvania State University.
The Penn State Course in College teaching **Certificate,Fall 2015**
Schreyer Institute for Teaching Excellence, Pennsylvania State University.